



**Instituto Politécnico de Bragança
Escola Superior de Tecnologia e Gestão**

Optimizing biogas production via ozone sludge pretreatment

Safaa Ahmad Mustafa Alqudah

The dissertation submitted to
**Escola Superior de Tecnologia e Gestão
Instituto Politécnico de Bragança**
Master Degree in
Chemical Engineering

Supervisor:

PhD Prof. Ramiro José Espinheira Martins

Braganca, Portugal
December 2025

DEDICATION

I dedicate my work to my beloved family, Alqudah. My parents, Ahmad alqudah and Naela alhamed, instilled in me the values of perseverance and determination. My siblings, Noor , Nidaa, Somaya, Dania, Hamza, and Bashar, have provided unwavering support and encouragement, serving as a source of strength to me.

I am thankful to them for always believing in me, boosting my confidence, and supporting all my decisions throughout my journey. I hope that my success will bring them as much happiness as they have filled me with since the day I was born.

To my dear Nabil Awawdeh and Elezabith Alqudah, whose guidance and wisdom have shaped my vision.

To my dear Portuguese, Professor Ramiro Martins, for assisting me in lighting my path and making life here much easier.

To my close friends, Khadija Reguag, Mariam Banirrached, and Soufiene also my friends that I met here in Portugal, Ikram and Saliha

My family, whose laughter and encouragement kept my academic journey smooth during the darkest days, sacrifices, and boundless love. I dedicate this paper to you for everything you have done and given me.

ACKNOWLEDGEMENTS

I would like to express my sincere gratitude to my supervisor, Professor Ramiro José Espinheira Martins, for sharing his knowledge with me. I am truly thankful for his patience, constant availability, and insightful guidance, which have been immensely valuable throughout the development of this work.

To the technician of the Chemical Processes Laboratory, Eng. Maria João Almeida Pinto Santos Afonso, for the support throughout the work.

Instituto Politécnico de Bragança for this opportunity.

ABSTRACT

Anaerobic digestion (AD) is the preferred method for handling wastewater sludge while producing renewable energy in the form of biogas. However, this process often occurs during the hydrolysis phase, which can prevent the system from working at maximum efficiency. This study examined the effect of ozone pre-treatment on methane generation from municipal sludge during mesophilic batch digestion. Ozone was applied at concentrations of 0%, 5%, and 10% for exposure times of 30, 60, and 90 s, respectively.

A series of anaerobic co-digestion experiments was then conducted using different inoculum-to-substrate (I/S) ratios of 1.0, 1.5, and 2.0. Methane production was continuously monitored using the AMPTS II system. The methane yield was 736 NmL CH₄ g⁻¹ VS at an ozone concentration of 4.41 L min⁻¹.

The Buswell–Mueller equation was applied to estimate the theoretical biochemical methane potential (TBMP), resulting in a value of approximately 517 mL CH₄ per gram of volatile solids (VS). Kinetic modeling using the modified Gompertz equation showed faster methane production rates and reduced lag times under the optimized pretreatment conditions. Overall, the data suggest that ozone pre-treatment, when carefully controlled, can significantly improve sludge biodegradability and enhance biogas yields, indicating a promising method for increasing energy recovery in wastewater treatment systems.

Furthermore, a comparative evaluation of four kinetic models (Gompertz, Logistic, Transference, and Cone) was conducted to identify the most suitable approach for describing biogas production kinetics under ozone pretreatment. Although all models provided statistically robust fits, the Logistic and Gompertz models demonstrated slightly superior consistency and interpretability across the range of experimental conditions. This careful model selection not only improved the reliability of methane yield predictions but also supported more informed process optimization. Overall, these findings emphasize that integrating robust kinetic modeling with innovative pretreatment strategies can significantly enhance biogas yield and process efficiency, offering valuable insights into advancing sustainable energy recovery from municipal sludge.

Keywords: Anaerobic digestion; biogas production; Co-digestion; Gompertz model; methane yield; ozone pretreatment; sludge solubilization ; wastewater sludge.

RESUMO

A digestão anaeróbia (DA) é um método preferível para tratar as lamas das águas residuais e produzir energia renovável sob a forma de biogás. No entanto, o processo é frequentemente interrompido durante a fase de hidrólise - um verdadeiro obstáculo que pode impedir que as coisas funcionem com a máxima eficiência. Este estudo examinou a forma como o pré-tratamento com ozono afecta a produção de metano a partir de lamas municipais sob digestão mesofílica em lote. O ozono foi introduzido em concentrações de 0%, 5% e 10%, com tempos de exposição de 30, 60 e 90 segundos. Foi então realizada uma série de experiências de co-digestão anaeróbia utilizando diferentes rácios de inóculo-substrato (I/S) - especificamente 1,0, 1,5 e 2,0. A produção de metano foi monitorizada continuamente utilizando o sistema AMPTS II. O resultado mais notável foi o rendimento ótimo de metano de 1380,9 NmL, obtido quando 10% de ozono foi aplicado durante 30 segundos a uma relação I/S de 1,5. Representando um rendimento em metano de 735,758 NmL CH₄ g⁻¹ VS com uma concentração de ozono de 4,41 L.min⁻¹.

A equação de Buswell e Mueller foi aplicada para estimar o potencial bioquímico teórico de metano (TBMP), chegando a um valor de aproximadamente 517 mL CH₄ por grama de sólidos voláteis (VS). A modelagem cinética usando a equação de Gompertz modificada mostrou taxas de produção de metano mais rápidas e tempos de atraso reduzidos sob condições de pré-tratamento otimizadas. No geral, os dados sugerem que o pré-tratamento com ozono, quando cuidadosamente controlado, pode melhorar significativamente a biodegradabilidade das lamas e aumentar a produção de biogás, apontando para um método promissor para aumentar a recuperação de energia em sistemas de tratamento de águas residuais.

Além disso, foi realizada uma avaliação comparativa de quatro modelos cinéticos - Gompertz, Logístico, Transferência e Cone - para identificar a abordagem mais adequada para descrever a cinética da produção de biogás sob pré-tratamento com ozono. Embora todos os modelos tenham fornecido ajustes estatisticamente robustos, os modelos Logístico e de Gompertz demonstraram consistência e interoperabilidade ligeiramente superiores em toda a gama de condições experimentais. Esta cuidadosa seleção de modelos não só melhorou a fiabilidade das previsões de produção de metano, como também apoiou uma otimização mais informada do processo. De um modo geral, estes resultados sublinham que a integração de uma modelação cinética robusta com estratégias inovadoras de pré-tratamento pode aumentar significativamente a produção de biogás e a eficiência do processo, oferecendo informações valiosas para o avanço da recuperação sustentável de energia a partir de lamas municipais.

Palavras-chave: Codigestão; Digestão anaeróbia; Lodo de águas residuais; Modelo de Gompertz; Pré-tratamento com ozono; Produção de biogás; Proporção inóculo-substrato; Rendimento de metano; Solubilização de lamas.

Index Of Figures

Figure 1: Anaerobic digestion (AD) biomass decomposition stages (hydrolysis, acidogenesis, acetogenesis, and methanogenesis) and key compounds.	7
Figure 2: Main factors and interactions influencing methane generation and the performance of the anaerobic digestion process.	9
Figure 3: Ultrasound pretreatment process.	12
Figure 4: Ozonation pretreatment process.	14
Figure 5: Ozone wastewater application diagram.	14
Figure 6: Comparison of increase in biogas/ methane production (B), capital cost, O&M (operation and maintenance) costs, and energy requirement (C) of sewage sludge pretreatment methods.	15
Figure 7: UV-Spectrophotometer JascoV-530.	18
Figure 8: COD calibration curve.	19
Figure 9: OxiTop®-OC 100 (3BOD analyser with the incubator).	20
Figure 10 : Ultrasonic set-up.	22
Figure 11: Concept of ozone synthesis and the ozone generator used in the experiment.	23
Figure 12: The AMPTS II system by Bioprocess Control. a) a digester unit, a CO ₂ absorption bottle, and a volumetric gas measurement unit; b) bioprocess control software.	23
Figure 13: Methane production for substrate compared with the theoretical methane yield.	31
Figure 14: Cumulative methane production for the various substrate samples tested.	31
Figure 15: Methane production rate over time for the various substrate samples analyzed.	32
Figure 16: Cumulative methane production over time for the various substrate samples in Trial 1.	32
Figure 17: Cumulative methane production for trial 2 over the course of the experimental period.	32
Figure 18: Cumulative Methane production (mL CH ₄ g ⁻¹ VS) using Gompertz Model fitting for all 0% Ozone pretreatment samples at varying I/S Ratios over time (Days).	41
Figure 19: Cumulative methane production using Gompertz Model fitting for all samples treated with 5% Ozone Pretreatment Over Time (Days).	41
Figure 20: Cumulative methane production using Gompertz Model fitting for all samples treated with 10% Ozone Pretreatment Over Time (Days).	42
Figure 21: ANOVA for the quadratic response of methane production.	50
Figure 22: Cube plot representing the interactive effects of ozone concentration (%), inoculum-to-substrate (I/S) ratio, and ozone contact time (s) on methane production (NmL) based on the Box–Behnken design (experiment 1).	50
Figure 23: 3D diagram of methane production based on the Box–Behnken design (experiment 1).	51
Figure 24: Contour graph of methane production based on the Box–Behnken design (experiment 1).	51
Figure 25: Scatter diagram of predicted vs actual methane production based on the Box–Behnken design (experiment 1).	52
Figure 26: Cumulative methane (CH ₄) production over time (days) for samples treated with varying ozone concentrations, exposure durations, and inoculum-to-substrate (I/S) ratios.	55
Figure 27: Methane (CH ₄) production rate over time (days) for samples subjected to varying ozone concentrations, exposure times, and inoculum-to-substrate (I/S) ratios.	56
Figure 28: Three-dimensional plot of interaction effects of ozone concentration (%), I/S ratio, and contact time (s) on methane yield (NmL) determined via a Box–Behnken experimental design.	59
Figure 29: 3D diagram of methane production (NmL).	60
Figure 30: Contour graph of methane production based on the Box–Behnken design (experiment 2).	61
Figure 31: Scatter diagram of predicted vs actual methane production based on the Box–Behnken design (experiment 2).	61
Figure 32: ANOVA results for the quadratic model of methane production.	62
Figure 33: Gompertz model fitting of cumulative methane production for untreated (0% ozone) samples over time.	65
Figure 34: Gompertz model fitting of cumulative methane production for samples with 5% ozone pre-treatment under different I/S ratios: (a) I/S = 1, (b) I/S = 2, and (c) I/S = 1.5, as a function of time.	66
Figure 35: Gompertz model fitting of cumulative methane production over time for 5% ozone pre-treated samples at varying I/S ratios.	67

Figure 36: Gompertz model fitting of cumulative methane production over time for 10% ozone-treated samples..... 68
Figure 37: Comparison of model fittings (Gompertz, Logistic, Transference, and Cone) with experimental cumulative CH₄ production for 10% ozone-treated samples (30 s) at I/S = 1.5. 73

Index Of Tables:

Table 1: COD Calibration curve (standard COD solution of 1000 mg L⁻¹)..... 18
Table 2: Physicochemical characteristics of wastewater sludge used for anaerobic digestion..... 24
Table 3: Nutrient supplementation for anaerobic digestion (Hu, 2013). 25
Table 4: Factor levels with variables. 27
Table 5: Box Behnken design (ozone pretreatment). 29
Table 6: Methane production as a function of ozone concentration, contact time, and I/S ratio (Experiment 1)..... 29
Table 7: Two-Factor ANOVA with replication, analyzing the effect of ozone percentage (A) and contact time (B) on methane production yield. 34
Table 8: Two-Factor ANOVA with replication analyzing the effect of I/S Ratio (C) and contact time (B) on methane production yield..... 35
Table 9: Changes in pH observed before and after 30 days of digestion. 37
Table 10: The impact of nutrient addition on methane production..... 40
Table 11: Mathematical models for methane production kinetics in anaerobic digestion..... 43
Table 12 : Estimated Gompertz model parameters for Experiment..... 43
Table 13: Estimated Logistic model parameters for Experiment 1. 44
Table 14: Estimated Transference model parameters for Experiment 1..... 44
Table 15: Estimated Cone model parameters for Experiment 1. 45
Table 16: Statistical comparison of models fits based on variance and F-Values for sample oz 10%, t(30s), I/S (2). 47
Table 17: F-Test Two-sample variance analysis for model comparison across all Experimental conditions supported the robustness of the Gompertz (M1), Logistic (M2), Transference (M3) and Cone (M4) models. 47
Table 18: Factor levels with variables for experiment 1..... 49
Table 19: Effect of ozone concentration, contact time, and I/S ratio on methane production (Experiment 2)..... 54
Table 20 : Overview of the anaerobic digestion phases in Experiment 2 with duration, key reactions, causes, and microbial groups..... 57
Table 21: Initial and final pH values for Experiment 2 (45 d)..... 58
Table 22: Factor Levels with variables for experiment 2 59
Table 23: Optimal operational conditions (ozone concentration, I/S ratio, and contact time) and their associated predicted methane yield. 63
Table 24: The Modified Gompertz Model analysis for methane production. 64
Table 25: Estimated Gompertz model parameters for 15 experimental samples from Experiment 2..... 69
Table 26: Estimated Logistic model parameters for 15 experimental samples from Experiment 2. 69
Table 27: Estimated Transference model parameters for 15 experimental samples from Experiment 2. 70
Table 28: 2 Estimated Cone model parameters for 15 experimental samples from Experiment 2..... 70
Table 29: Statistical comparison of model fits based on variance and F-values for the sample Oz 10%–30 s (I/S 1.5).... 73
Table 30: Model performance comparison for Oz 10% 30sec, I/S(1.5) Volume [NmL] condition, analysis of the four models. 73
Table 31: F-test two-sample variance analysis for model comparison across all experimental conditions confirmed the robustness of the Gompertz (M1), Logistic (M2), Transference (M3), and Cone (M4) models. 75

Index of Abbreviations

- AD - Anaerobic Digestion
- AMPTS II - Automatic Methane Potential Test System II
- ANOVA - Analysis of Variance
- AOPs - Advanced Oxidation Processes
- AWWA - American Water Works Association
- Bmax - Maximum Biogas Potential
- BOD - Biological Oxygen Demand
- BMP - Biochemical Methane Potential
- C/N - Carbon to Nitrogen ratio
- COD - Chemical Oxygen Demand
- DBPs - Disinfection By-Products
- DS - Oven-dried Sludge
- DS7 - Sun-dried Sludge for Seven Days
- DS15 - Sun-dried Sludge for 15 Days
- HRT - Hydraulic Retention Time
- I/S (or IS) - Inoculum-to-Substrate ratio
- O&M - Operation and Maintenance
- OLR - Organic Loading Rate
- R² - R-squared (coefficient of determination)
- Rmax - Maximum Production Rate
- SA - Sludge Ash
- SEE - Standard Error of Estimate
- SRT - Solid Retention Time
- TAC - Total Alkalinity
- TBMP - Theoretical Biochemical Methane Potential
- TS - Total Solids

- US - Ultrasound
- UV - Ultra Violet
- VFA / VFAs - Volatile Fatty Acid(s)
- VS - Volatile Solids
- WAS - Waste-Activated Sludge
- WOS - Wet Oxidized Sludge
- WTP - Water Treatment Plant
- WWTP / WWTPs - Wastewater Treatment Plant(s)

Table of Contents

1	<i>Introduction</i>	1
1.1	Anaerobic Sludge Digestion in Wastewater Treatment Plants (WWTPs)	1
1.1.1	Ozone Pretreatment.....	1
1.1.2	Ultrasound Pretreatment	1
1.2	Case study.....	2
2	<i>Objectives</i>	3
3	<i>State Of the Art</i>	3
3.1	Wastewater Treatment in Portugal	3
3.1.1	Liquid Line	4
3.1.2	Solid Line.....	4
3.1.3	Deodorization Line	4
3.2	Pretreatment Technologies for Enhanced Biogas Production	4
3.2.1	Thermal Pretreatment.....	4
3.2.2	Ultrasound Pretreatment	4
3.2.3	Ozone Pretreatment.....	5
3.2.4	Physical/Mechanical Pretreatment.....	5
3.3	Stages of Sludge Generation	5
3.3.1	Preliminary Treatment.....	5
3.3.2	Primary Treatment.....	5
3.3.3	Secondary (Biological) Treatment.....	5
3.3.4	Tertiary Treatment (Optional)	5
3.4	Sludge Thickening and Dehydration	6
3.5	Anaerobic Digestion (Optional)	6
3.6	Final Disposal or Recovery	6
3.7	The Main Factors Influencing Sludge Generation	6
3.8	Anaerobic Digestion	6
3.9	Influence of Operational Parameters on Methane Production and Anaerobic Digestion Efficiency	8
3.9.1	Temperature.....	9
3.9.2	pH.....	9
3.9.3	Hydraulic Retention Time (HRT)	9
3.9.4	Organic Loading Rate (OLR).....	9
3.9.5	Organic composition.....	10
3.9.6	Volatile fatty acids (VFAs).....	10
3.9.7	Mixing/Stirring	10
3.9.8	Toxicity/disinfection.....	10
3.9.9	Retention Time.....	10
3.9.10	Moisture	10
3.10	Physical/Mechanical Pretreatment Processes	11

3.10.1	Ultrasound in Wastewater Pre-treatment.....	11
3.10.2	Ozone in Wastewater Pretreatment	13
4	<i>Methodology</i>	16
4.1	Temperature.....	16
4.2	pH	16
4.2.1	Optimising Microbial Activity	17
4.2.2	Detecting Imbalances Early	17
4.2.3	Preventing System Failures.....	17
4.3	Chemical oxygen demand (COD)	17
4.4	Biological oxygen demand (BOD).....	19
4.5	Volatile solid (VS)	20
4.6	Total Solids (TS)	20
4.7	Volatile fatty acid:	20
4.7.1	Determination of Volatile Fatty Acids (VFAs) by The Titration Method.....	21
4.7.2	Principle.....	21
4.7.3	Procedure	21
4.8	Pretreatment.....	22
4.8.1	Ultrasound	22
4.8.2	Ozonation	22
5	<i>Materials and Methods</i>	23
5.1	Study Site and Experimental Overview.....	23
5.2	Substrate and Inoculum Collection:	23
5.3	Sludge Characterization	24
5.4	Ozone Pretreatment Procedure	25
5.5	Experimental Design for Anaerobic Digestion	25
5.6	Nutrient Supplementation	25
5.7	Theoretical Methane Potential (TBMP)	26
5.8	Box Behnken design.....	26
5.9	Methane Production Modeling	27
6	<i>Results</i>	28
6.1	Experiment 1	28
6.1.1	Effect of Ozone Pretreatment on Methane Yield	28
6.1.2	Influence of I/S Ratio	34
6.1.3	pH Behavior before and after digestion	37
Impact of Elevated pH and Ammonia on Methane Production in Anaerobic Digestion	39	
6.1.4	Kinetic Modeling Using Modified Gompertz Equation	40
6.1.5	Evaluation of Multiple Mathematical Models for Anaerobic Digestion Performance in Experiment 1	42
6.1.6	Comprehensive Model Evaluation Using F-Test for Variance and best Fit Criteria, for the comparison for all models	47

6.1.7	Performing a Box-Behnken design experiment.....	49
6.1.8	Three-Dimensional Response Surface Analysis of Methane Yield	52
6.1.9	Limitations and Justification for Experiment 2	53
6.2	Experiment 2	54
6.2.1	Effect of Ozone Pretreatment on Methane Yield	54
6.2.2	Influence of I/S Ratio	57
6.2.3	Effect of Anaerobic Digestion on pH Values	57
6.2.4	Theoretical vs. Experimental Methane Yield	58
6.2.5	Performing a Box-Behnken design experiment.....	58
	62
6.2.6	Fit Response Surface Model.....	62
6.2.7	ANOVA and Model Adequacy	63
6.2.8	The Optimal Conditions (Hypothetical Result):	63
6.2.9	Modified Gompertz Model.....	63
6.2.10	Gompertz Model fitting	64
6.2.11	Evaluation of Mathematical Models for Anaerobic Digestion Performance in Experiment 2	68
6.2.12	Comparative Analysis of Kinetic Models Using F-Test: Oz 10%, 30 sec, I/S = 1.5 Condition	72
6.2.13	Comprehensive Model Evaluation Using F-Test for Variance and best Fit Criteria, for the comparison of all models	74
7	Discussion.....	76
7.1	Impact of Ozone Concentration and Contact Time.....	76
7.2	Role of Inoculum-to-Substrate Ratio.....	76
7.3	Methane Kinetics and Gompertz Model.....	77
7.4	Integration with Literature and Novelty	77
7.5	Practical Implications and Environmental Significance.....	77
7.6	Comparison between kinetic model's fittings	78
8	Conclusions.....	79
9	References.....	80

1 Introduction

1.1 Anaerobic Sludge Digestion in Wastewater Treatment Plants (WWTPs)

Wastewater Treatment Plants (WWTPs) are essential for reducing water pollution because they filter pollutants from sewage, maintain water bodies, and are appropriate for various applications. Sludge treatment is a crucial part of WWTPs, and anaerobic digestion (AD) is a standard method for stabilizing both primary and secondary sludges. This process is often referred to as anaerobic sludge stabilisation or methane fermentation. AD reduces the organic content of sludge by 40-55% (Appels et al., 2008), making it a crucial step before drying or incineration. A further benefit of anaerobic digestion is its ability to generate biogas, which can be recovered as renewable energy and thus increases the environmental sustainability of the overall process.

Anaerobic sludge digestion has long been a standard process in wastewater treatment plants (WWTPs) because it simultaneously produces biogas and reduces sludge volume. In doing so, it enhances the overall sustainability of WWTPs by converting organic waste into useful energy carriers such as fuel, electricity, and heat. The anaerobic digestion process comprises several stages, with hydrolysis being a crucial yet often rate-limiting step in which complex organic matter is broken down into simpler molecules that are later converted into biogas. Since the efficiency of hydrolysis strongly influences total biogas yield, it has become a central focus of recent research and technological development. Hydrolysis efficiency is influenced by several operational parameters, including temperature, pH, mixing intensity, particle size, and sludge composition, all of which govern how readily complex organics are solubilized.

Various pretreatment methods have been developed and studied to overcome the challenges associated with hydrolysis, targeting these parameters to improve cell disruption, surface area, and substrate accessibility (Tyagi & Lo, 2011). These pretreatment techniques aim to break down complex organic materials before the anaerobic digestion process, thereby enhancing the hydrolysis step and increasing the overall methane production. Two of the most promising pretreatment methods are:

1.1.1 Ozone Pretreatment

Ozone pretreatment involves the use of ozone to oxidize complex organic compounds in sludge, breaking them down into simpler, and more biodegradable forms. This method has been shown to significantly enhance hydrolysis, leading to higher biogas yields. Additionally, ozone pretreatment can help reduce sludge toxicity, making it more amenable to anaerobic digestion (Tyagi & Lo, 2011).

1.1.2 Ultrasound Pretreatment

Wastewater sludge is treated using high-frequency ultrasound to vibrate the sludge and create cavitation bubbles. Upon collapse, these bubbles release a large amount of concentrated energy,

which breaks down the cell walls of microorganisms and releases organic matter inside the cells. Methane production increases as a result of this process, which also improves hydrolysis and increases the availability of substrates for methanogenesis (Zhou et al., 2015).

In addition to pretreatment, another inventive technique to increase biogas production is co-digestion, in addition to pretreatment. Co-digestion is the simultaneous digestion of sludge with additional organic waste, such as agricultural residues, food waste, or industrial byproducts. It increases microbial activity and improves the nutrient balance, resulting in increased biogas yields. Recent research has shown that co-digestion can improve methane production, reduce the addition of external chemicals, and mitigate digestion instability (Nguyen et al., 2021).

Newly developed pretreatment and co-digestion methods have the potential to significantly enhance biogas production in anaerobic sludge digesters. Specifically, methane production was enhanced by pretreatment with ozone and ultrasound prior before hydrolysis. In addition, co-digestion offers an attractive strategy for improving biogas yield through the synergistic properties of various organic substrates. These advances supplement worldwide objectives to improve waste management and renewable energy generation, in the name of the evolution of WWTP's sustainability and efficiency (Nguyen et al., 2021).

1.2 Case study

The main objective of a Wastewater Treatment Plant (WWTP) is to eliminate pollutants and contaminants from sewage wastewater, thereby preventing changes in water quality and protecting the intended uses of water bodies.

Anaerobic digestion is a widely used process for stabilizing primary and secondary sludge. This process, also referred to as methane fermentation or anaerobic sludge stabilization, reduces the organic matter content of the sludge by 40-55%. This is a critical step in the treatment of sludge before drying and incineration, because it optimizes the post-treatment process and reduces costs. Moreover, the biogas produced during this process can serve as an energy source.

This study aimed to examine recent technological advances in promoting biogas generation in anaerobic sludge digesters, including pretreatment and co-digestion methods.

Anaerobic sludge digestion has been a common practice in WWTPs for many years and is recognized as an effective and environmentally sustainable technology for producing energy, such as heat, electricity, and fuel for vehicles. The hydrolysis step is a limiting factor in the anaerobic digestion process, and pretreatment or hydrolysis induction techniques have been investigated to optimize this process. These methods increase methane production through combined processes involving thermal, chemical, biological, physical/mechanical, and the later release of simpler compounds.

2 Objectives

Sludge pre-treatment technologies are most often used to promote the production of methane and biogas. This study aimed to identify the recent advances in pretreatment and co-digestion related to enhancing biogas production from anaerobic sludge digesters. In WWTPs, the anaerobic digestion of sludge has been a standard practice for many years. It is widely recognized as a clean and potentially carbon-neutral method for generating electricity and heat, as well as producing fuels for transportation. Hydrolysis is another limiting step in anaerobic digestion, and pre-treatment or hydrolysis induction techniques have been proposed to improve this process. This methane is produced at high rates by a combined process of thermal, chemical, biological, and physical/mechanical methods and releases simpler compounds later.

This study focused on the following:

- A detailed review of recent anaerobic digestion studies and progress in technology.
- Sludge and Inoculum Characterization (Description of the physical and biochemical properties of sludge and inoculum with potential for methane production).
- Hands on the Biochemical Methane Potential (BMP) Assay with Pretreatment using ultrasound and ozone and the effect of ultrasound and ozone pretreatment on methane.

3 State Of the Art

3.1 Wastewater Treatment in Portugal

Water is a vital natural resource that supports ecosystems and biological activities; therefore, keeping it pure is essential. Sewage, often known as wastewater, is contaminated with human waste and presents health and environmental hazards. Wastewater must be appropriately treated before it is released into the environment to protect public health and ecosystems.

Urban wastewater treatment in Portugal is regulated by the Regulation (ECN no. 1882/2003 and Directive 91/271/EEC, which was revised by Directive 98/15/.EC (POLÍTICAS, 2009) Águas de Trás-os-Montes and Alto Douro, which are a component of the Águas do Norte Group, handle wastewater treatment in Bragança (Tundisi & Matsumura-Tundisi, 2011). Physical and biological treatments are applied during the treatment process to produce residues, such as sludge, sand, and lipids. The Fervença River receives the treated water output. The treatment system consists of three main components: air deodorization, which removes unpleasant odors; solid treatment, which manages and processes the generated sludge; and liquid treatment, which purifies the wastewater before discharge.(Carvalho, 2010; Oliveira, 2017; POLÍTICAS, 2009).

The treatment process includes physical, biological, and tertiary treatments, which generate residues such as solids, sands, fats, and sludge. The treated effluent is then discharged into the Fervença River (Oliveira, 2017).

The treatment process is divided into three main lines:

3.1.1 Liquid Line

Involves preliminary, primary, secondary (biological), and tertiary treatment. Preliminary treatment removes coarse solids and fats; primary treatment removes suspended solids; and secondary treatment uses anoxia and aeration to remove nutrients and organic matter. Tertiary treatments disinfect effluents using chlorine, ozone, or UV radiation (Oliveira, 2017).

3.1.2 Solid Line

Manages sludge with high organic content. Sludge volume is reduced through thickening and anaerobic digestion, in which bacteria break down organic matter into biogas. Sludge is then processed for disposal or recovery (Oliveira, 2017).

3.1.3 Deodorization Line

It focuses on odor control using physical, chemical, or biological methods, such as activated carbon or chemical scrubbers (Oliveira, 2017).

The primary goal of wastewater treatment plants (WWTPs) is to remove contaminants from sewage and maintain the water quality for intended purposes. This goal was addressed in the issue statement. An essential stage before additional treatments, such as drying and incineration, anaerobic digestion dramatically lowers the organic matter content of primary and secondary sludge, thus reducing post-treatment costs (Li et al., 2024). In addition, this process generates biogas, which is used as an energy source. This study examined pretreatment and co-digestion techniques and new technological developments aimed at improving biogas production in anaerobic sludge digesters. Anaerobic sludge digestion is a recognized technique for producing energy that is both efficient and sustainable.

3.2 Pretreatment Technologies for Enhanced Biogas Production

Anaerobic digestion efficiency can be increased using pretreatment techniques, which accelerate the breakdown of complex organic matter and produce more methane.

3.2.1 Thermal Pretreatment

Sludge is preheated to a high temperature (usually 150 – 200 °C) to decompose complex organic molecules and increase their accessibility to microorganisms for digestion. It has been demonstrated that thermal hydrolysis increases biogas output while decreasing sludge volume and enhancing dewaterability (Bougrier et al., 2008).

3.2.2 Ultrasound Pretreatment

Greater methane production results from the disruption of cell walls and improved solubilization of sludge caused by the ultrasound waves. It has been demonstrated that this technique works well for increasing sludge's biochemical methane potential (BMP) (Li et al., 2024).

3.2.3 Ozone Pretreatment

Ozonation increases the biodegradability of organic matter by oxidizing and breaking down complex molecules. It works especially well to break down waste-activated sludge (WAS), which increases biogas yield (Weemaes et al., 2000).

3.2.4 Physical/Mechanical Pretreatment

These methods include high-pressure homogenization and mechanical disintegration, which improve sludge solubilization by breaking down the cell walls and complex organic matter (Tyagi & Lo, 2011). Wastewater sludge is generated as a byproduct of wastewater treatment in treatment plants. It consists of residual semi-solid material that remains after the wastewater has been treated and the water has been removed.

3.3 Stages of Sludge Generation

3.3.1 Preliminary Treatment

Screening: Coarse solids, such as plastics, rags, and other large debris, were removed from the raw wastewater. Waste from this stage is usually sent to landfills or incinerated.

Grit Removal: Sand, gravel, and other heavy inorganic materials were separated. This reduces wear and tear of the equipment and prevents blockage (Carlsson et al., 2012).

3.3.2 Primary Treatment

Sedimentation: Wastewater is held in sedimentation tanks, allowing heavier solids to settle at the bottom. This settled material forms the **primary sludge**, which is rich in organic matter (Neumann et al., 2016).

3.3.3 Secondary (Biological) Treatment

Biological Processes: Microorganisms in aeration tanks break down the organic materials in wastewater. Secondary sludge is formed when surplus microorganisms and biomass settle in secondary clarifiers. This sludge is frequently mixed with primary sludge for additional processing because it usually has a higher water content (Neumann et al., 2016).

3.3.4 Tertiary Treatment (Optional)

In some cases, additional treatment is used to remove pollutants and nutrients, which can result in the production of more sludge or other byproducts (Neumann et al., 2016).

3.4 Sludge Thickening and Dehydration

Thickened sludge from the primary and secondary treatments was used to reduce the water content of the mixture. This procedure produces a more manageable and concentrated sludge (Carlsson et al., 2012).

3.5 Anaerobic Digestion (Optional)

Thickened sludge can undergo anaerobic digestion, where bacteria break down the organic matter, reducing the volume of sludge and producing biogas (methane). This digested sludge is often referred to as **biosolid** (Nguyen et al., 2021).

3.6 Final Disposal or Recovery

The final sludge product can be treated further, dried, used in agricultural applications, incinerated, or disposed of in landfills (Nguyen et al., 2021).

3.7 The Main Factors Influencing Sludge Generation

The quantity and properties of the sludge are influenced by the type of wastewater (domestic, industrial, or combined). The volume and composition of sludge can be affected by various treatment technologies and the effectiveness of these procedures. The operating parameters of a treatment plant, including the temperature, pH, and retention duration, can affect the amount of sludge produced. Because of the volume generated and the need to reduce its environmental impact through safe disposal or beneficial reuse, sludge management is an essential component of wastewater treatment.

Co-Digestion: Boosting Biogas Yield

Co-digestion is an additional biogas production strategy that involves combining sludge with other organic substrates such as food waste or agricultural residues. Co-digestion can boost methane yields and increase overall digestion efficiency by adding substrates with a higher organic content or distinct qualities (Li et al., 2024).

3.8 Anaerobic Digestion

Anaerobic digestion (AD) is the process by which microorganisms break down the organic components of any material into a gaseous mixture (such as CH₄, CO₂, H₂, H₂S, etc.) in the absence of oxygen. This breakdown occurred through a series of biochemical events. For some bacterial species involved in this process to thrive, the environment must be anaerobic (oxygen-free). AD typically occurs in closed spaces (Meegoda et al., 2018). The generated biogas was placed in a

temporary storage before being utilized for several purposes. The primary commercial applications of biogas are the generation of electricity and heat. Digestate is used to describe organic matter and the remaining sediments in the vessel after AD, and can be divided into liquid and solid components. Both can be used as fertilizers in agricultural settings and can provide important nutrients for plants (Meegoda et al., 2018).

AD occurs in several steps and involves intricate interactions with several microorganisms. These microbial communities work together to break down the complex biomass polymers at different stages, resulting in a gaseous mixture. The four main stages of AD biochemical reactions are hydrolysis, acidogenesis, acetogenesis, and methanogenesis (Figure 1). Various bacterial groups exhibit varying degrees of activity at each stage, and the products of each stage are utilized as inputs for subsequent phases (Meegoda et al., 2018).

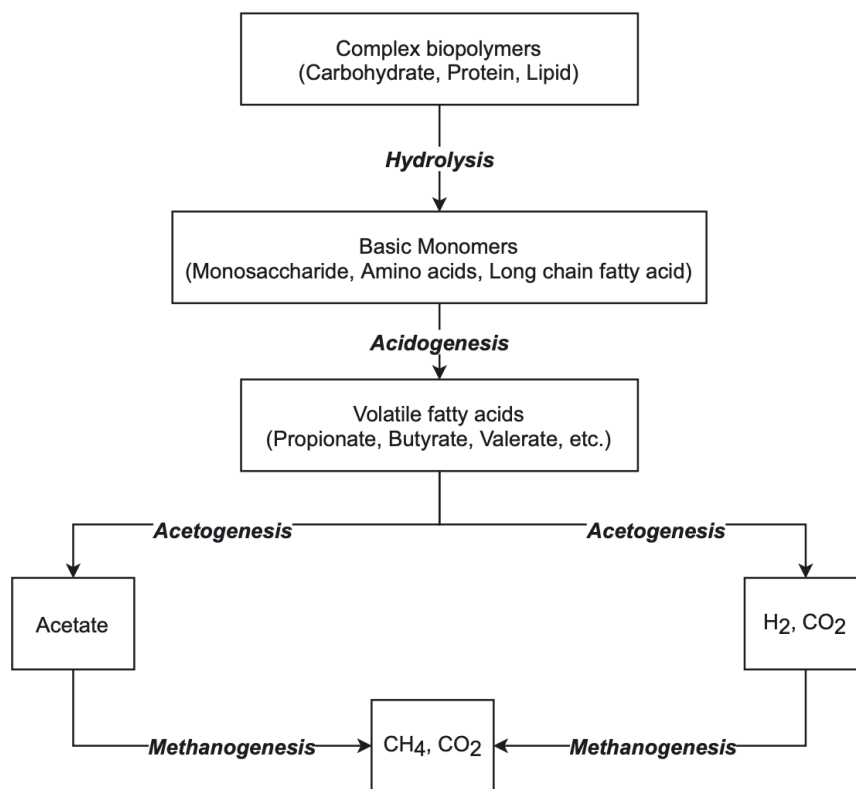
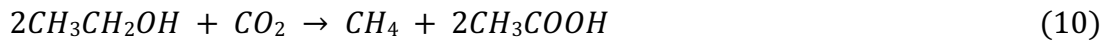
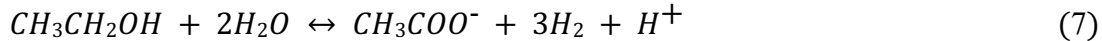
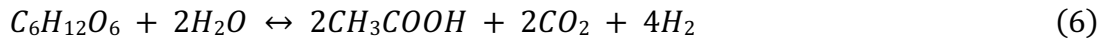
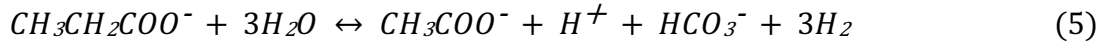
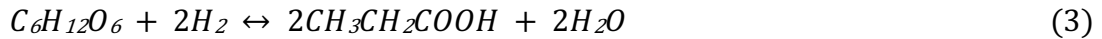
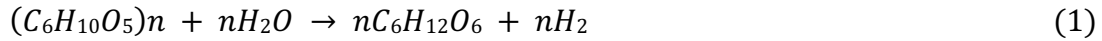


Figure 1: Anaerobic digestion (AD) biomass decomposition stages (hydrolysis, acidogenesis, acetogenesis, and methanogenesis) and key compounds.

The digestive process consists of several phases, the first of which is hydrolysis, in which water and extracellular enzymes break down complex polymers, such as cellulose and starch, into simpler components (glucose and amino acids). The process by which acidogenic bacteria further degrade hydrolysis products into volatile fatty acids and alcohols is known as acidogenesis. At the next stage, methanogens can readily use some of these products. Acetogenesis then converts these products into acetate, CO₂, H₂, and a few long-chain fatty acids, with the help of acetogenic bacteria. To sustain thermodynamic feasibility at this stage, bacteria need to participate in a mutualistic relationship in which they consume each other's waste products (Al Seadi et al., 2013).

Methane is produced during the final stage, known as methanogenesis, when all intermediate products from the previous phases combine. This stage is strictly anaerobic, because methanogenic bacteria cannot thrive in the presence of oxygen. Two distinct bacterial species, acidophilic and hydrogenophilic, convert acetate (CH_3COOH) and hydrogen (H_2) into carbon dioxide (CO_2) and methane (CH_4). Acidophilic bacteria convert acetate to CH_4 and CO_2 , whereas hydrogenophilic bacteria convert H_2 and CO_2 to CH_4 (Meegoda et al., 2018). The chemical reactions defining this level are depicted in Equations 1–10 (Junior et al., 2021).



3.9 Influence of Operational Parameters on Methane Production and Anaerobic Digestion Efficiency

Several operational and environmental factors play a crucial role in determining the efficiency of anaerobic digestion (AD) and the amount of methane produced. These parameters influence microbial activity, the stability of the digestion environment, and the overall conversion of organic matter into biogas. Key variables include substrate composition, which determines the carbon-to-nitrogen (C/N) ratio and biodegradability of the feedstock, as well as temperature, which affects microbial growth rates and enzymatic reactions. Additionally, pH, moisture content, and agitation help maintain optimal metabolic conditions for methanogenic bacteria.

Operational controls such as organic loading rate (OLR), hydraulic retention time (HRT), and pretreatment methods significantly impact process stability and methane yield. Imbalances can lead to the accumulation of inhibitory compounds, such as volatile fatty acids (VFAs), or the suppression of sensitive microbial communities. By properly managing these parameters, AD systems can operate at higher efficiency, maintain process stability, and enhance overall biogas production.

The main elements influencing methane generation and the anaerobic digestion process are illustrated in Figure 2 (Meegoda et al., 2018).

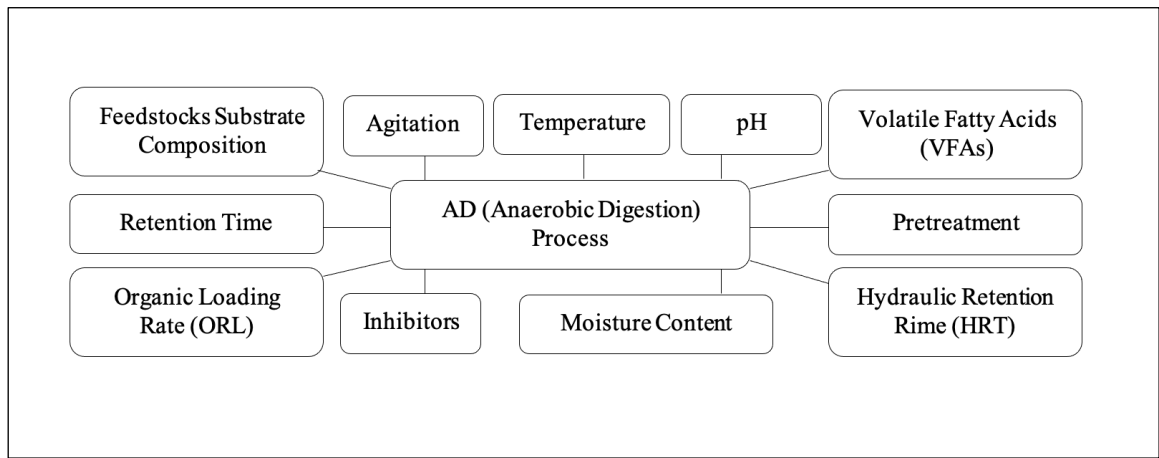


Figure 2: Main factors and interactions influencing methane generation and the performance of the anaerobic digestion process.

3.9.1 Temperature

- Mesophilic (30 – 40 °C) and thermophilic (50 – 60 °C) conditions: The rates of digestion and microbial activity are significantly influenced by temperature. Although thermophilic digestion requires more energy, it can accelerate the breakdown of organic matter and increase methane production in mesophilic conditions, which are very common (Li et al., 2011).
- Temperature variation: Temperature variations have the potential to decrease efficiency and slow down the activity of microorganisms (Angelidaki & Ahring, 1994).

3.9.2 pH

- **Optimum pH range (6.5 – 7.5)** (Ripley et al., 1986): Methanogenic microbes are pH-sensitive. Methane can be produced under highly alkaline or acidic conditions by altering the microbial activity. Maintaining the pH requires buffering or adjusting the raw materials (Amani et al., 2010).

3.9.3 Hydraulic Retention Time (HRT)

- Impact on digestion time: HRT is the duration of the substrate residence in the digester. A longer hydraulic retention time (HRT) may reduce the nutrient processing capacity of the system, while enhancing substrate digestibility and promoting higher methane production. A brief HRT decreases bioavailability and inhibits digestion (Neves et al., 2008).

3.9.4 Organic Loading Rate (OLR)

- Bed Feed: The amount of organic material fed into the digester is indicated by the OLR. To sustain microbial activity, the optimal OLR maintains a balance in the supply of organic matter.

Excess OLR can cause acidosis, dysfunction, and death of microorganisms ([Angelidaki et al., 2003](#); [Rajagopal et al., 2013](#)).

3.9.5 Organic composition

- **Carbon to nitrogen (C/N):** For optimal digestion, a balanced C/N ratio, typically between 20:1 and 30:1, is essential. While too much nitrogen can be toxic, too little nitrogen inhibits microbial growth.
- **Organic matter:** Biomass production increases with the amount of organic matter in the bed. Methane emissions can be enhanced by digestion with various substances such as sewage and food waste ([Qiuyuan et al., 2023](#)).

3.9.6 Volatile fatty acids (VFAs)

Monitoring VFA levels ensures that they do not exceed toxic thresholds, and that methane production continues ([Demirel & Scherer, 2008](#); [Liu et al., 2012](#)).

3.9.7 Mixing/Stirring

- **Distribution of substrate and microorganism:** Mixing prevents the formation of sludge layers, distributes nutrients evenly, and maintains temperature in the digester. Poor mixing reduces the digestion efficiency and methane production ([Karim et al., 2005](#)).

3.9.8 Toxicity/disinfection

- **Ammonia and Sulphur:** High levels of ammonia, heavy metals, or sulfur in the substrate can inhibit microbial activity and reduce methane production. Ammonia toxicity is commonly observed when protein-based ingredients are used ([Chen et al., 2008](#)).

3.9.9 Retention Time

- **Solid retention time (SRT):** Methane production and sludge digestion were enhanced by longer SRTs. Methane production was negatively affected by decreased SRT, and biomass potential was lost ([Bolzonella et al., 2005](#)).

3.9.10 Moisture

Access of microbes to water: While moisture is necessary for microbial activity, too much moisture can dilute the substrate and decrease the amount of available organic matter to produce methane. Maximum relative humidity promotes microbial decomposition ([Riffat et al., 1999](#)).

By controlling these parameters, the efficiency of AD (hence methane production) can be enhanced, leading to an increase in biomass yield and sound waste management practices.

AD can handle a range of feedstock types from various sources. In practice, virtually any biodegradable organic material can be anaerobically digested to produce methane gas. In principle, any biodegradable organic matter can be anaerobically digested to produce biogas, such as AD feedstock from different sources. Feedstock for AD should be readily biodegradable and free of any toxic components that would impact bacteria. Some feedstocks require pre-treatment to enhance biodegradability. Multiple feedstocks can be mixed and digested, but some feedstock combinations can degrade performance and even halt the AD process.

In this study, it will focus on the pretreatment to enhance the hydrolysis step—which is a limiting factor in the anaerobic digestion process—pretreatment or hydrolysis induction techniques will be studied. These methods enhance methane production by utilizing a combination of thermal, physical/mechanical, chemical, and biological processes and the release of simpler compounds in subsequent stages.

Wastewater treatment, particularly in industrial contexts, is critical for reducing environmental impacts and ensuring water reuse. Pretreatment processes are vital for enhancing the efficiency of subsequent treatment steps. Recent research has focused on improving these pretreatment technologies, particularly physical/mechanical processes and ultrasound and ozone applications. An overview of the latest advancements in this area is presented.

3.10 Physical/Mechanical Pretreatment Processes

These processes serve as the first line of defense in wastewater treatment with the aim of removing large particles and debris, reducing solids, and protecting downstream treatment units. The common techniques include screening, grit removal, and filtration.

Recent research and developments in physical/mechanical pretreatment processes, such as advanced screening technology, are contemporary screening devices that enhance the effectiveness of suspended solid removal by handling higher flow rates with smaller mesh sizes. These developments have reduced the strain on biological treatment systems. Improved grit chambers are a type of grit removal system developed to better capture finer particles. This reduces the wear on equipment and guarantees a more efficient operation of chemical and biological processes downstream. Additionally, to improve the particle removal efficiency, dynamic filtration systems, such as membrane filtration systems and continuous backwash filters, are being investigated. Membrane bioreactors that integrate biological processes with filtration have become more popular because of their efficient purification methods and compact design (and Eddy et al., 2002).

3.10.1 Ultrasound in Wastewater Pre-treatment

Ultrasound (US) has emerged as an innovative technique for enhancing wastewater treatment processes. The application of high-frequency sound waves (ultrasound) induces cavitation, which disrupts solid particles, breaks down complex compounds, and enhances biological and chemical treatment efficiencies, as illustrated in Figure 3 (Zhao & Baik, 2012).

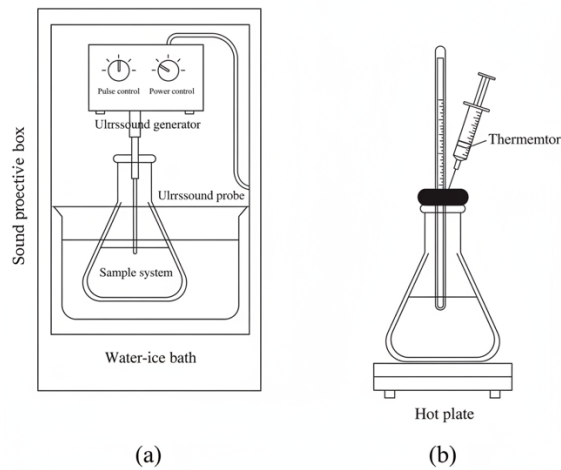


Figure 3: Ultrasound pretreatment process.

Previous research on the application of ultrasound as a pretreatment method in wastewater treatment has primarily focused on enhancing sludge disintegration. Ultrasound disrupts cellular structures within the sludge, which improves its biodegradability and consequently reduces sludge volume. Studies have demonstrated that integrating ultrasound pre-treatment into anaerobic digestion processes can increase methane production by 30 to 50% (Nickel, 2000).

Microbial Cell Disruption: microbial cells in wastewater are broken up by the cavitation effect of ultrasonic waves, which facilitates the release of intracellular components. This increases the amount of organic matter that can be broken down, thereby increasing the efficiency of biological processes (Pilli et al., 2011).

Emerging Contaminants: studies have concentrated on the use of ultrasonography to degrade microplastics, medications, and other newly discovered pollutants in wastewater. Research has indicated that ultrasonic waves can break down intricate organic pollutants, thereby increasing their accessibility for further treatment procedures (Pilli et al., 2011).

Sludge was pretreated with ultrasonic waves, which were subjected to continuous compression and decompression cycles. Cavitation occurs when this process produces microbubbles that collapse violently. Extreme conditions are created by collapse, with pressures above 500 bar and temperatures as high as 5000 K (Braguglia et al., 2011). This releases shear forces that break down the sludge flocs, cell walls, and membranes, thereby enhancing the hydrolysis of volatile solids.

Ultrasound improves anaerobic digestion by increasing the availability of macromolecules, such as proteins and carbohydrates, and is used to improve sludge dehydration. The process involves several steps: hydromechanical shear forces, formation of radicals (e.g., $\bullet\text{OH}$, $\bullet\text{O}$, $\bullet\text{H}$), thermal decomposition of volatile substances, and temperature increase (Neumann et al., 2016).

The efficiency of ultrasonic disintegration depends on factors such as the sludge solid content and the specific energy applied. Low frequencies are effective for increasing methane yield due to the release of macromolecular components during anaerobic digestion.

Particularly in Europe, ultrasonic pretreatment has been thoroughly investigated in lab, pilot, and full-scale experiments. Several commercial products for biogas production are currently available in the market. The method works best with secondary sludge and has very short retention times, but to be practical, biogas generation must balance out the high energy consumption of the process (Ruiz-Hernando et al., 2013).

This study focused on the ultrasonic pretreatment of wastewater sludge and its impact on biogas production and the anaerobic digestion process.

3.10.2 Ozone in Wastewater Pretreatment

Ozone (O_3) is a powerful oxidizing agent that has been increasingly used in wastewater pretreatment. Its high oxidation potential makes it highly effective for breaking down organic pollutants, pathogens, and even certain heavy metals.

Recent research has highlighted the following points:

- **Advanced Oxidation Processes (AOPs):** These treatments, which produce hydroxyl radicals ($\cdot OH$), are created when ozone is mixed with other substances such as UV light or hydrogen peroxide. These radicals have even greater oxidizing power than ozone. Research has demonstrated that AOPs can dramatically reduce refractory organic substances, medications, and colorants, which do not respond well to conventional methods (Von Gunten, 2003).
- **Pathogen Inactivation:** A broad variety of pathogens, including bacteria, viruses, and protozoa, can be rendered inactive by ozone. It is being researched as a potential substitute for chlorine-based disinfection methods, which can result in toxic disinfection byproducts (DBPs) (Esplugas et al., 2007).
- **COD and BOD Reduction:** It has been demonstrated that ozone oxidation reduces the Biological and Chemical Oxygen Demands of wastewater (BOD and COD), enhancing the efficiency of secondary and tertiary treatment procedures. Studies have indicated that the application of ozone as a pretreatment can eliminate up to 70 – 90% of the COD from wastewater (Bakhshi et al., 2018).

Ozonation

Ozone, a gas with high oxidation potential, is used to pretreat sludge for the partial oxidation and hydrolysis of biodegradable organic matter, enhancing biogas production, as shown in Figures 4 and 5 as it illustrate in (Hammadi et al., 2016). The ozonation process involves sequential reactions that rupture sludge flocs, solubilize organic materials, and oxidize released compounds. The efficiency of this process depends on ozone dosage, mass transfer, and reaction kinetics. However, excessive ozone can lead to over-mineralization and reduced methane production. The ideal ozone dose ranges from 0.05 to 0.5 g O_3 g⁻¹ TS, depending on sludge characteristics (Zhen et al., 2017).

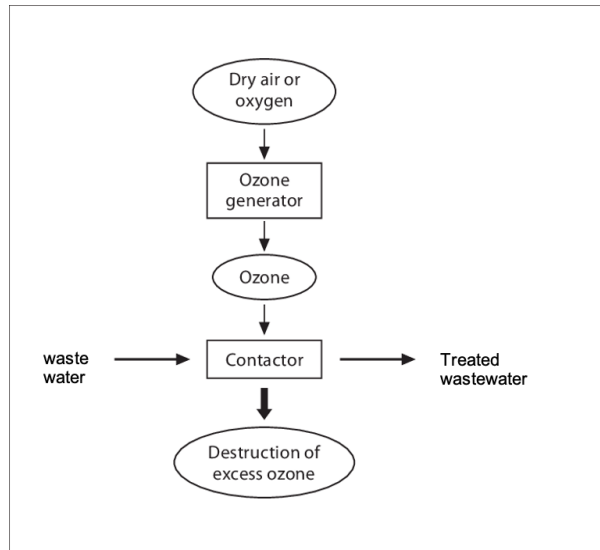


Figure 4: Ozonation pretreatment process.

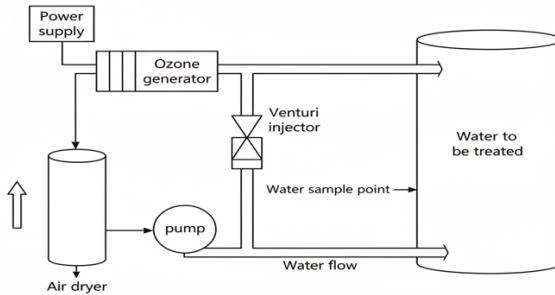


Figure 5: Ozone wastewater application diagram.

Ozonation is effective in disintegrating sludge and increasing methane production, but it is energy-intensive. The commercials are available, offering significant sludge reduction and enhanced dewaterability. Ozone also oxidizes most organic and inorganic compounds, releasing intracellular materials and nutrients like phosphorus and nitrogen (Tyagi & Lo, 2011).

Although numerous reports exist on ozone, only a few studies have been conducted on microwave-assisted ozone technology. The combined treatment improved sludge biodegradability and the release of nutrients, particularly phosphorus. Several studies have shown that the combination of ozonation and microwave methods with acidic (H_2SO_4) and alkaline pretreatment significantly increases not only sludge solubilization but also enhances the efficiency of phosphorus recovery. For five minutes treatment, as shown in Figure 6 (Junior et al., 2021). For example, 579% more

phosphorus was released when acid pretreatment was followed by ozonation and microwave treatment (Tyagi & Lo, 2011; Zhen et al., 2017).

The purpose of this study was to determine how ozonation, a pretreatment of wastewater sludge, affects biogas production during anaerobic digestion.

Integrated Pretreatment Approach

- **Ultrasound and Ozone Combination:** As alternative to standalone ultrasound or ozonation, few studies have reported the use of ultrasound combined with ozone in pretreatment systems. The combination of both techniques shows a synergistic effect and improves the degradation of complex compounds such as persistent organic pollutants and pharmaceutical residues. The combination of these techniques significantly increases the rate of contaminant degradation for each technique (Bakhshi et al., 2018).
- **Hybrid physical and chemical pretreatment:** New research focuses on integrating physical/mechanical processes with chemical treatments, such as ozone or ultrasound. For instance, coupling fine screening or filtration with ozone treatment improves the removal of delicate particulate matter and enhances the oxidation efficiency (Wang & Xu, 2012).

Integrating advanced physical/mechanical processes with innovative technologies, such as ultrasound and ozone, shows great promise for improving wastewater pretreatment. Ongoing research is geared towards making these methods more energy-efficient, cost-effective, and capable of handling the increasingly complex nature of modern wastewater streams. As these technologies continue to develop, they are expected to play an essential role in sustainable wastewater management.

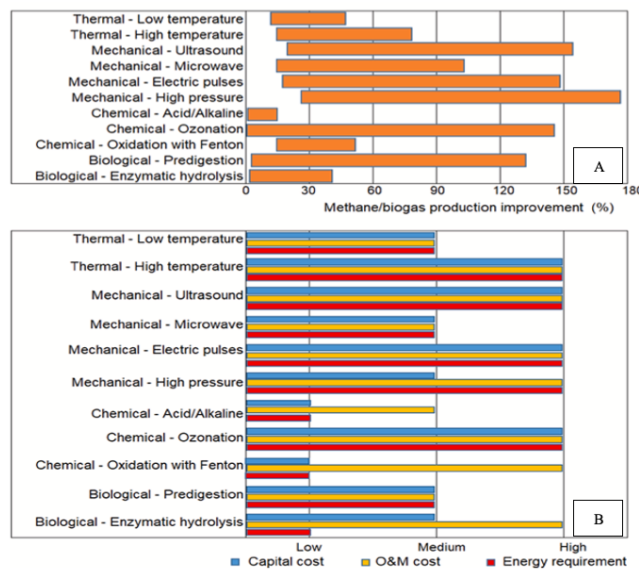


Figure 6: Comparison of increase in biogas/ methane production (A), capital cost, O&M (operation and maintenance) costs, and energy requirement (B) of sewage sludge pretreatment methods.

Pretreatment with ozone has a high oxidizing potential. The potent oxidation potential of ozone makes it a highly effective decomposer for organic materials. It can increase the release of nutrients such as phosphorus and improve biodegradability by solubilizing and mineralizing sludge

components. The boost biogas production is illustrated in Figure 6. Ozonation significantly boosts the production of methane and biogas, with gains of up to 150% (Junior et al., 2021). Ozone pretreatment is a valuable tool for enhancing anaerobic digestion because it oxidizes and lyses microorganisms, promoting sludge disintegration and improving sedimentation and dewatering. It can reduce sludge volume by up to 80 % and increase methane yield, but its high energy demand and operating costs require careful optimization of ozone dosage to achieve net energy and cost benefits. (Kalogo et al., 2012).

By improving the availability of macromolecules, such as proteins and carbohydrates, for anaerobic digestion, ultrasound pretreatment dramatically increases sludge solubilization and boosts biogas production. With short retention times, ultrasonic pretreatment can increase methane/biogas production by more than 100%, as shown in Figure 6. Ultrasound is a time-efficient technique that requires only a few seconds of retention time to produce noticeable effects (Junior et al., 2021). Ultrasound is a widely studied pretreatment with proven benefits in improving sludge solubilization and methane yield, although its high energy consumption presents a challenge. Studying ultrasound can help to optimize energy efficiency while maximizing biogas production. Both ozone and ultrasound are highly effective in enhancing biogas production. Research on these methods can lead to improved efficiency, cost-effectiveness, and scalability of wastewater treatment processes (Junior et al., 2021; Tyagi & Lo, 2011).

4 Methodology

This study was carried out at the Instituto Politécnico de Bragança from April 2024 . The sludge was collected in April 2024.

Sludge characterisation

The characterisation of sludge (substrate) and inoculum for biogas production can affect the methane yield product due to the presence of organic substances and heavy metals, so the sludge characterisation under analysis is essential. Sludge characterization included the analysis of pH, total solids (TS), volatile solids (VS), carbon content (%), and organic matter (%). The analytical techniques applied to these parameters were based on the Standard Methods for the Examination of Water and Wastewater, 23rd edition (Apha Awwa, 2017).

4.1 Temperature

Temperature was defined as the controlled incubation temperature inside the AMPTS II bioprocess system. The Automatic Methane Potential Test System (AMPTS II) is used to study anaerobic digestion by continuously measuring the volume of biogas, specifically methane, produced during the tests.

4.2 pH

The pH measuring instrument utilized was the HANNA model Edge, which yielded immediate results before and after digestion. Measuring the pH of samples before and after anaerobic digestion is essential for ensuring the efficiency and stability of the digestion process, particularly in biogas production. The main reasons for monitoring the pH and a well-buffered system are as follows:

4.2.1 Optimising Microbial Activity

Anaerobic digestion relies on a group of microorganisms that break down the organic matter. Methanogenic bacteria, responsible for producing methane, thrive in a neutral pH range of approximately 6.5-7.5:

- At **pH < 6.5**, acidogenesis dominates and methane production decreases significantly;
- Ammonia toxicity can occur at a **pH > 8.0**, which also inhibits methanogens.

A well-buffered system helps to maintain a stable pH within the optimal range. Deviations from this range can inhibit their activity, leading to reduced biogas yield (Qaseem et al., 2016).

4.2.2 Detecting Imbalances Early

Monitoring the pH, in conjunction with the ratio of Volatile Fatty Acids (Fosua et al., 2023) to the Total Alkalinity (TAC), provides indicators of potential process imbalances. A low pH suggests acid accumulation, whereas a high pH indicates ammonia inhibition. Therefore, buffering allows pre-adjustments to maintain optimal conditions (Sánchez et al., 2000).

4.2.3 Preventing System Failures

Significant pH fluctuations can lead to system upsets, such as acid crashes or ammonia toxicity, which may necessitate the restarting of the digestion process. Adjusting the pH helps prevent such occurrences by enabling proactive management (Gonde, 2023).

By integrating pH monitoring into the anaerobic digestion process, operational efficiency and safeguarding against potential disruptions can be enhanced.

In this study, the pH was adjusted between 7.2-7.6 to control the optimum conditions for methane production.

4.3 Chemical oxygen demand (COD)

COD was measured using the Standard Method 5220D, and the samples were digested at 150 °C for 2 h in a HANNA HI 839800 COD digester. The samples will be analysed with a UV spectrophotometer (Jasco 530) as shown in Figure 7.

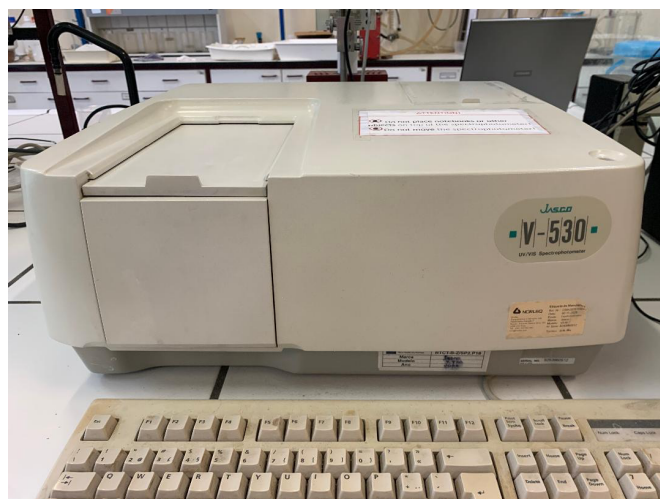


Figure 7: UV-Spectrophotometer JascoV-530.

The Chemical Oxygen Demand (COD) of the wastewater samples was measured using the standard dichromate reflux method. Before analysis, all COD digestion vials (16 mm borosilicate tubes with Teflon-lined caps) were rinsed with 20% H₂SO₄ to remove contaminants. A procedural blank using distilled water was prepared for spectrophotometer calibration. The wastewater sample was homogenized, diluted when necessary, and an aliquot was measured with a Class A volumetric pipette into a 25 mL volumetric flask, filled to the mark, and mixed thoroughly.

For digestion, each vial received 1.5 mL of potassium dichromate digestion solution, 2.5 mL of sample, and 3.5 mL of sulfuric acid reagent. The vials were sealed, gently mixed to control the exothermic reaction, and placed in a COD digestion block at 150 °C for 2 hours. After cooling, the vials were shaken, allowed to settle, and analyzed at 600 nm using a spectrophotometer zeroed with the blank. COD values were calculated from absorbance and expressed as mg O₂ L⁻¹.

Standard Calibration Curve for COD

Table 1 presents the data used to construct the COD calibration curve, and Figure 8 illustrates the corresponding graph.

Table 1: COD Calibration curve (standard COD solution of 1000 mg L⁻¹).

Sample Number	V (Volume) (std to 100 ml)	COD (mg O ₂ L ⁻¹)	Absorbance
1	5	50	0.006
2	10	100	0.0208
3	30	300	0.0822
4	50	500	0.1638
5	70	700	0.1942
6	90	900	0.2490
7	100	1000	0.2856

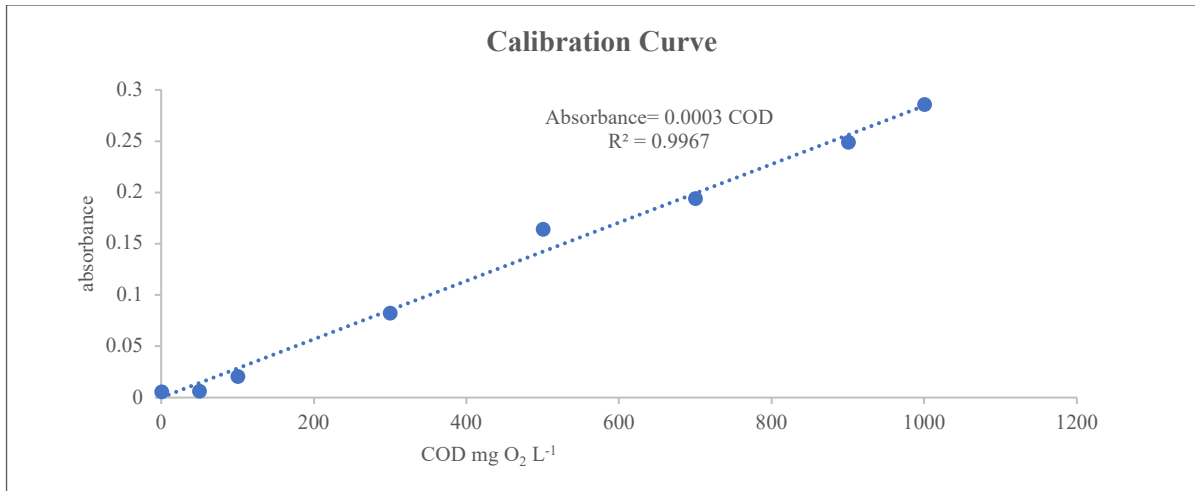


Figure 8: COD calibration curve.

The figure presents a linear chemical oxygen demand (COD) calibration curve, evidencing a strong coefficient of determination $R^2=0.9967$, which indicates excellent linearity between absorbance and COD concentration over the tested range.

4.4 Biological oxygen demand (BOD)

To assess the anaerobic biodegradability of the wastewater samples using OxiTop®-OC 100, as shown in Figure 9, the system was set for a 5-day incubation period.

- a) **Sample Preparation:**
 - Each sample bottle was filled with 250 mL of the wastewater sample at a certain volume, according to the manual.
- b) **Incubation:**
 - The setup was placed in a thermostatic cabinet or an incubator set at 20 ± 1 °C.
 - The system was operated continuously for five days.
- c) **Data Collection and Analysis:**
 - The OxiTop meter records pressure changes over time, reflecting oxygen consumption.
 - Data were analyzed to determine BOD, expressed in mg O₂ consumed per liter per day.



Figure 9: OxiTop®-OC 100 (3BOD analyser with the incubator).

4.5 Volatile solid (VS)

The procedure is introduced in the manual Standard Procedures for the Examination of Water & Wastewater (Apha Awwa, 2017), and the calculation is applied according to Equation 11.

$$VS (mgL^{-1}) = \frac{(m_1 - m_2) \cdot 1000}{V} \quad (11)$$

Where

m_1 = weight of residue + dish or filter after ignition, mg

m_2 = weight of (filter + dried residue) + dish before ignition, mg

V = sample volume, mL

4.6 Total Solids (TS)

The total solids were determined using the 2540 B Method and dried at 103–105 °C. The procedure was performed according to the Standard Procedures for the Examination of Water & Wastewater (Apha Awwa, 2017), and the concentration was determined by Equation 12.

$$TS (mgL^{-1}) = \frac{(m_1 - m_0) \cdot 1000}{V} \quad (12)$$

Where

m_1 = weight of dried residue + dish, mg

m_0 = weight of dish, mg

V = sample volume, mL

4.7 Volatile fatty acid:

4.7.1 Determination of Volatile Fatty Acids (VFAs) by The Titration Method

The titration method for determining volatile fatty acids (VFAs) in samples such as digestates or wastewater is based on the neutralization of organic acids with a strong base. This is a simple and widely used procedure in anaerobic digestion analysis to monitor the process stability.

4.7.2 Principle

The volatile fatty acids, primarily acetic, propionic, and butyric acids, present in the samples were titrated with a standard sodium hydroxide (NaOH) solution. The titration was performed after adjusting the pH of the sample to eliminate interference from carbonates and bicarbonates.

4.7.3 Procedure

a) **Sample Preparation:**

- The sample was filtered, if necessary, to remove suspended solids that may interfere with the analysis.
- The filtered sample (50 mL) was pipetted into an Erlenmeyer flask.

b) **Acidification:**

Add 1 mL of sulfuric acid (H₂SO₄, 1 N) to the sample to lower the pH below 2.0, converting carbonates and bicarbonates into carbon dioxide (CO₂), which can be released by gentle stirring.

c) **Neutralization:**

After acidification, the pH was adjusted to approximately 7.0, using 0.1 N NaOH.

d) **Titration:**

- Two to three drops of phenolphthalein were added as an indicator.
- Titrate the solution with 0.1 N NaOH until a light pink color appears, which indicates the endpoint.

e) **Calculation:**

- The volume of NaOH (Moharir et al.) used in the titration was recorded.
- The VFA concentration was calculated based on the volume of NaOH used.

The VFA concentration is expressed as mg of acetic acid per liter (mg HAcL⁻¹) and can be calculated using Equation 13:

$$VFAs = \frac{V_{NaOH} \times N_{NaOH} \times 60 \times 1000}{V_{sample}} \quad (13)$$

Where:

- V_{NaOH} = Volume of NaOH used in titration units
- N_{NaOH} = Normality of the NaOH solution (eqL^{-1}).
- V_{sample} = Volume of sample titrate units.
- 60 is the equivalent weight of acetic acid (the reference VFA), in mg per milliequivalent, used to express VFAs as mg acetic acid per liter.

4.8 Pretreatment

4.8.1 Ultrasound

The pre-treatment of the wastewater sludge (substrate) is planned to be connected with an ultrasound generator for a certain time, as shown in Figure 10, to study the effect of ultrasound pretreatment on the anaerobic digestion process and biogas production yield.

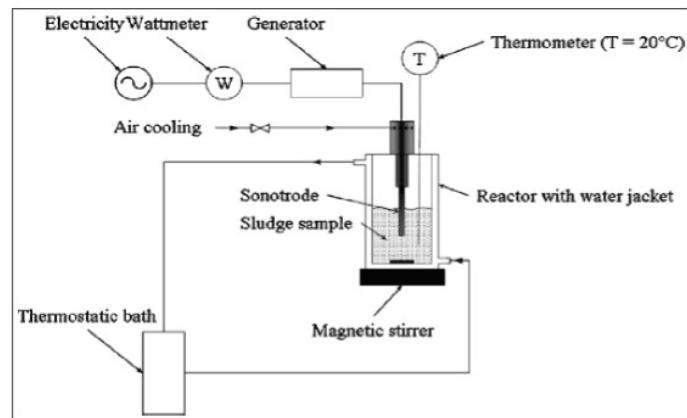


Figure 10 : Ultrasonic set-up.

Although ultrasound pretreatment was intended for working on it, ozone pretreatment was the sole method used due to testing and scheduling conflicts. Ultrasound pre-treatment will be the focus of future work.

4.8.2 Ozonation

An ozone generator was employed for sludge pretreatment prior to anaerobic digestion (Figure 11). Ozone was applied at a specific concentration to evaluate its effect on the anaerobic digestion process and biogas production yield.

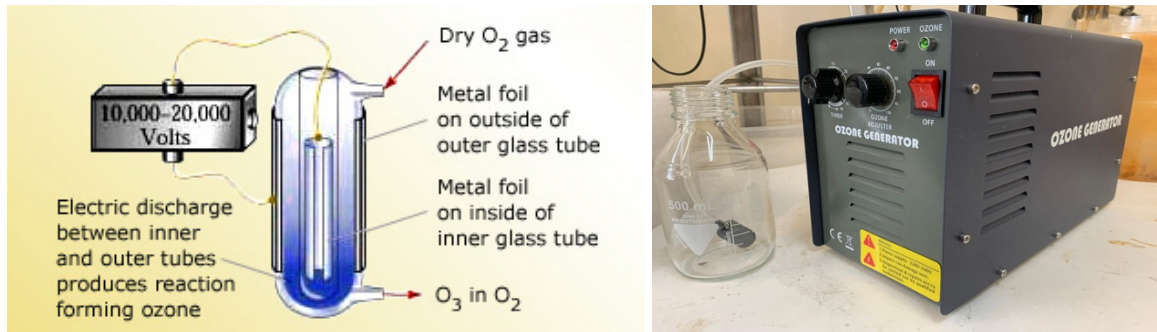


Figure 11: Concept of ozone synthesis and the ozone generator used in the experiment.

5 Materials and Methods

5.1 Study Site and Experimental Overview

The study was carried out in Bragança, Portugal, at the Instituto Politécnico de Bragança, which is located in Bragança, to study the effect of ozone pretreatment on the performance of the anaerobic digestion (AD) system in sludge from a wastewater treatment plant. A set of batch-mode biochemical methane potential (BMP) tests was performed under mesophilic conditions (35 ± 2 °C) using the Automated Methane Potential Test System (AMPTS II) provided by Bioprocess Control. AMPTS II possesses components such as a digester unit, CO₂ absorption bottle, and volumetric gas measurement unit, which help in the accurate monitoring and quantification of biogas production throughout the experiment. The experimental setup and components of the AMPTS II system are illustrated in Fig. 12.



Figure 12: The AMPTS II system by Bioprocess Control. a) a digester unit, a CO₂ absorption bottle, and a volumetric gas measurement unit; b) bioprocess control software.

5.2 Substrate and Inoculum Collection:

This work relied on the Porto Wastewater Treatment Plant (WWTP)(ETAR Gaia litoral_ lama digerida) as the source of municipal wastewater sludge used as a substrate, a facility with a long-track record of treating urban sewage. The inoculum was obtained from a local treatment plant with anaerobic digesters that were operated under stable conditions. Both the substrate and inoculum were carefully analyzed before the experiments to determine the physicochemical parameters essential for optimizing the anaerobic digestion (AD) process. These parameters included total solids (TS), volatile solids (VS), chemical oxygen demand (COD), biochemical oxygen demand (BOD), volatile fatty acids (VFA), and pH. The elemental composition (C, H, O, N, and S) of the substrate was derived from typical values reported in the literature for municipal wastewater sludge (Sichler et al., 2022). Table 2 provides a comprehensive summary of the physicochemical properties of wastewater sludge used in this study.

Table 2: Physicochemical characteristics of wastewater sludge used for anaerobic digestion.

Parameter	Value	Unit	Note/Source
COD	1130.33	mg O ₂ L ⁻¹	Average from 50 mL dilution sample
BOD	3840	mg O ₂ L ⁻¹	After analysis for 22.5 mL sample
BOD/COD Ratio	≈ 3.4	-	Indicates highly biodegradable substrate
VS (Volatile Solids)	16.8472	% (dry weight basis)	After analysis
TS (Total Solids)	19.6818	%	After analysis
VFA (Volatile Fatty Acids)	9000	mg L ⁻¹ (as acetic acid)	Based on NaOH titration (75 mL)
C (Carbon)	50%	% (dry weight)	Based on literature for municipal sludge (Sichler et al., 2022)
H (Hydrogen)	6.7%	%	From literature (Sichler et al., 2022)
O (Oxygen)	31.6%	%	From literature (Sichler et al., 2022)
N (Nitrogen)	7.1%	%	From literature(Sichler et al., 2022)
S (Sulfur)	~0.6%	%	From literature(Sichler et al., 2022)
Theoretical Methane Yield	≈ 517	mL CH ₄ g ⁻¹ VS	Calculated with Buswell & Mueller including sulfur(Buswell & Mueller, 1952)

5.3 Sludge Characterization

To ensure accurate and reliable results, the wastewater sludge was characterized using the Standard Methods for the Examination of Water and Wastewater (Apha Awwa, 2005, 2017). Standardized analytical methods were used to ensure reliable evaluation of anaerobic digestion performance. Total solids (TS) and volatile solids (VS) were determined according to Method 2540B, while chemical oxygen demand (COD) was measured using Method 5220D with a HANNA HI 839800 reactor and JASCO V-530 spectrophotometer. The pH of each sample was continuously monitored with a HANNA Edge digital pH meter, and volatile fatty acids (VFAs) were quantified by alkaline titration with NaOH, including pH measurements after 45 days to assess intermediate acid

accumulation. Together, these measurements provided comprehensive monitoring of key physicochemical parameters governing biogas production. (Apha Awwa, 2005, 2017).

5.4 Ozone Pretreatment Procedure

The ozone pretreatment of wastewater sludge was conducted using a custom-built ozone generator. The sludge samples were exposed to ozone at concentrations of 0, 5, and 10% with ozone contact times of 30, 60, and 90 s. Ozone was chosen as the pretreatment agent because of its strong oxidative potential, which facilitates the disruption of cell walls and the solubilization of complex organic matter. The goal of ozone pretreatment was to enhance the biodegradability of the sludge and improve the subsequent methane yield during anaerobic digestion. Following pretreatment, ozone-treated sludge samples were used in anaerobic batch digestion trials to assess the impact of ozone exposure on the digestion process.

5.5 Experimental Design for Anaerobic Digestion

Anaerobic digestion was conducted in 500 mL reactors, each with a working volume of 400 mL and 100 mL headspace. Three different inoculum-to-substrate (I/S) ratios were tested: 1.0, 1.5, and 2.0 (wet weight basis). Before sealing, nitrogen gas was purged to establish anaerobic conditions. After sealing, the reactors were incubated at 35 ± 2 °C for 45 days. The CO₂ generated was absorbed by a 3M NaOH solution in the scrubbing unit, and the volume of methane produced was continuously monitored and recorded under standard temperature and pressure (STP) conditions. The AMPTS II system provides real-time measurements of the methane production.

5.6 Nutrient Supplementation

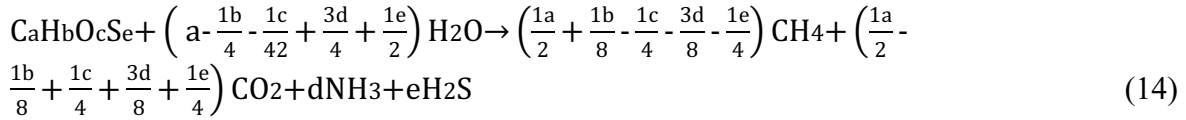
To ensure adequate microbial activity during anaerobic digestion, essential micronutrients and trace elements were added to the reactors following a modified nutrient composition from prior studies. Nutrient solution was added to each reactor in experiment (2) to maintain optimal conditions for microbial growth and methane production. The detailed composition of nutrient supplementation is outlined in Table 3.

Table 3: Nutrient supplementation for anaerobic digestion (Hu, 2013).

Solution	Dosage vials (ml)	Constituents	Mass (mg/350 mL)
Micronutrient	1.2	MgSO ₄ .7H ₂ O	18.9
Trace element	0.12	FeSO ₄ .7H ₂ O	522.8
	0.12	CoCl ₂ .6H ₂ O	0.42
	0.12	ZnCl ₂	10.5
	0.12	NiCl ₂ .6H ₂ O	0.0105
	0.12	EDTA	0.21
	0.12	CuSO ₄	5.9

5.7 Theoretical Methane Potential (TBMP)

The theoretical methane potential (TBMP) was calculated using the empirical Buswell and Mueller equation, which is based on the elemental composition of the substrate (C, H, O, N, S). The molecular formula for the sludge was derived as $C_{223}H_{356}O_{106}N_{27}S$, leading to an estimated theoretical methane potential of approximately 517 mL CH_4 gVS^{-1} . The Buswell and Mueller equation 14 (Buswell & Mueller, 1952) for the anaerobic digestion of organic matter is:



$$TBMP \text{ (ml } CH_4 \text{ g}^{-1} \text{ VS)} = \frac{22.4 * \left(\frac{a}{2} + \frac{b}{8} - \frac{c}{4} - \frac{3d}{8} - \frac{e}{4} \right)}{12.017a + 1.0079b + 15.999c + 14.9967d + 32.065e} \quad (15)$$

$$a = \frac{a_{ultimass}}{mmc} = \frac{a_{ultimass}}{12.0107} \quad (16)$$

$$b = \frac{b_{ultimass}}{mmH} = \frac{b_{ultimass}}{1.0079} \quad (17)$$

$$c = \frac{c_{ultimass}}{mmO} = \frac{c_{ultimass}}{15.999} \quad (18)$$

$$d = \frac{d_{ultimass}}{mmN} = \frac{d_{ultimass}}{14.0067} \quad (19)$$

$$e = \frac{e_{ultimass}}{mmS} = \frac{e_{ultimass}}{32.065} \quad (20)$$

where:

Ultimass : ultimate (elemental) analysis mass fraction

5.8 Box Behnken design

A Box–Behnken experimental design (BBD) was employed to investigate the combined effects of ozone concentration, inoculum-to-substrate (I/S) ratio, and contact time on methane production. This statistical design enables the evaluation of nonlinear and interaction effects among variables while requiring fewer experimental runs compared to full factorial designs.

Three levels (low, medium, high) were defined for each factor, as shown in Table 4. Ozone concentration (%) was designated as Factor A, the I/S ratio as Factor B, and contact time (s) as

Factor C. Methane yield was used as the response variable. All experiments were performed in randomized order to minimize systematic error.

Table 4: Factor levels with variables.

Factor	Variable	Low (-1)	Medium (0)	High (+1)
A	Ozone concentration (%)	0	5	10
B	I/S Ratio	0	1.0	2.0
C	Contact time (s)	30	60	90

Analysis of Variance (ANOVA)

Analysis of variance (ANOVA) was performed to evaluate the statistical significance of the individual factors (ozone concentration, I/S ratio, and contact time), as well as their interaction and quadratic effects, on methane production. The ANOVA results were generated using the Box–Behnken design model and included assessment of the linear, interaction (two-factor), and second-order (quadratic) terms.

The significance of each term was determined using the F-test and its associated p-value. Factors with $p < 0.05$ were considered statistically significant contributors to the variation in methane yield. The coefficient of determination (R^2), adjusted R^2 , and predicted R^2 were used to evaluate the model's goodness of fit and predictive capability. A high R^2 value indicated that a substantial proportion of the variability in methane production was explained by the model.

The lack-of-fit test was also examined to verify whether the model adequately represented the experimental data. A non-significant lack-of-fit ($p > 0.05$) indicated that the predicted values were consistent with the observed methane yields. Additionally, the adequate precision value was used to assess the signal-to-noise ratio; values greater than 4 were considered desirable and reflective of a reliable model.

Residual diagnostic plots—including normal probability plots, residuals vs. predicted values, and residuals vs. run order—were analyzed to ensure that ANOVA assumptions (normality, independence, and homoscedasticity of residuals) were satisfied. These diagnostic checks confirmed the validity of the model for predicting methane yield under the tested operating conditions.

5.9 Methane Production Modeling

The kinetics of methane production were modeled using the Modified Gompertz Equation, which is widely applied to describe cumulative methane production over time in anaerobic digestion systems. Equation 21 can be expressed as follows:

$$B(t) = B_{max} \cdot \exp \left\{ -\exp \left[\frac{R_{m,e}}{B_{max}} (\lambda - t) + 1 \right] \right\} \quad (21)$$

where:

B(t): Cumulative methane (NmL) at time t
B_{max}: Maximum methane potential (NmL)
R_{max}: Maximum methane production rate (NmL day⁻¹)
λ: Lag phase (Syaichurrozi et al.)
e: Euler's number (~2.718)

Model parameters, including the maximum methane production rate and lag phase duration, were extracted via nonlinear regression analysis, which was used to interpret the microbial activity, production efficiency, and impact of varying ozone pretreatment conditions on the AD process.

6 Results

6.1 Experiment 1

Effect of Ozone Pretreatment on Methane Production in Anaerobic Digestion

The primary aim of Experiment 1 was to assess the influence of ozone pretreatment on the methane yield during anaerobic digestion (AD) of municipal wastewater sludge. The hypothesis was that ozone exposure, by enhancing sludge disintegration and solubilizing organic matter, would increase the bioavailability of substrates and improve methane generation.

Ozone pretreatment was applied at 0%, 5%, and 10% concentrations with contact times of 0, 30 s, and 60 s. Anaerobic digestion was conducted at three inoculum-to-substrate (I/S) ratios of 0, 1.5, and 2.0, over 30 days under mesophilic conditions, using the AMPTS II system. Methane production was modeled using the Modified Gompertz equation.

6.1.1 Effect of Ozone Pretreatment on Methane Yield

This study investigated the influence of ozone pretreatment on methane yield using a Box–Behnken design, as outlined in Table 5. The experimental design involved three independent variables—ozone concentration (A), contact time (B), and inoculum-to-substrate (I/S) ratio (C)—each tested at three coded levels (-1, 0, +1), allowing for the modeling of nonlinear effects and interactions through a second-order polynomial regression. A total of 15 runs, including 3 center points, were conducted in a single block and replicate to ensure consistency and estimate experimental error. This response surface methodology efficiently explored the combined and individual effects of the three factors on methane production, without requiring a full factorial design. The structured distribution of experimental conditions enabled the detection of curvature and interactions in the response surface, supporting reliable optimization of the pretreatment parameters to enhance anaerobic digestion performance.

Table 5: Box Behnken design (ozone pretreatment).

Box-Behnken design				
Factors:	3	Replicates:	1	
Base runs:	15	Total runs:	15	
Base Blocks:	1	Total Blocks:	1	
Center points:	3			
Design Table				
Run	Blk	A	B	C
1	1	-1	-1	0
2	1	1	-1	0
3	1	-1	1	0
4	1	1	1	0
5	1	-1	0	-1
6	1	1	0	-1
7	1	-1	0	1
8	1	1	0	1
9	1	0	-1	-1
10	1	0	1	-1
11	1	0	-1	1
12	1	0	1	1
13	1	0	0	0
14	1	0	0	0
15	1	0	0	0

After 30 days of digestion for experiment 1, the experimental methane production with different ozone concentrations, exposure times, and I/S ratios is summarized in Table 6.

Table 6: Methane production as a function of ozone concentration, contact time, and I/S ratio (Experiment 1).

Sample	Condition	VS of I (g)	VS of S (g)	Mass of I (g)	Mass of S (g)	Methane (NmL CH ₄)	Methane production/S (mL CH ₄ g ⁻¹ VS)	Theoretical yield (mL CH ₄ g ⁻¹ VS)
1 Blank1	oz (0), I/S (0)	18.83	0	350	0	1152	61.2	517
2 Blank2	oz (0), I/S (0)	18.83	0	350	0	835	44.3	517
3 No treatment	oz (0), I/S(2)	16.24	8.12	301.81	48.19	2164	161	517
4 No treatment	oz (0), I/S(2)	16.24	8.12	301.81	48.19	3614	340	517

Table 6: Methane production as a function of ozone concentration, contact time, and I/S ratio (Experiment 1) (cont.).

Sample	Condition	VS of I (g)	VS of S (g)	Mass of I (g)	Mass of S (g)	Methane (NmL CH ₄)	Methane production/S (mL CH ₄ g ⁻¹ VS)	Theoretical yield mL CH ₄ g ⁻¹ VS	
5	oz5%-30sec1	oz5%, t(30s), I/S (2)	16.24	8.12	301.81	48.19	3517	328	517
6	oz5%-30sec2	oz5%, t(30s), I/S (2)	16.24	8.12	301.81	48.19	1345	60.1	517
7	oz5%-60sec1	oz5%, t(60s), I/S (2)	16.24	8.12	301.81	48.19	861	0.51	517
8	oz5%-60sec2	oz5%, t(60s), I/S (2)	16.24	8.12	301.81	48.19	1019	19.915	517
9	oz5%-30sec1	oz5%, t(30s), I/S (1.5)	15.53	10.35	288.57	61.43	7861	680.326	517
10	oz5%-30sec2	oz5%, t(30s), I/S (1.5)	15.53	10.35	288.57	61.43	1909	105.195	517
11	oz5%-60sec1	oz5%, t(60s), I/S (1.5)	15.53	10.35	288.57	61.43	4105	317.408	517
12	oz5%-60sec2	oz5%, t(60s), I/S (1.5)	15.53	10.35	288.57	61.43	5223	425.446	517
13	oz 10%-30sec1	oz 10%, t(30s), I/S (2)	16.24	8.12	301.81	48.19	4799	485.494	517
14	oz 10%-30sec2	oz 10%, t(30s), I/S (2)	16.24	8.12	301.81	48.19	516	530.395	517

Table 6 and Figure 13 presents a comparison between the experimental methane production from the substrate and the theoretical yield calculated using Buswell and Mueller's equation. The results show that, while most experimental values were below the theoretical maximum, two data points closely approached the predicted yield. This positive outcome demonstrates that, under certain conditions, the process can achieve methane production levels near the theoretical potential, highlighting the effectiveness of the applied pretreatment and operational strategies in optimizing biogas recovery.

Figure 14 presents a comprehensive summary of the cumulative methane production over time (in days) from the anaerobic digestion of municipal wastewater sludge under multiple experimental conditions. Owing to the inclusion of replicate trials in the experimental design, this figure was further divided into Figures 16 and 17, each representing distinct sets of replicate trials to clearly illustrate the variability and reproducibility of the results. Additionally, Figure 15 depicts the methane *accumulation flow rate*, that is, the daily rate of methane production, plotted against time for the same set of samples. Collectively, these figures provide a detailed visual representation of both the *total methane yield* and *temporal production dynamics* under varying ozone pretreatment and inoculum-to-substrate ratios. The trends observed in these figures provide key insights into the kinetics of biogas generation, which are further discussed below.

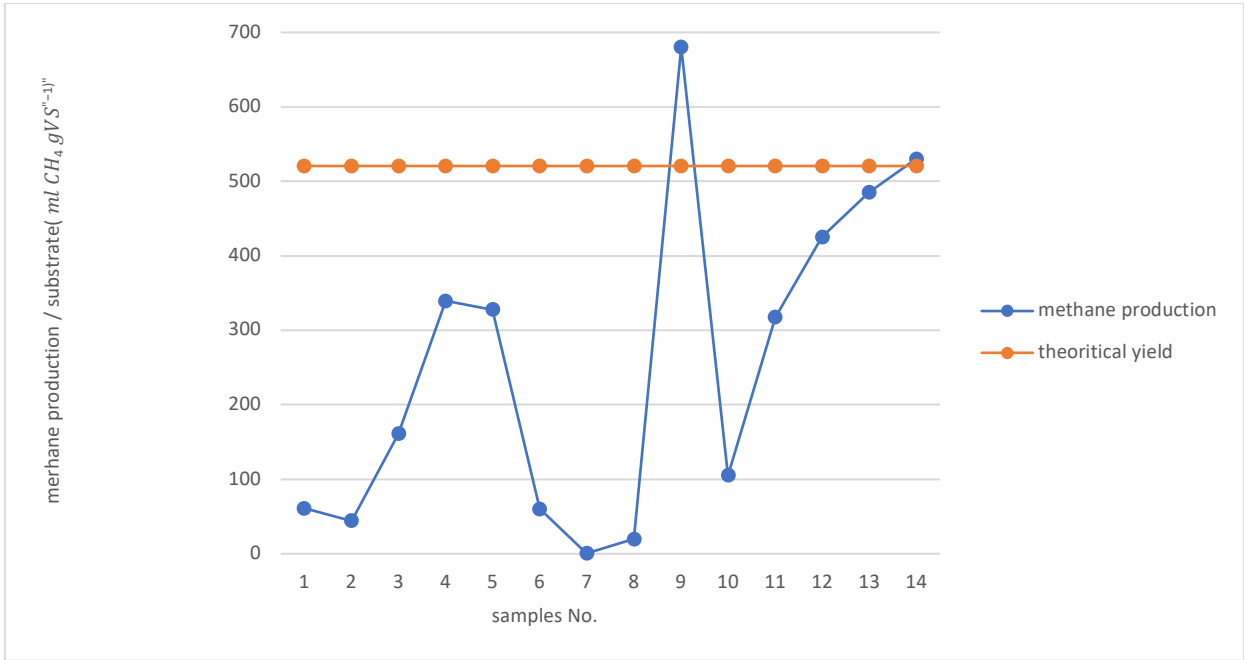


Figure 13: Methane production for substrate compared with the theoretical methane yield.

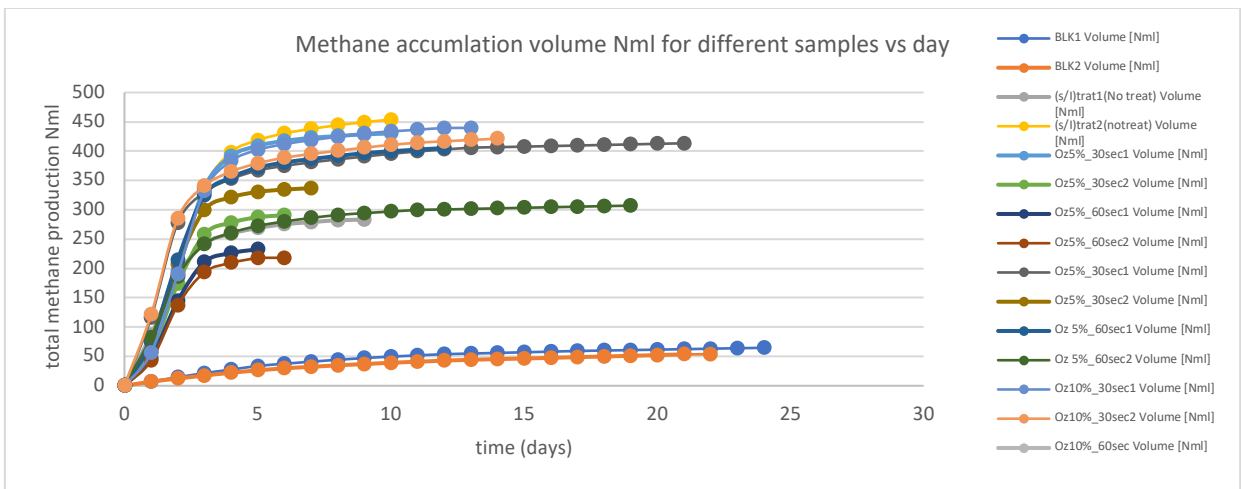


Figure 14: Cumulative methane production for the various substrate samples tested.

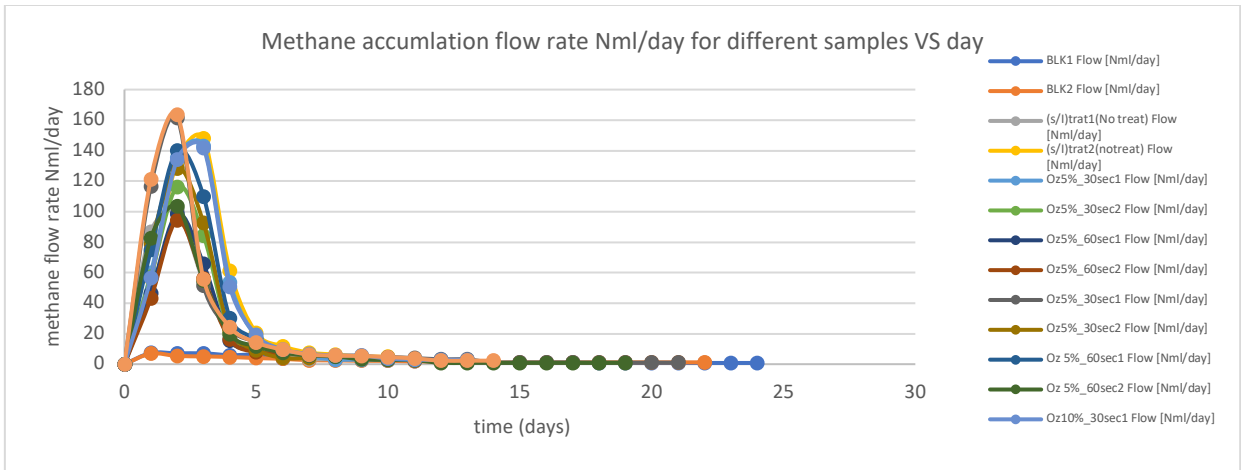


Figure 15: Methane production rate over time for the various substrate samples analyzed.

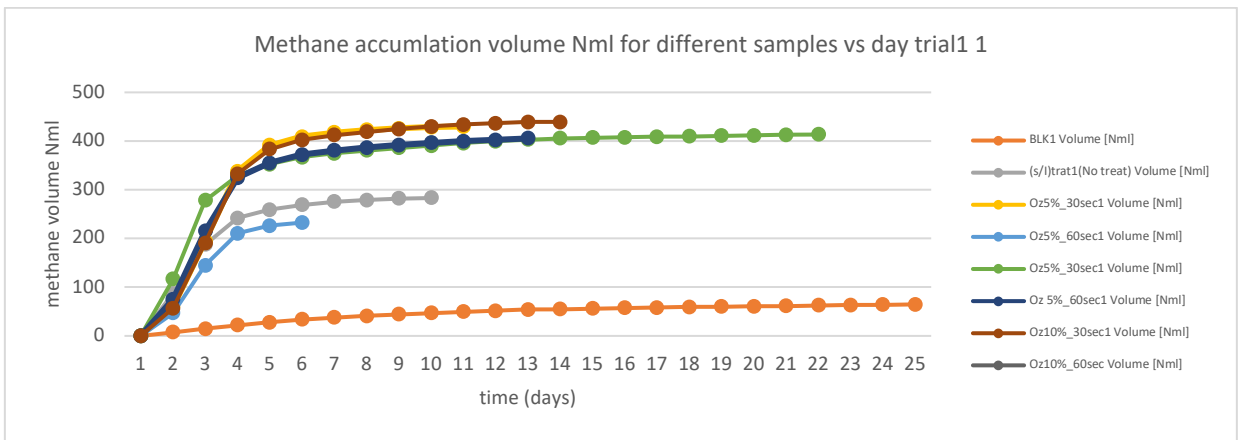


Figure 16: Cumulative methane production over time for the various substrate samples in Trial 1.

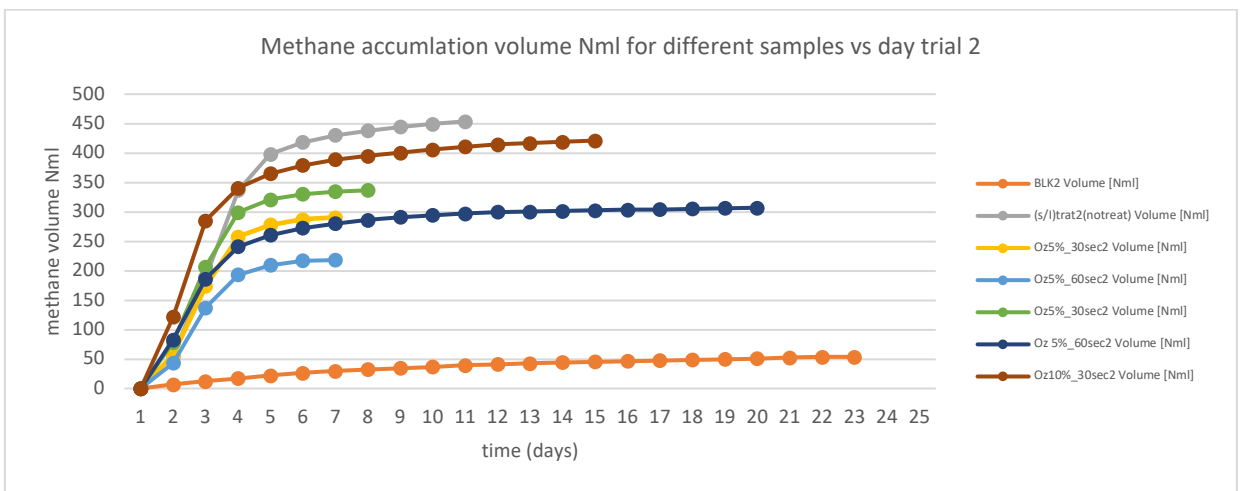


Figure 17: Cumulative methane production for trial 2 over the course of the experimental period.

The experimental data on methane production from ozone-pretreated sludge revealed important trends regarding the impact of ozone dosage on anaerobic digestion efficiency. The untreated sludge (0% ozone) exhibited a relatively high methane yield of approximately 340 mL CH₄ g⁻¹ VS, suggesting that the raw sludge was inherently biodegradable. Among all conditions tested, the highest methane yield was recorded at around 680 mL CH₄ g⁻¹ VS for the sample pretreated with 5% ozone for 30 seconds at an inoculum-to-substrate (I/S) ratio of 1.5. Interestingly, this value exceeded the theoretical biochemical methane potential (BMP) of 517 mL CH₄ g⁻¹ VS, which may be attributed to experimental variation, residual gas accumulation, or rapid microbial consumption of readily biodegradable compounds released during pretreatment.

Methane production remained notably high for the 10% ozone–30 second condition, reaching approximately 530 mL CH₄ g⁻¹ VS, further confirming that moderate ozone pretreatment enhances sludge digestibility. However, this value did not surpass the theoretical BMP, and in most other conditions, methane yields also fell below this theoretical limit. This trend indicates that while ozone pretreatment is beneficial, its effectiveness plateaus or slightly declines at higher dosages—likely due to the formation of inhibitory oxidation by-products that suppress microbial activity.

The data reinforce the notion that moderate ozone exposure (especially 5% for 30–60 seconds) significantly improves methane yield, aligning with the hypothesis that partial oxidation enhances substrate bioavailability. Nevertheless, notable variability among replicates, such as methane yields ranging from 60 to 327 mL CH₄ g⁻¹ VS under identical pretreatment conditions (5% ozone for 30 seconds), suggests the presence of operational inconsistencies. These could stem from uneven ozone dispersion, sludge heterogeneity, or other uncontrolled experimental factors. Overall, while ozone pretreatment has been validated as an effective strategy for enhancing anaerobic digestion, optimizing dosage and operational consistency remains critical to achieving reproducible and maximized methane production.

The theoretical methane yield represents the maximum possible methane production based on complete anaerobic degradation of organic matter. However, actual methane production is often lower because of incomplete degradation, loss of intermediates, and inefficiencies in microbial processes. In this study, while certain treatments, such as "oz5%-30sec1" with a methane production of 680 mL CH₄ g⁻¹ VS, approached the theoretical yield, they still fell short, indicating that complete conversion of organic matter was not achieved.

Several factors can cause methane production to fall short of the theoretical expectations.

- Substrate composition: The presence of lignin, hemicellulose, and other complex compounds can make substrates more resistant to microbial degradation, reducing the methane yield.
- Microbial activity: The efficiency of methanogenic microbes can be influenced by factors such as pH, temperature, and presence of inhibitory substances ([Afroze et al., 2023](#)).

The addition of trace elements and nutrients plays a crucial role in enhancing the efficiency of anaerobic digestion. Trace elements like iron (Fe), nickel (Ni), and cobalt (Co) are essential for the activity of key enzymes involved in methane production. For instance, supplementation with 1 mg L⁻¹ of Fe has been shown to increase methane yield by approximately 68%. Similarly, the

combination of Ni²⁺ (1 mg L⁻¹) and Co²⁺ (0.1–0.5 mg L⁻¹) has been reported to enhance methane production by 16–23% (Mary et al., 2024).

Beyond macronutrients, microorganisms also require trace elements such as potassium, magnesium, manganese, iron, copper, and zinc for cell function. Although municipal wastewater often contains these in adequate amounts, certain conditions may necessitate supplementation to ensure optimal microbial activity (Afroze et al., 2023).

In this study, although trace elements were not explicitly tested, their absence could have limited methanogenic activity, thereby reducing methane production. The observed methane yields, even under optimized ozone treatments, suggest that supplementation with appropriate trace elements could further enhance process efficiency (Ataa Fosua et al., 2023).

6.1.2 Influence of I/S Ratio

The results of experiment 1 focused on the relationship between methane production yield and ozone % with contact time, as shown in Table 7. The I/S ratio with contact time is related to the methane production yield, as shown in Table 8.

- In this two-factor ANOVA with replication analysis in table 7, it was compared the means of different levels of factors A and B on a response variable.

- From the results, we can see that factor A is not significant as indicated by the p-values. AB has a significant effect on the response variable, as indicated by the low p-values of the main effects.

Table 7: Two-Factor ANOVA with replication, analyzing the effect of ozone percentage (A) and contact time (B) on methane production yield.

$y = 2088.1 + 402.6x_1 + -1618.55x_2 + -872.5x_1x_2$			
A= ozone %, B=contact time			
SUMMARY	B-	B+	Total
A-			
Count	2	2	4
Sum	4862.4	1879.6	6742
Average	2431.2	939.8	1685.5
Variance	2359226.42	12418.88	1531973.09
A+			
Count	2	2	4
Sum	9962.8	0	9962.8

Table 7: Two-Factor ANOVA with replication, analyzing the effect of ozone percentage (A) and contact time (B) on methane production yield (cont.).

Average	4981.4	0	2490.7
Variance	66466.58	0	8293604.18
Total			
Count	4	4	
Sum	14825.2	1879.6	
Average	3706.3	469.9	
Variance	2976404.35	298547.64	

ANOVA							
Source of Variation	SS	df	MS	F	P-value	F crit	
Sample	1296694.08	1	1296694.08	2.1273742	0.21844311	7.70864742	Factor A is not significant P>0.05
Columns	20948569.9	1	20948569.9	34.3685129	0.00422626	7.70864742	Factor B and significant P<0.05
Interaction	6090050	1	6090050	9.99142008	0.03415386	7.70864742	AB interaction is significant at P<0.05
Within	2438111.88	4	609527.97				
Total	30773425.9	7					

The interaction between factors A and B was found to be statistically significant, as indicated by a p-value below the 0.05 threshold. Specifically, the F-value for factor A was 2.127 with a corresponding p-value of 0.21844, suggesting that factor A alone does not have a significant effect on the response variable. In contrast, factor B demonstrated a strong and statistically significant influence, with an F-value of 34.368 and a p-value of 0.004226. Although factor A does not appear to independently affect the response, the significant interaction between A and B suggests that their combined effect plays an important role in shaping the outcome. This implies that while factor B has a clear main effect, the influence of factor A may become relevant only in the context of its interaction with factor B.

Table 8: Two-Factor ANOVA with replication analyzing the effect of I/S Ratio (C) and contact time (B) on methane production yield.

$y = 3229.8 + 1544.3x_1 + -428.05x_2 + 317.65x_1x_2$ C= I/S ratio %, B=contact time			
SUMMARY	C-	C+	Total
B-			
Count	2	2	4
Sum	4862.4	1879.6	6742

Table 8 : Two-Factor ANOVA with replication analyzing the effect of I/S Ratio (C) and contact time (B) on methane production yield (cont.).

Average	2431.2	939.8	1685.5
Variance	2359226.42	12418.88	1531973.09
B+			
Count	2	2	4
Sum	9769	9327.4	19096.4
Average	4884.5	4663.7	4774.1
Variance	17716723.4	625185.62	6130220.55
Total			
Count	4	4	
Sum	14631.4	11207	
Average	3657.85	2801.75	
Variance	8698210.23	4835011.9	

ANOVA							
Source of Variation	SS	df	MS	F	P-value	F crit	
Sample	19078899.9	1	19078899.9	3.68433146	0.12735047	7.70864742	Factor B is not significant P>0.05
Columns	1465814.42	1	1465814.42	0.28306381	0.62287803	7.70864742	Factor C is not significant P>0.05
Interaction	807212.18	1	807212.18	0.15588096	0.7131254	7.70864742	BC interaction is not significant P>0.05
Within	20713554.3	4	5178388.58				
Total	42065480.8	7					

In this two-factor ANOVA with replication, the effects of factors C and B on the response variable were assessed. The analysis revealed that neither factor C nor factor B exerted a statistically significant influence on the response, as evidenced by their respective high p-values. Specifically, factor C yielded an F-value of 3.68 with a p-value of 0.10, while factor B produced an F-value of 0.283 and a p-value of 0.623. These results indicate that the variation observed in the response variable cannot be attributed to changes in either factor C or B. Moreover, the interaction between the two factors was also found to be statistically insignificant, as the interaction term's p-value exceeded the 0.05 threshold. Overall, the findings suggest that within the tested experimental conditions, neither the individual factors nor their interaction had a meaningful effect on the response variable.

Statistical analysis: ANOVA for factorial interactions

A two-way ANOVA with replication was conducted to evaluate the interaction effects of ozone concentration, contact time, and the inoculum-to-substrate (I/S) ratio on methane production. The analysis revealed that ozone concentration (Factor A) did not have a statistically significant main effect on methane yield ($p = 0.218$). This lack of significance may be attributed to high experimental variability and the non-linear nature of the dose–response relationship, which can obscure clear trends. In contrast, contact time (Factor B) emerged as a significant factor ($p = 0.0042$), suggesting that the duration of ozone exposure exerts a meaningful influence on the digestion performance, likely by altering the degree of sludge solubilization and biodegradability.

Notably, the interaction between ozone concentration and contact time (A*B) was also statistically significant ($p = 0.034$), indicating that the methane yield is not determined by these variables independently, but rather by their combined effect. This interaction suggests a complex relationship where the effectiveness of ozone pretreatment is modulated by the duration of exposure.

In a separate ANOVA examining the relationship between contact time and I/S ratio (B vs. C), neither the main effects nor their interaction were statistically significant. This outcome implies that beyond a certain contact time threshold—particularly between 30 and 60 seconds—the influence of ozone duration on methane yield becomes marginal, or that experimental variability obscured any potential differences. These findings underscore the importance of optimizing both ozone concentration and contact time jointly, rather than in isolation, to achieve improved anaerobic digestion outcomes.

6.1.3 pH Behavior before and after digestion

The study focused on testing the pH behavior before and after 30 d of digestion, as shown in Table 9. Digestion is used to monitor biochemical changes during anaerobic breakdown of organic waste (sludge waste). Initially, the pH indicates the acidity or alkalinity of the raw substrate, which influences microbial activity. During digestion, microorganisms decompose the organic matter, producing intermediate acids and later methane, which significantly affects pH levels. By analyzing the pH after 30 days, researchers can assess whether the system remains stable, identify potential process imbalances (such as acid accumulation or ammonia release), and determine if the digestion process is effective and near completion. This helps to optimize the retention time and improve the overall digestion efficiency.

Table 9: Changes in pH observed before and after 30 days of digestion.

Sample	Initial pH	Final pH
1 Blank1	7.52	9.27
2 Blank2	7.51	9.12
3 No treatment	7.53	9.30
4 No treatment	7.55	9.25
5 oz5%-30sec1	7.54	9.40

Table 9: Changes in pH observed before and after 30 days of digestion (cont.).

	Sample	Initial pH	Final pH
6	oz5%-30sec2	7.56	9.34
7	oz5%-60sec1	7.51	9.20
8	oz5%-60sec2	7.52	9.26
9	oz5%-30sec1	7.72	8.92
10	oz5%-30sec2	7.55	9.22
11	oz5%-60sec1	7.56	9.33
12	oz5%-60sec2	7.56	9.39
13	oz10%-30sec1	7.53	9.28
14	oz10%-30sec2	7.52	9.39
15	oz10%-60sec1	7.52	9.35

The initial pH of the sludge was mildly alkaline, ranging from 7.51 to 7.72. Following anaerobic digestion, the pH levels increased notably, reaching values between 9.12 and 9.4 across all treatment groups. This rise in pH aligns with typical post-digestion biochemical processes, such as ammonification and the removal of CO₂, which contribute to alkalization. Notably, even in reactors subjected to ozone pretreatment, there was no evidence of acidification, suggesting that the oxidative conditions did not disrupt the buffering capacity or microbial stability of the system. The consistently elevated pH values post-digestion are particularly significant, as they may be associated with the sub-theoretical methane yields observed in certain cases. This relationship highlights the potential influence of high alkalinity on microbial activity or metabolic pathways within the anaerobic digestion process.

The main reason for increasing the pH to 9.12–9.4 after digestion:

1. Ammonia accumulation from protein degradation:
 - During anaerobic digestion, the degradation of nitrogenous compounds (especially proteins from the sludge) leads to the release of ammonia (NH₃/NH₄⁺). At mesophilic temperatures and slightly alkaline conditions, ammonium ions (NH₄⁺) partially dissociate into free ammonia (NH₃), which raises the pH (Rajagopal et al.).
 - Municipal sludge is typically rich in organic nitrogen, and in the study, the elemental composition included ~7.1% nitrogen. This would favor significant ammonia release, especially with efficient breakdown triggered by ozone pretreatment (Nakakubo et al., 2008).
2. Carbon dioxide (CO₂) removal via scrubbing:

The AMPTS II system includes a CO₂ absorption unit using NaOH, which removes CO₂ from the gas phase. CO₂ is acidic in aqueous media, and its removal shifts the equilibrium toward alkalinity (i.e., the pH increases). And, the continual removal of CO₂ without any buffering in the system

can drive the pH above 9.0. However, in this study, the samples were buffered before starting the digestion process; therefore, so the CO₂ reason is not applicable.

Impact of Elevated pH and Ammonia on Methane Production in Anaerobic Digestion

Elevated pH levels are closely associated with reduced methane production during anaerobic digestion (AD). This is primarily due to the inhibitory effects of high pH on methanogenic archaea, the key microbial group responsible for methane generation. The optimal pH range for methanogenic activity is generally between 6.8– and 7.8. However, when pH levels exceed 8.5, and particularly beyond 9.0, methanogenic activity is significantly suppressed (Nakakubo et al., 2008).

One major mechanism underlying this inhibition is the formation of free ammonia (NH₃). As proteins degrade during anaerobic digestion, they release amino acids that are subsequently deaminated, producing ammonia in the form of ammonium ions (NH₄⁺). At mesophilic temperatures (typically 35–40 °C) and slightly alkaline pH, the chemical equilibrium shifts from NH₄⁺ toward the formation of free NH₃ (Rajagopal et al.).

This form of ammonia is highly toxic to acetoclastic methanogens, disrupting proton gradients across their cell membranes and leading to cellular energy depletion (Mary et al., 2024).

Moreover, high concentrations of ammonia can further elevate the pH of the system's pH, creating a positive feedback loop that exacerbates NH₃ formation and intensifies its inhibitory effects.

Despite these challenges, the microbial community can adapt under prolonged exposure to high ammonia concentrations. Certain ammonia-tolerant methanogens may become enriched, particularly especially when supported by appropriate micronutrient supplementation. The addition of trace elements, such as cobalt (Co), nickel (Ni), selenium (Se), and molybdenum (Mo), has been shown to enhance microbial resilience and methanogenic performance under ammonia stress. Furthermore, essential micronutrients including iron (Fe), zinc (Zn), copper (Cu), and manganese (Yasar et al.) serve as cofactors for key enzymes involved in the methanogenesis pathway, thereby supporting metabolic activity and microbial growth (Afroze et al., 2023).

Table 10 summarizes the rationale for behind nutrient addition in Experiment 2 and its impact on methane production. Nutrients such as trace metals—cobalt (Co), nickel (Ni), molybdenum (Mo), and selenium (Se)—were added to address methanogen inhibition, as these elements are essential cofactors for enzymes involved in methanogenesis, thereby improving the resilience and activity of methanogens. Additionally, a broader nutrient mix was used to correct for imbalanced microbial activity and , to correct for imbalanced microbial activity, a broader nutrient mix was used to enhance the overall health and function of the microbial community. Together, these interventions led to improved digestion efficiency, resulting in an increased biogas yield and higher methane content.

Table 10: The impact of nutrient addition on methane production.

Problem	Nutrient Solution	Impact on Methane Production
Methanogen inhibition	Add trace metals (Co, Ni, Mo, Se)	Supports enzyme activity and resilience
Imbalanced microbial activity	Nutrients improve microbial health	Enhances biogas and methane output

6.1.4 Kinetic Modeling Using Modified Gompertz Equation

Kinetic modeling of the experimental data revealed a clear enhancement in the maximum methane production rates (R_{max}) in the samples treated with ozone compared to the untreated controls. For untreated sludge, R_{max} values ranged between approximately 111 and 159 Nml CH_4 d^{-1} , reflecting the baseline activity of the native microbial community. In contrast, ozone pretreatment at 5% concentration for 30 seconds ($I/S = 1.5$) resulted in a modest increase in R_{max} to approximately 141–145 Nml CH_4 d^{-1} . An even more pronounced effect was observed with 10% ozone exposure for the same duration at a higher I/S ratio (2.0), where the R_{max} values rose to approximately 153–154 Nml CH_4 d^{-1} .

These increases in R_{max} indicate that ozone pretreatment facilitates more efficient substrate hydrolysis and accelerates the onset of methanogenesis in the rumen. Moreover, the lag phases (λ) across all conditions remained consistently short (less than one day)—less than one day—, suggesting that microbial communities adapted rapidly to the pretreated sludge, despite the oxidative environment introduced by ozone. This kinetic behavior supports the conclusion that carefully optimized ozone pretreatment enhances both the rate and onset of methane production, offering a practical strategy for improving the efficiency of anaerobic digestion.

Figure 18 shows the cumulative methane production curves for all samples without ozone pretreatment, along with the Gompertz model fittings. The figure shows how the measured and predicted methane yields (mL $CH_4 \cdot g^{-1}$ VS) changed over time for both the control and substrate samples at different inoculum-to-substrate ratios. The close alignment between the experimental data points and the fitted curves highlights the model's ability to accurately reflect the progression of methane generation under these baseline conditions. While Figure 19 displays cumulative methane production profiles for samples subjected to 5% ozone pretreatment, again with Gompertz model fitting. This figure illustrates the impact of ozone treatment and varying I/S ratios on methane yields over time. The model captures the enhanced production rates and yields observed in the pretreated samples, emphasizing the positive effect of ozone on anaerobic digestion performance and the reliability of the Gompertz model in describing these dynamics.

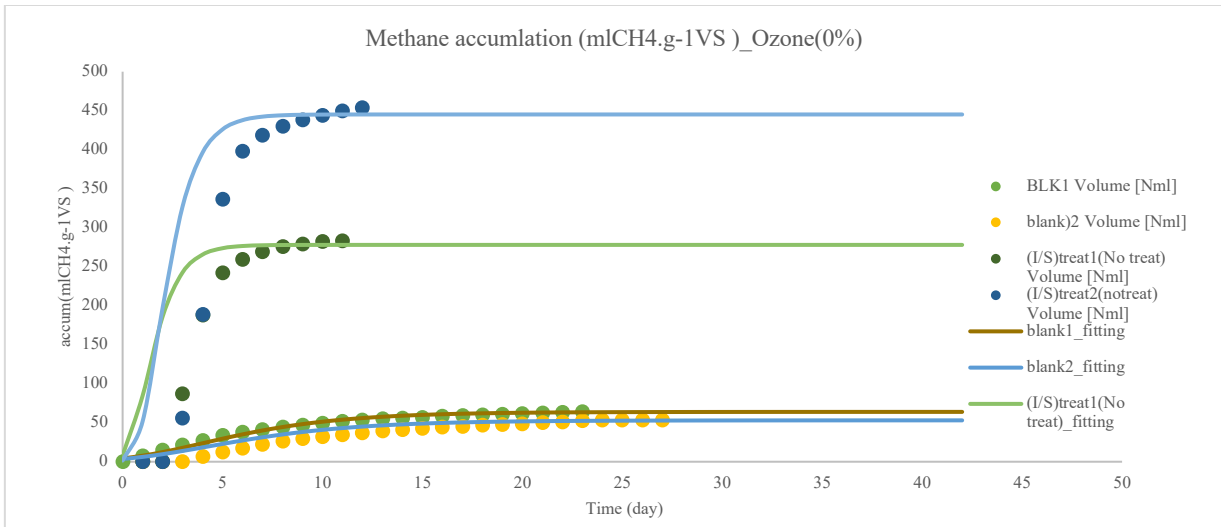


Figure 18 Cumulative Methane production (mL CH₄ g⁻¹ VS) using Gompertz Model fitting for all 0% Ozone pretreatment samples at varying I/S Ratios over time (Days).

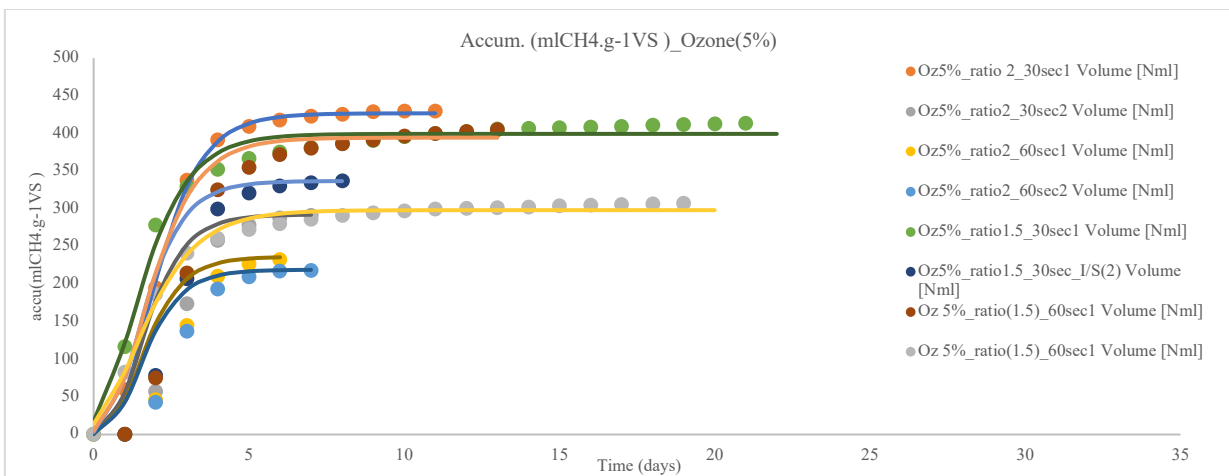


Figure 19: Cumulative methane production using Gompertz Model fitting for all samples treated with 5% Ozone Pretreatment Over Time (Days).

Figure 20 summarized a clear illustration of how methane production progresses over time in samples treated with 10% ozone pretreatment. The experimental data points for both tested I/S ratios are closely tracked by the Gompertz model curves, reflecting a rapid increase in methane accumulation during the initial days, followed by a plateau as the process stabilizes. This strong agreement between observed and predicted values shows that the Gompertz model effectively captures the dynamic changes in methane yield under these conditions. The figure highlights not only the efficiency of ozone pretreatment in enhancing biogas production but also the model's reliability in representing real process behavior, making it a valuable tool for understanding and optimizing anaerobic digestion performance.

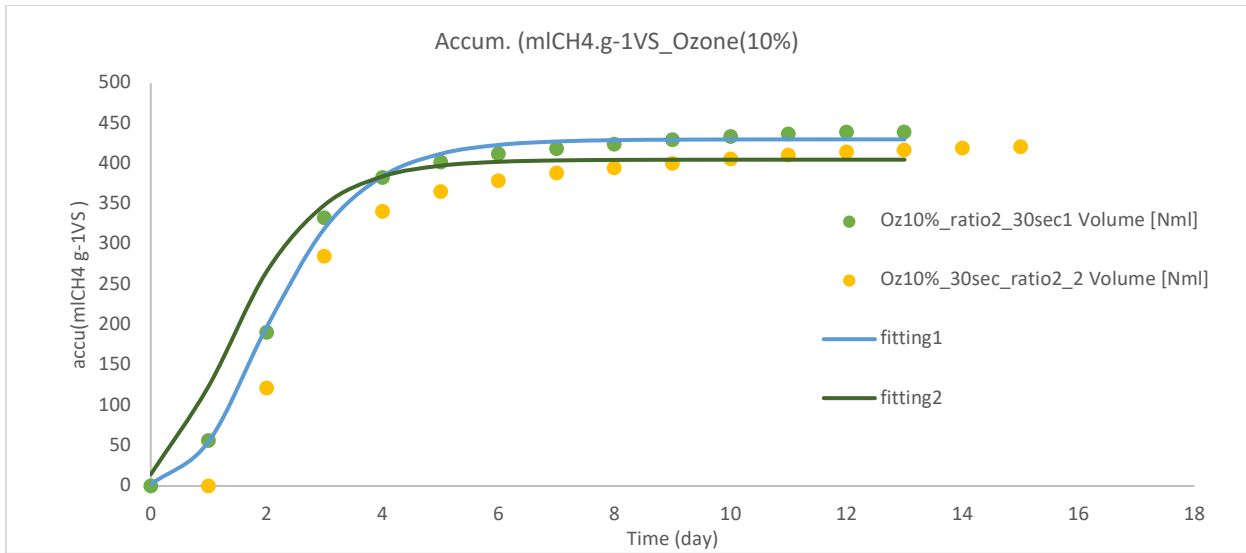


Figure 20: Cumulative methane production using Gompertz Model fitting for all samples treated with 10% Ozone Pretreatment Over Time (Days).

The Gompertz model effectively captures the methane production dynamics of both untreated samples in Experiment 1, despite variability between replicates due to the biological complexity of anaerobic digestion. For sample (s1)1 (No treat), the model indicates moderate biogas potential ($B_{max} = 278 \text{ Nml}$), a steady production rate ($R_{max} = 111 \text{ mL} \cdot \text{d}^{-1}$), and a short lag phase ($\lambda = 0.23 \text{ d}$), suggesting rapid microbial activation. In contrast, sample (s1)2 (No treat) shows a substantially higher biogas potential ($B_{max} = 445 \text{ Nml}$) and production rate ($R_{max} = 159 \text{ mL} \cdot \text{d}^{-1}$), with a longer lag phase ($\lambda = 0.76 \text{ d}$), indicating more complex substrate degradation. The 60% increase in B_{max} between replicates highlights the model's ability to reflect substrate or inoculum heterogeneity. Although formal goodness-of-fit metrics are not provided, the biologically plausible parameters and consistent trends confirm that the Gompertz model is a reliable tool for describing sigmoidal methane production patterns in anaerobic digestion.

6.1.5 Evaluation of Multiple Mathematical Models for Anaerobic Digestion Performance in Experiment 1

Anaerobic digestion (AD) is a widely adopted technology for the treatment of municipal wastewater, and is particularly effective in stabilizing sewage sludge and generating biogas. Various mathematical and mechanistic models have been developed to better understand, simulate, and optimize this complex biological process. These models range from empirical formulations to detailed mechanistic frameworks that capture AD biochemical and microbial dynamics. The main types of models applied in municipal wastewater treatment are summarized in Table 11, based on classifications reported by (Zhang et al., 2021; Li et al., 2012).

Table 11: Mathematical models for methane production kinetics in anaerobic digestion.

Model	Equation	Reference
Modified Gompertz Equation	$M = B_{max} * \exp\left(-\exp\left[\frac{R_{max} * e}{B_{max}}(\lambda - t) + 1\right]\right)$	(Zhang et al., 2021); (Li et al., 2012)
Logistic function	$M = \frac{B_{max}}{1 + \exp\left[\frac{4R_{max} * (\lambda - t)}{B_{max}} + 2\right]}$	(Zhang et al., 2021); (Li et al., 2012)
Trasference function	$M = B_{max} * \left(1 - \exp\left[\frac{R_{max} * (t - \lambda)}{B_{max}}\right]\right)$	(Li et al., 2012)
Cone function	$M = \frac{B_{max}}{(1 + (Kt)^{-n})}$	(Achinas & Euverink, 2019)

where:

- Bmax: Maximum methane production potential (mL g⁻¹ VS)
- Rmax : Maximum methane production rate (mL g⁻¹ VS d⁻¹)
- λ : lag phase time (d)
- K: Biogas production rate constant (d⁻¹)
- n: Shape factor
- t= production time (d)

Tables 12 to 15 display the fitting parameters derived from each model applied to the 14 samples in Experiment 1.

Table 12 : Estimated Gompertz model parameters for Experiment.

Sample	Bmax (mL g ⁻¹ VS)	Rmax (mL g ⁻¹ VS d ⁻¹)	Lag time, λ (d)	R ²
1 BLANK_1	63.9	5.9	0	0.9860
2 BLANK_2	53.1	4.6	0	0.9830
3 (s/I)1(No treat)	278	111	0.24	0.9978
4 (s/I)2(No treat)	445	159	0.76	0.9985
5 Oz5%_ratio2_30sec1	427	163	0.74	0.9989
6 Oz5%_ratio2_30sec2	292	130	0.59	0.9993
7 Oz5%_ratio2_60sec1	236	109	0.60	0.9990
8 Oz5%_ratio2_60sec2	219	102	0.60	0.9998
9 Oz5%_ratio1.5_30sec1	399	142	0.15	0.9830

Table 12 : Estimated Gompertz model parameters for Experiment (cont.).

Sample	Bmax (mL g ⁻¹ VS)	Rmax (mL g ⁻¹ VS d ⁻¹)	Lag time, λ (d)	R ²
10 Oz5%_ratio1.5_30sec2	337	146	0.49	0.9991
11 Oz5%_ratio1.5_60sec1	394	145	0.49	0.9970
12 Oz5%_ratio1.5_60sec2	298	96	0.13	0.9898
13 Oz10%_ratio2_30sec1	430	153	0.71	0.9974
14 Oz10%_ratio2_30sec2	405	154	0.20	0.9889

Table 13: Estimated Logistic model parameters for Experiment 1.

Sample	Bmax (mL g ⁻¹ VS)	Rmax (mL g ⁻¹ VS d ⁻¹)	Lag time, λ (d)	R ²
1 BLANK_1	60.4	5.65	5.07	0.9778
2 BLANK_2	51.0	4.06	5.59	0.9731
3 (s/I)1(No treat)	277	94.5	0.53	0.9931
4 (s/I)2(No treat)	439	164	2.23	0.9963
5 Oz5%_ratio2_30sec1	422	167	2.12	0.9979
6 Oz5%_ratio2_30sec2	286	134	1.78	0.9982
7 Oz5%_ratio2_60sec1	230	113	1.73	0.9985
8 Oz5%_ratio2_60sec2	215	105	1.73	0.9978
9 Oz5%_ratio1.5_30sec1	397	147	1.61	0.9713
10 Oz5%_ratio1.5_30sec2	332	148	1.71	0.9973
11 Oz5%_ratio1.5_60sec1	332	148	1.71	0.8557
12 Oz5%_ratio1.5_60sec2	296	97.4	1.76	0.9789
13 Oz10%_ratio2_30sec1	426	158	2.19	0.9942
14 Oz10%_ratio2_30sec2	402	160	1.56	0.9789

Table 14: Estimated Transference model parameters for Experiment 1.

Sample	Bmax (mL g ⁻¹ VS)	Rmax (mL g ⁻¹ VS d ⁻¹)	Lag time, λ (d)	R ²
1 BLANK_1	1000	3.62	0.05	0.6131
2 BLANK_2	97615	3.00	0.00	0.7325
3 (s/I)1(No treat)	9000	42.0	0.00	0.4230
4 (s/I)2(No treat)	1694889	59.5	0.00	0.6278
5 Oz5%_ratio2_30sec1	555184	57.4	0.00	0.5663
6 Oz5%_ratio2_30sec2	1317240	60.1	0.00	0.8213
7 Oz5%_ratio2_60sec1	6432381	55.2	0.00	0.8943
8 Oz5%_ratio2_60sec2	495321	45.4	0.00	0.8097
9 Oz5%_ratio1.5_30sec1	405	202	0.05	0.9858

Table14 : Estimated Transference model parameters for Experiment 1 (cont.).

Sample	Bmax (mL g ⁻¹ VS)	Rmax (mL g ⁻¹ VS d ⁻¹)	Lag time, λ (d)	R ²
10 Oz5%_ratio1.5_30sec2	179728	62.1	0.00	0.6978
11 Oz5%_ratio1.5_60sec1	411	178	0.14	0.9750
12 Oz5%_ratio1.5_60sec2	303	141	0.06	0.9912
13 Oz10%_ratio2_30sec1	453	174	0.21	0.9648
14 Oz10%_ratio2_30sec2	415	214	0.05	0.9871

Table 15: Estimated Cone model parameters for Experiment 1.

Sample	Bmax (mL g ⁻¹ VS)	Lag time, λ (d)	K (d ⁻¹)	n	R ²
1 BLANK_1	74.9	0.00	0.167	1.290	0.9997
2 BLANK_2	77.0	0.08	0.104	1.008	0.9997
3 (s/I)1(No treat)	291.4	0.21	0.793	1.875	0.9996
4 (s/I)2(No treat)	462.9	0.22	1.027	1.664	0.9804
5 Oz5%_ratio2_30sec1	435.1	0.00	0.487	3.025	0.9978
6 Oz5%_ratio2_30sec2	303.4	0.00	0.575	2.802	0.9981
7 Oz5%_ratio2_60sec1	247.2	0.00	0.582	2.812	0.9985
8 Oz5%_ratio2_60sec2	226.4	0.00	0.593	2.867	0.9994
9 Oz5%_ratio1.5_30sec1	872.9	0.998	0.036	0.190	0.9941
10 Oz5%_ratio1.5_30sec2	348.2	0.00	0.607	2.640	0.9976
11 Oz5%_ratio1.5_60sec1	404.2	0.00	0.544	2.530	0.9986
12 Oz5%_ratio1.5_60sec2	322.5	1.34	2.229	0.817	0.9459
13 Oz10%_ratio2_30sec1	437.4	0.00	0.476	2.875	0.9982
14 Oz10%_ratio2_30sec2	445.4	0.77	1.539	0.932	0.9999

To enable a meaningful comparison between models, an F-test was conducted to assess the differences in variance. This analysis will help identify specific variations among the samples. The discussion should also consider the methodology used and the sum of squared errors (SSE) associated with each model.

To analyze the samples collectively, the complete F-test results across experimental conditions offer a stronger statistical basis for model comparison. The evaluation of methane production kinetics using Gompertz, Logistic, Transference, and Cone models reveal distinct differences in their fitting accuracy and biological relevance.

The Gompertz model (Table 12) consistently provided excellent fits, with R² values ranging from 0.983 to 0.999 across all treatments. It reliably estimates key kinetic parameters, such as the maximum methane potential (Bmax), methane production rate (Rmax), and lag phase (λ), all within biologically plausible ranges. Notably, treated samples (*Oz5%_ratio2_30sec1*,

Oz10%_ratio2_30sec1) show high B_{max} and R_{max} values with minimal lag phases, supporting the Gompertz model's robustness and interpretative value.

The Logistic model (Table 13) also performed well, with most of the R^2 values exceeding 0.97. However, some anomalies, such as a low R^2 of 0.856 for *Oz5%_ratio1.5_60sec1* and overestimated lag times (~5 d for blank samples), suggest reduced consistency. Although B_{max} and R_{max} remain comparable to those in the Gompertz model, the inflated lag phases and occasional lower R^2 values weaken its reliability.

In contrast, the Transference model (Table 14) shows greater variability and generally poorer performance, with many R^2 values below 0.7 (0.423 for No treat, 0.566 for *Oz5%_ratio2_30sec1*). While isolated samples (*Oz5%_ratio1.5_60sec2*, $R^2 = 0.991$) showed acceptable fits, the frequent occurrence of biologically implausible B_{max} values (e.g., >1,000,000 mL g⁻¹ VS) and inconsistent model behavior limited their suitability for comprehensive kinetic analysis in this experiment.

The Cone model (Table 15) demonstrates excellent statistical performance with R^2 values frequently at or near 1.000, suggesting a perfect or near-perfect fit. However, some anomalies appear in parameter estimates: B_{max} values for some samples are excessively high (e.g., 872.94 for *Oz5%_ratio1.5_30sec1*), and extreme parameter values for n and K occasionally lack clear biological justification. Nevertheless, the Cone model provides highly accurate curve fitting, especially for pretreated samples such as *Oz10%_ratio2_30sec2* ($R^2 = 1.000$), suggesting a strong potential for modeling complex degradation behaviors when carefully parameterized.

Considering both statistical robustness and biological interpretability, the Gompertz model emerged as the best-fitting model for this experimental dataset. It offers consistently high R^2 values, realistic estimates for B_{max} , R_{max} , and lag time, and clearly differentiates between the treatment effects. While the Cone model fits well numerically, its parameter interpretation is less transparent, and the Logistic and Transference models show limitations in either fit quality or predictive reliability.

Comprehensive models evaluation and Statistical comparison of models fits based on variance and F-Values for sample oz 10%, t(30s), I/S (2):

Under the experimental condition of 10% ozone pretreatment for 30 seconds with an I/S ratio of 2, the performance of four kinetic models in the table 16—Gompertz, Logistic, Transference, and Cone—was evaluated in terms of their ability to fit cumulative methane production data. Among them, the Gompertz model demonstrated the most consistent and accurate fit, as reflected in its lowest variance (2337), indicating minimal deviation from the observed data. The Cone (25389) and Transference (2718) models followed closely, showing comparable levels of precision. In contrast, the logistic model exhibited the highest variance (4449), suggesting less reliability in predicting experimental outcomes. F-ratio comparisons further reinforced these findings; the M2/M1 and M2/M3 ratios (1.90 and 1.64, respectively) confirmed that the logistic model had significantly greater variability than the Gompertz and Transference models. Meanwhile, the close proximity of the M3/M1 (1.16), M4/M1 (1.09), and M3/M4 (1.07) ratios indicates a stable and comparable performance among the Gompertz, Cone, and Transference models. Overall, while all models could generally represent the data, the Gompertz model proved to be the most statistically

robust, with the Cone and Transference models also offering strong and consistent performance, unlike the less reliable logistic model under this specific treatment condition.

Table 16: Statistical comparison of models fits based on variance and F-Values for sample oz 10%, t(30s), I/S (2).

oz 10%, t(30s), I/S (2) Volume [Nml]				F value					
Models	Bmax	S (variance)	Models	M1	M2	M3	M4	m2/m1	1.904
Gompertz (M1)	404.953	2336.960	M1					m2/m3	1.637
Logistic (M2)	401.550	4449.103	M2	1.904		1.637	1.752	m3/m1	1.163
Trans (M3)	414.843	2718.372	M3	1.163				m4/m1	1.086
Cone (M4)	445.380	2538.755	M4	1.086				m2/m4	1.752
								m3/m4	1.071

6.1.6 Comprehensive Model Evaluation Using F-Test for Variance and best Fit Criteria, for the comparison for all models

In addition to individual model fitting, the study conducted a comprehensive variance-based statistical analysis across all 14 samples using four kinetic models: Gompertz, Logistic, Transference, and Cone. F-tests for two-sample variances were performed between each pair of models to assess whether the differences in model performance were statistically significant. The analysis used a critical F-value of 2.58, based on a significance level of $\alpha = 0.05$, and degrees of freedom $df_1 = df_2 = 13$. This threshold served as the criterion for determining whether the observed differences in the model variance could be attributed to random variations or reflected a statistically significant difference in predictive performance. As summarized in Table 17, this approach allowed for a rigorous comparison of model variability across all experimental conditions and further supported the robustness of the Logistic, Gompertz, and Cone models, while identifying significant discrepancies associated with the Transference model.

Table 17: F-Test Two-sample variance analysis for model comparison across all Experimental conditions supported the robustness of the Gompertz (M1), Logistic (M2), Transference (M3) and Cone (M4) models.

Data analysis F-Test Two-Sample for Variances									
	M2/M1			M3/M1			M4/M1		
	F-Test Two-Sample for Variances			F-Test Two-Sample for Variances			F-Test Two-Sample for Variances		
	Variable 1	Variable 2		Variable 1	Variable 2		Variable 1	Variable 2	
Mean	3522.6086	735.0910	Mean	47268.8	735.091	Mean	16360.633	735.09107	
Variance	67577946.5	1244198.41	Variance	7.045E+09	1244198	Variance	1068093440	1244198.42	
Observations	14	14	Observations	14	14	Observations	14	14	
df	13	13	df	13	13	df	13	13	
F	54.3144		F	5662.1323		F	858.4590		

Table 17: F-Test Two-sample variance analysis for model comparison across all Experimental conditions supported the robustness of the Gompertz (M1), Logistic (M2), Transference (M3) and Cone (M4) models (cont.).

	M3/M2		M4/M2		M3/M4		
	F-Test Two-Sample for Variances		F-Test Two-Sample for Variances		F-Test Two-Sample for Variances		
	Variable 1	Variable 2	Variable 1	Variable 2	Variable 1	Variable 2	
P(F<=f) one-tail	3.83E-09				P(F<=f) one-tail	7.48361E-17	
F Critical one-tail	2.57692			2.5769	F Critical one-tail	2.5769	
Mean	47268.8024	3522.60868 6	Mean	16360.634	3522.6087	Mean	47268.8024 16360.6336 6
Variance	7044816007	67577946.5 1	Variance	1.068E+09	67577947	Variance	704481600 106809344 7 0
Observations	14	14	Observations	14	14	Observations	14 14
df	13	13	df	13	13	df	13 13
F	104.2472		F	15.8053		F	6.595692
P(F<=f) one-tail	6.09355E-11		P(F<=f) one-tail	7.201E-06		P(F<=f) one-tail	0.000866
F Critical one-tail	2.576927		F Critical one-tail	2.57692		F Critical one-tail	2.576927

The results presented in Table 17 offer a detailed statistical comparison of the variance among four commonly used kinetic models—Gompertz (M1), Logistic (M2), Transference (M3), and Cone (M4)—using the F-test two-sample variance analysis. The analysis revealed a clear trend: the Gompertz model consistently demonstrated significantly lower variance compared to the other models, as evidenced by F-values far exceeding the critical threshold (e.g., $F = 54.3$ for M2/M1, $F = 5662$ for M3/M1, and $F = 858$ for M4/M1, all with p-values well below 0.001). These results highlight the statistical robustness and stability of the Gompertz model in capturing methane production dynamics under various experimental conditions. In contrast, the transference model exhibited the highest variance among all comparisons (e.g., M3 vs. M1 and M3 vs. M2), suggesting that its predictive performance was less consistent and more sensitive to changing parameters. The Cone and Logistic models, while somewhat more stable than transference, still displayed significantly higher variances than Gompertz, indicating relatively lower reliability. Collectively, this analysis supports the conclusion that the Gompertz model is best suited for modeling anaerobic digestion kinetics in this study, offering both statistical soundness and practical dependability in its predictions.

6.1.7 Performing a Box-Behnken design experiment

A Box-Behnken design experiment was performed to analyze methane production based on factors such as the ozone percentage, I/S ratio, and contact time. It defines the factor levels using the variables for experiment 1 in Table 18.

Table 18: Factor levels with variables for experiment 1.

Factor	Variable	Low (-1)	Medium (0)	High (+1)
A	Ozone concentration (%)	0	5	10
B	I/S Ratio	0	1.0	2.0
C	Contact time (s)	0	30	60

Additionally, the figures (21–25) collectively present a comprehensive statistical and graphical analysis of methane production under various experimental conditions using the Box–Behnken design from Experiment 1.

Figure 21 illustrates the results of the ANOVA, indicating the statistical significance of the quadratic model used to predict methane production. This is followed by Figure 22, which shows a cube plot capturing the interaction effects among three key variables: ozone concentration, inoculum-to-substrate (I/S) ratio, and ozone contact time. These interactions are further visualized in Figure 23, where a 3D surface plot highlights the response behavior of methane production across varying levels of these factors. Figure 24 shows a contour plot of the same response surface, offering a clearer two-dimensional representation of the interaction zones that optimize methane output. Figure 25 presents a scatter plot comparing the predicted and actual methane production values, demonstrating the model’s predictive accuracy and validating the statistical fit achieved through the experimental design.

Together, these visualizations support a rigorous evaluation of the process parameters and model performance for optimizing anaerobic digestion for methane generation.

ANOVA for 2FI model

Response 1: methane yeild

Source	Sum of Squares	df	Mean Square	F-value	p-value	
Model	3.851E+05	6	64190.30	2.01	0.1920	not significant
A-ozone %	10010.35	1	10010.35	0.3127	0.5935	
B-ratio	41245.03	1	41245.03	1.29	0.2937	
C-contact time	3515.38	1	3515.38	0.1098	0.7501	
AB	1758.21	1	1758.21	0.0549	0.8214	
AC	6352.03	1	6352.03	0.1984	0.6695	
BC	11844.33	1	11844.33	0.3700	0.5622	
Pure Error	2.241E+05	7	32014.61			
Cor Total	6.092E+05	13				

Factor coding is **Coded**.
Sum of squares is **Type III - Partial**

The **Model F-value** of 2.01 implies the model is not significant relative to the noise. There is a 19.20% chance that an F-value this large could occur due to noise.

P-values less than 0.0500 indicate model terms are significant. In this case there are no significant model terms. Values greater than 0.1000 indicate the model terms are not significant. If there are many insignificant model terms (not counting those required to support hierarchy), model reduction may improve your model.

Figure 21: ANOVA for the quadratic response of methane production.

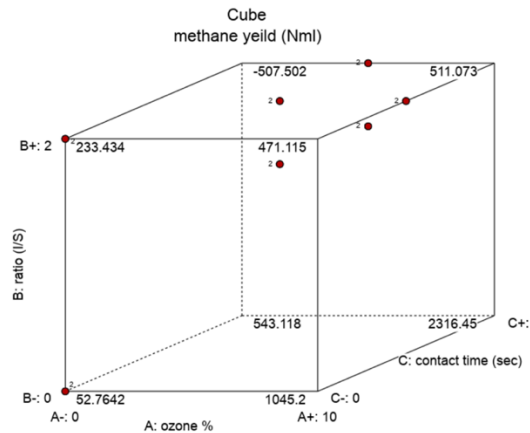


Figure 22: Cube plot representing the interactive effects of ozone concentration (%), inoculum-to-substrate (I/S) ratio, and ozone contact time (s) on methane production (Nml) based on the Box–Behnken design (experiment 1).

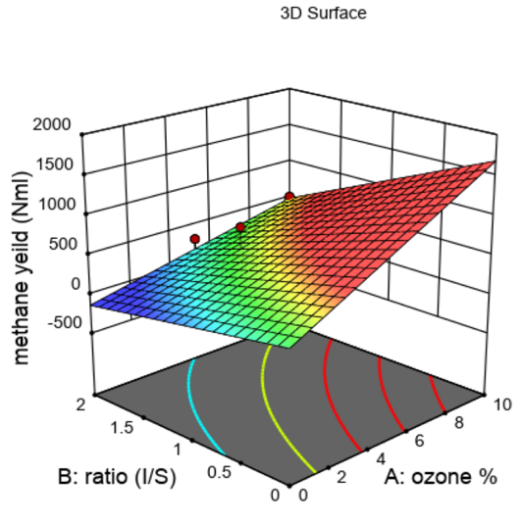


Figure 23: 3D diagram of methane production based on the Box–Behnken design (experiment 1).

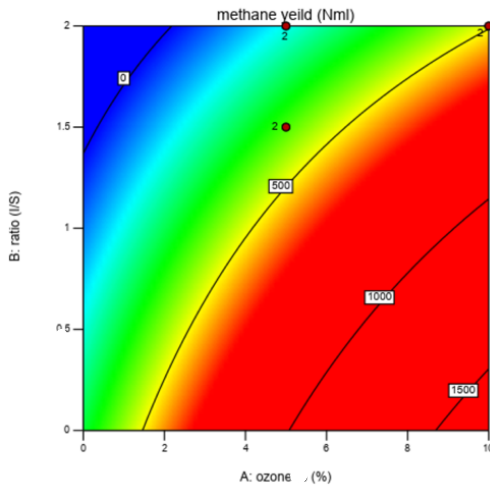


Figure 24: Contour graph of methane production based on the Box–Behnken design (experiment 1).

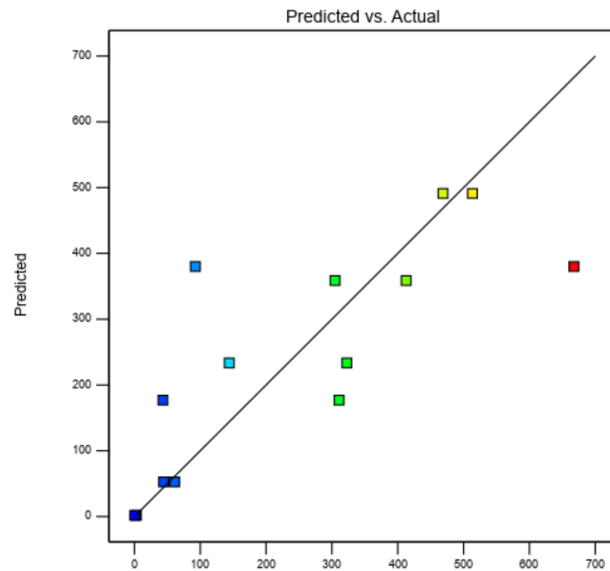


Figure 25: Scatter diagram of predicted vs actual methane production bed on the Box–Behnken design (experiment1).

6.1.8 Three-Dimensional Response Surface Analysis of Methane Yield

A three-dimensional (3D) response surface methodology was employed to visualize the interaction effects of three critical process parameters—ozone concentration (A: 0%, 5%, 10%), ozone contact time (B: 0, 30, 60 s), and the inoculum-to-substrate (I/S) ratio (C: 0.0, 1.0, 2.0)—on methane production during anaerobic digestion, expressed as mL CH₄ per gram volatile solids (VS). These relationships are illustrated in Figures 21 through 25.

The significance of these interactions was first confirmed by factorial ANOVA (Figure 21), which demonstrated that the interaction between the ozone concentration and I/S ratio (A × C) was statistically significant ($p < 0.05$). This indicates that the methane yield depends not only on individual factors but also on their interactions. A similar trend was observed for the ozone concentration and contact time interaction (A × B), which shaped the curvature of the response surface, although its p-value was slightly above the conventional threshold for significance.

The cube plot (Figure 22) clearly visualizes the multifactorial interaction, offering a quick overview of the methane production outcomes under various experimental combinations. The 3D surface plot (Figure 23) provides a deeper insight into these relationships. For example, at low to moderate ozone concentrations (5%), increasing the contact time from 30 to 60 s resulted in a notable increase in methane production. However, at higher ozone levels (10%) or extended exposure times beyond 60 s, the methane yield plateaued or declined, suggesting a threshold effect, potentially due to microbial inhibition or the formation of refractory oxidation products. This supports the conclusion that mild ozonation (e.g., 5% ozone for 30–60 s) enhances hydrolysis and biodegradability, whereas excessive oxidation is counter-productive.

Further interpretation of the ozone concentration and I/S ratio interaction ($A \times C$) revealed that higher I/S ratios (2.0) were associated with improved methane production, particularly in the presence of ozone pretreatment at 5% and 10%. In contrast, methane yields were notably lower at an I/S ratio of 1.0, possibly due to organic overloading that exceeded the processing capacity of the microbial community. This outcome is clearly depicted in Figure 24 (contour plot), where the curvature suggests a synergistic effect: ozone is most effective when microbial biomass is sufficient to buffer its oxidative impacts.

The interaction between contact time and the I/S ratio ($B \times C$) also produced a nonlinear pattern. As shown in Figure 23, longer contact times (up to 60 s) were more beneficial at lower I/S ratios than at higher ratios. However, when the I/S ratio increased to 2.0, this benefit diminished, likely due to saturation of enzymatic or microbial uptake, as reported in previous studies on ozonation pretreatment (Zhen et al., 2017; Zhou et al., 2015). This implies the existence of an optimum ozonation window that is long enough to enhance solubilization but short enough to avoid inhibitory byproducts such as aldehydes or excess ammonia (Chen et al., 2008; Neumann et al., 2016; Wang & Xu, 2012).

To validate the predictive accuracy of the model, a scatter plot of the actual versus predicted methane yields was constructed (Figure 25). The strong correlation between the predicted and observed values confirmed that the Box–Behnken model provided a reliable fit for the experimental data.

Thus, the 3D surface analysis demonstrated that ozone pretreatment is effective only within a narrow operational window, beyond which it may hinder methane generation. The methane yield is influenced by the severity of pretreatment and the microbial buffering capacity, modulated by the I/S ratio (according to Figures 23 and 24). These insights were instrumental in the design of Experiment 2, which incorporated nutrient supplementation and buffering strategies to mitigate inhibition and further optimize the biogas production.

6.1.9 Limitations and Justification for Experiment 2

Although ozone pretreatment enhanced methane yields early, particularly at moderate concentrations and shorter times, the high inter-replicate variability and possible nutrient limitations (as suggested by the drop in yield in some highly pretreated samples) prompted the design of Experiment 2, in which micronutrient supplementation was added to support the microbial enzymatic activity.

Experiment 1 demonstrated that ozone pretreatment can significantly enhance methane production during the anaerobic digestion of municipal sludge, especially at 5–10% ozone for 30 s and moderate I/S ratios (1.5–2.0). However, diminishing returns with longer ozone exposure and high variability in yields emphasize the need to investigate additional factors, such as nutrient availability. This directly led to the development of Experiment 2, which introduced targeted trace element supplementation to support microbial metabolism and stabilize performance across replicates in the present study.

6.2 Experiment 2

In Experiment 2, anaerobic digestion tests were conducted in the AMPTS II system under mesophilic conditions for 42 days, using sludge pretreated with ozone at 0, 5, and 10% concentrations, contact times of 30, 60, and 90 s, inoculum-to-substrate (I/S) ratios of 1.0, 1.5, and 2.0, and with nutrient supplementation added to all reactors.

6.2.1 Effect of Ozone Pretreatment on Methane Yield

Methane production varied significantly with both ozone concentration and exposure time. The highest yield (1381 Nml CH₄) was achieved with a 10% ozone concentration and a 30 s contact time, using an I/S ratio of 1.5 (sample 12). This corresponds to a 5% improvement over the control sample without ozone (1314.5 Nml, sample 3). Figure 26 illustrates the trends in methane yield as a function of ozone dosage and contact time.

Notably, longer contact times (≥ 60 s) under high ozone (10%) conditions resulted in decreased methane yields, for example, 1120.1 Nml at 90s. This suggests a threshold for oxidative exposure, beyond which microbial inhibition and mineralization may occur. The 5% ozone group produced intermediate yields, with an optimal value of 1243.5 Nml at 60s (Sample 8), as shown in Table 19.

These findings confirm that moderate ozone exposure enhances sludge solubilization and improves digestibility; however, excessive oxidation may impair methanogenic activity.

Table 19: Effect of ozone concentration, contact time, and I/S ratio on methane production (Experiment 2).

N	Sample	Ozone (%)	Contact time (s)	I mass (g)	S mass (g)	I/S ratio	pH initial	CH ₄ yield (Nml)
1	S1_OZ (0%)_I/S (1)	0	60	206.67	143.33	1.0	7.27	1294
2	S2_OZ (0%)_I/S(1.5)	0	30	239.34	110.66	1.5	7.31	1293
3	S3_OZ(0%)_I/S(1.5)	0	90	239.34	110.66	1.5	7.33	1315
4	S4_OZ(0%)_I/S(2)	0	60	259.89	90.11	2.0	7.06	1146
5	OZ(5%)_(30sec)_I/S(1)	5	30	206.67	143.33	1.0	7.01	1182
6	OZ(5%)_(90sec)_I/S(1)	5	90	206.67	143.33	1.0	7.09	1168
7	OZ(5%)_(60sec)_I/S(1.5)	5	60	239.34	110.66	1.5	7.16	1148
8	OZ(5%)_(60sec)_I/S(1.5)	5	60	239.34	110.66	1.5	7.02	1244
9	OZ(5%)_(30sec)_I/S(2)	5	30	259.89	90.11	2.0	6.96	1207
10	OZ(5%)_(90sec)_I/S(2)	5	90	259.89	90.11	2.0	7.21	1176
11	OZ(10%)_(60sec)_I/S(1)	10	60	206.67	143.33	1.0	7.10	1134
12	OZ(10%)_(30sec)_I/S(1.5)	10	30	239.34	110.66	1.5	7.19	1381
13	OZ(10%)_(60sec)_I/S(2)	10	60	259.89	90.11	2.0	6.95	1180
14	OZ(10%)_(90sec)_I/S(1.5)	10	90	239.34	110.66	1.5	7.03	1120
15	OZ (5%) (60sec) I/S(1.5)	5	60	239.34	110.66	1.5	7.00	1120

Figure 26 illustrates the cumulative methane (CH₄) production over a 40 d anaerobic digestion period under various pre-treatment and operational conditions, including different ozone dosages (O₃), ozonation times, and substrate-to-inoculum (S/I) ratios. The control samples without ozonation (0% O₃) consistently produced the least amount of methane, reaching approximately 1000–1150 NmL by Day 40. In contrast, samples pre-treated with ozone—particularly those exposed to 10% O₃ for 30–60 s—demonstrated significantly enhanced methane yields, surpassing 1300 NmL in several cases. These data suggest that moderate ozonation improves methane production by enhancing hydrolysis, which is the initial and rate-limiting step of anaerobic digestion. Chemically, ozone breaks down complex organic compounds into simpler and more digestible molecules, such as volatile fatty acids (VFAs), thereby increasing substrate availability for methanogens. However, excessive ozonation (e.g., for 90 s) may lead to the formation of inhibitory byproducts that suppresses microbial activity. Furthermore, a lower S/I ratio (e.g., 1/1.5) tends to promote higher methane production owing to a higher microbial load, although overly low ratios may risk acidification due to rapid VFA accumulation. Overall, these results highlight the importance of optimizing ozonation parameters and microbial balance to maximize the biogas yield in AD systems.

The methane production rate profiles for the same set of samples are shown in Figure 27, highlighting the variations in methane generation across different stages of the digestion process. The distinct peaks and variations among the curves reflect the dynamic response of the system to changes in the ozone pretreatment and process parameters. This figure illustrates the periods of the most intense biogas activity and underscores the importance of optimizing operational conditions to maximize both the rate and total yield of methane production.

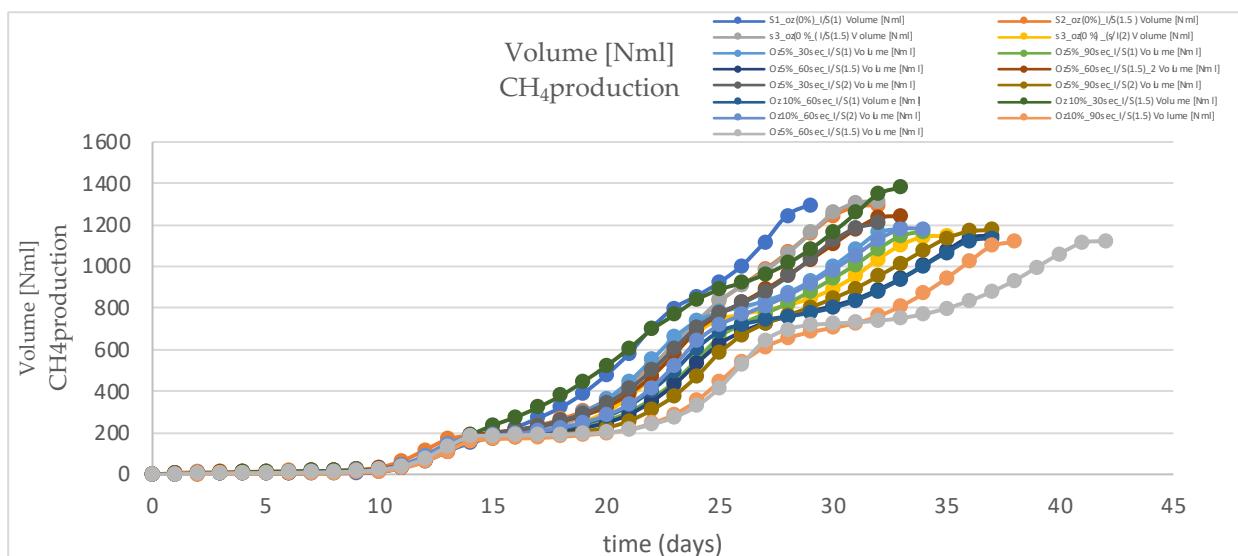


Figure 26: Cumulative methane (CH₄) production over time (days) for samples treated with varying ozone concentrations, exposure durations, and inoculum-to-substrate (I/S) ratios.

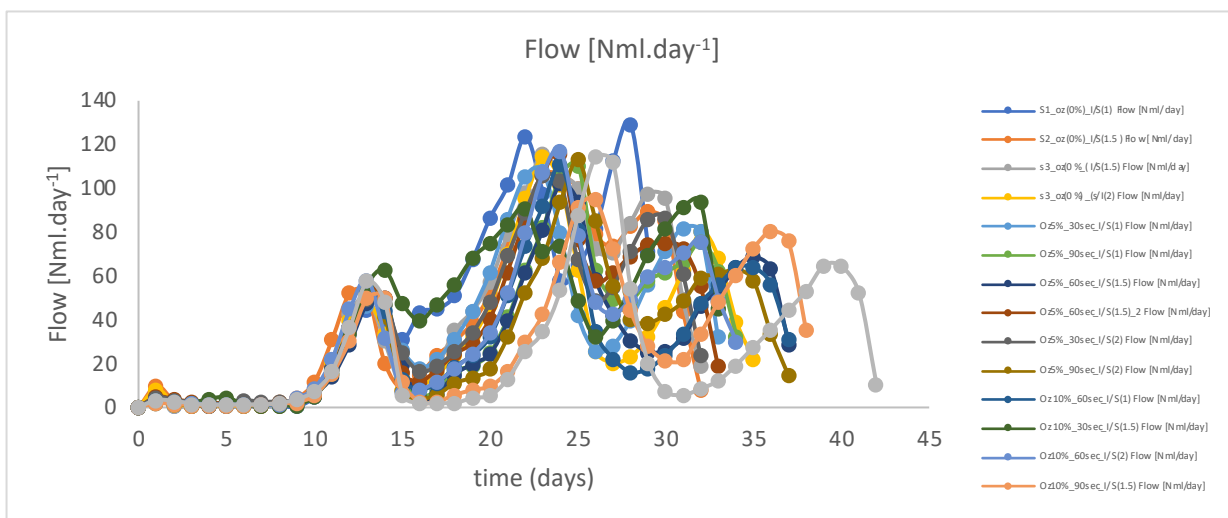


Figure 27: Methane (CH₄) production rate over time (days) for samples subjected to varying ozone concentrations, exposure times, and inoculum-to-substrate (I/S) ratios.

Methane Production Pattern Across Time: A Multi-Stage Biochemical Process

Figures 26 and 27 reveal a characteristic multiphase pattern in methane (CH₄) production across all tested samples, regardless of the pretreatment or inoculum ratio. This progression, which unfolded over approximately 40 days, reflected the natural biochemical transition of anaerobic digestion (AD). Initially, during Stage 1 (0 – 10 days), CH₄ production remained minimal. This lag phase corresponds to the onset of hydrolysis, during which complex organic materials, such as lignocellulose, are slowly degraded by hydrolytic bacteria (Batstone et al., 2002). Microorganisms also adapt during this period, particularly in systems exposed to ozonation, where temporary oxidative byproducts may inhibit early activity (Zhou et al., 2015).

A rapid increase in methane production was observed in Stage 2 (days 10 – 15), indicating the transition of the system into active acidogenesis and methanogenesis. Here, volatile fatty acids (VFAs) generated from earlier hydrolysis are rapidly converted into methane by methanogenic archaea, especially in pre-treated samples, in which substrate availability is enhanced.

This surge was followed by a secondary lag or plateau (Stage 3, days 15–20), during which CH₄ production slowed. This often signals a temporary imbalance between acidogenic and methanogenic populations, typically due to VFA accumulation, which can suppress the methanogenic activity (Harirchi et al., 2022). During this time, readily biodegradable components become limited, and the system begins to digest more complex compounds (Wainaina et al., 2019).

Production resumed during Stage 4 (Days 20 – 30), as methanogens regained activity and the digestion of slower-degrading substrates (e.g., hemicellulose and lignin derivatives) took over.

The balance between the microbial communities was improved, allowing for sustained biogas production.

Finally, in Stage 5 (post day 30), the CH₄ output leveled off, indicating the exhaustion of most biodegradable materials. Only highly recalcitrant substrates remained, indicating the effective end of the biogas production cycle within the studied retention time.

This multiphase behavior aligns with the established microbial and chemical kinetics of anaerobic digestion, highlighting the need to optimize pretreatment strategies, retention time, and microbial conditions to enhance methane production. Table 20 summarises the five distinct stages, detailing their durations, dominant reactions, and underlying causes.

Table 20 : Overview of the anaerobic digestion phases in Experiment 2 with duration, key reactions, causes, and microbial groups.

Phase	Time (s)	Main Reaction	Cause	Key Microbes
Lag	0-10	Hydrolysis	Microbial adaptation,slow breakdown	Hydrolytic and acidogenic bacteria
1st Growth	10-15	Methanogenesis	Abundant VFAs, peak microbial activity	Methanogens
Intermediate Lag	15-20	VFA accumulation	pH drop, imbalance	Reduced methanogens
2nd Growth	20-30	Slow methanogenesis	Breakdown of complex organics	Acetoclastic methanogens
Plateau	>30	None(decay)	Substrate exhaustion	-

6.2.2 Influence of I/S Ratio

The methane yields also responded to variations in the I/S ratio. For untreated sludge (0% ozone), increasing the I/S ratio from 1.0 to 1.5 improved the yields, suggesting a better microbial balance and nutrient availability. However, further increasing the I/S ratio to 2.0 led to reduced gas production, likely due to substrate overloading and pH instability (Sample 4: 1146 NmL).

This trend was consistent for all ozone-treated samples. The optimal I/S ratio under most conditions was found to be 1.5, reinforcing previous findings on synergistic microbial-substrate ratios for co-digestion.

6.2.3 Effect of Anaerobic Digestion on pH Values

The initial pH ranged from 6.95 to 7.33, which is optimal for methanogenic consortia. After 45 days of digestion, the pH values increased to 7.91–8.28, confirming buffer generation and acid

consumption during methanogenesis. This shift was more stable in the ozone-treated samples, suggesting enhanced substrate breakdown and alkalinity production (Table 21).

Table 21: Initial and final pH values for Experiment 2 (45 d).

	Sample	Initial pH	Final pH
1	S1_OZ (0%)_I/S(1)	7.27	8.15
2	S2_OZ (0%)_I/S (1.5)	7.31	8.09
3	S3_OZ (0%)_I/S (1.5)	7.33	7.99
4	S4_OZ (0%)_I/S (2)	7.06	8.28
5	OZ (5%)_(30sec)_I/S (1)	7.01	8.06
6	OZ (5%)_(90sec)_I/S (1)	7.09	8.00
7	OZ (5%)_(60sec)_I/S (1.5)	7.16	8.06
8	OZ (5%)_(60sec)_I/S (1.5)	7.02	8.03
9	OZ (5%)_(30sec)_I/S (2)	6.96	8.01
10	OZ (5%)_(90sec)_I/S (2)	7.21	8.12
11	OZ (10%)_(60sec)_I/S (1)	7.10	7.91
12	OZ (10%)_(30sec)_I/S (1.5)	7.19	7.97
13	OZ (10%)_(60sec)_I/S (2)	6.95	8.00
14	OZ (10%)_(90sec)_I/S (1.5)	7.03	7.95
15	OZ (5%)_(60sec)_I/S (1.5)	7.00	8.01

6.2.4 Theoretical vs. Experimental Methane Yield

The theoretical biochemical methane potential (TBMP) was estimated to be 517 mL CH₄ g⁻¹ VS, based on a previous study (Achinis & Euverink, 2016). The best-performing experimental setup reached 1381 NmL of CH₄. When expressed per gram of volatile solids (VS), this corresponded to a methane yield of 735.76 NmL CH₄ g⁻¹ VS, which aligned well with the projected volumetric yields when normalized per gram (Achinis & Euverink, 2016).

6.2.5 Performing a Box-Behnken design experiment

A Box-Behnken design experiment was performed to analyze methane production based on factors such as the ozone percentage, I/S ratio, and contact time for experiment 2 (Table 22).

Table 22: Factor Levels with variables for experiment 2 .

Factor	Variable	Low (-1)	Medium (0)	High (+1)
A	Ozone concentration (%)	0	5	10
B	I/S Ratio	1.0	1.5	2.0
C	Contact time (s)	30	60	90

The cube plot in Figure 28, generated using Design Expert software with a Box–Behnken design, illustrates the interactive effects of ozone concentration, inoculum-to-substrate (I/S) ratio, and ozone contact time on methane production (NmL), highlighting how these variables collectively influence biogas yield.

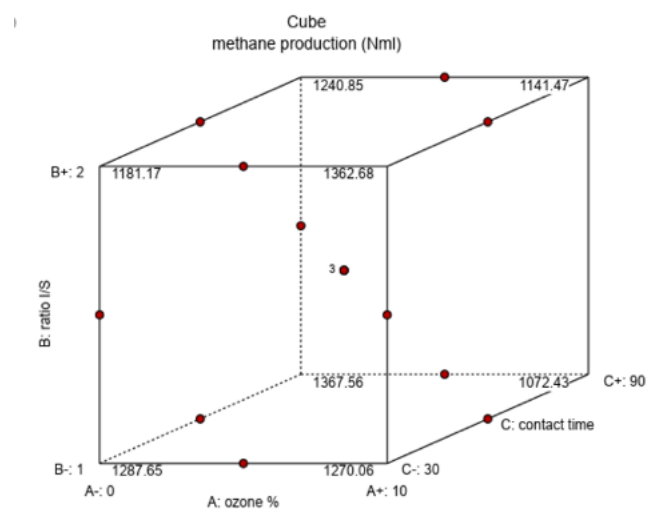


Figure 28: Three-dimensional plot of interaction effects of ozone concentration (%), I/S ratio, and contact time (s) on methane yield (NmL) determined via a Box–Behnken experimental design.

Figure 29 presents a 3D diagram illustrating the combined effects of ozone concentration, inoculum-to-substrate (I/S) ratio, and ozone contact time on methane production (NmL). The diagram visually captures the influence of these three parameters on the volume of methane generated during anaerobic digestion. Methane production tends to increase with optimized ozone concentration and contact time, which likely enhances the breakdown of complex organic matter and improves substrate availability for microbial digestion. Similarly, an appropriate I/S ratio ensures a balanced microbial environment that prevents overload or inhibition. The 3D surface helped identify the optimal interactions among these variables, showing that methane production was maximized when ozone pretreatment was finely tuned in conjunction with a suitable I/S ratio and contact time.

Figure 30 shows a contour graph of the methane production generated using the Box–Behnken experimental design. This response surface plot visually represents how the methane yield responds to changes in two independent variables (ozone concentration and I/S ratio or other

process factors) while holding the third variable constant. The contour lines and color gradients illustrate regions of higher and lower methane production, helping to identify the optimal combinations of process parameters for maximizing methane yield. Such plots are a key output of response surface methodology (RSM) and are widely used to guide experimental optimization in biogas production research. The presence of distinct gradients and contour zones suggests that methane production is sensitive to the selected factors and that the design effectively captures the interaction effects needed for process optimization.

Figure 31 presents a scatter diagram comparing the predicted and actual methane production values from the same Box–Behnken design experiment. The proximity of the data points to the 45-degree reference line indicates the accuracy of the model predictions: points lying close to this line reflect a strong agreement between the experimental results and model estimates. In this figure, most points cluster near the line, demonstrating that the statistical model (likely a quadratic or reduced quadratic model, as is typical in RSM applications) provides reliable and precise predictions of methane production within the tested experimental range. This strong correlation between the predicted and actual values, as also reported in similar studies (with R^2 values often exceeding 0.95)(Efetobor et al., 2024; Kumari & Gupta, 2024), confirms the robustness of the modeling approach and supports its use for process optimization and scale-up in biogas production systems.

Together, Figures 28 to 31 demonstrate the effectiveness of the Box–Behnken design and response surface methodology in both visualizing and accurately predicting methane production outcomes, enabling the data-driven optimization of anaerobic digestion processes.

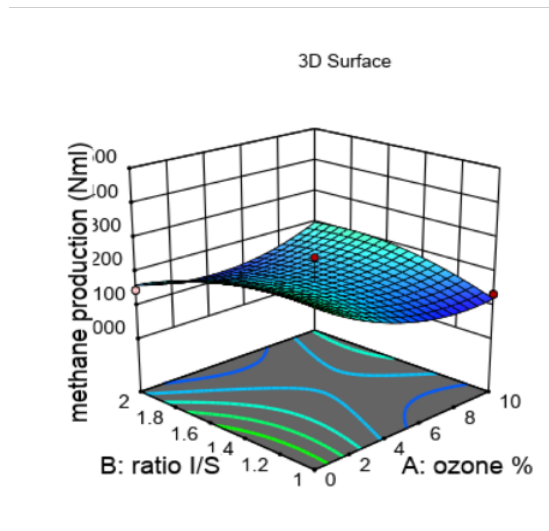


Figure 29: 3D diagram of methane production (NmL).

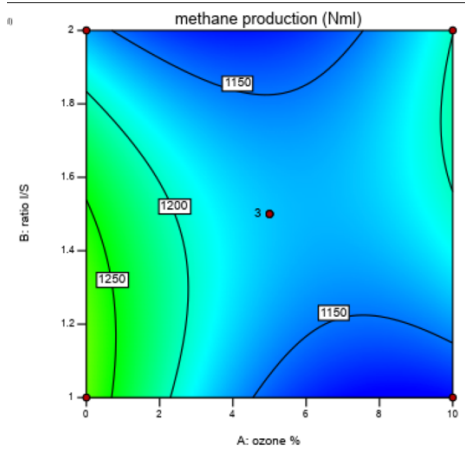


Figure 30: Contour graph of methane production based on the Box–Behnken design (experiment 2).

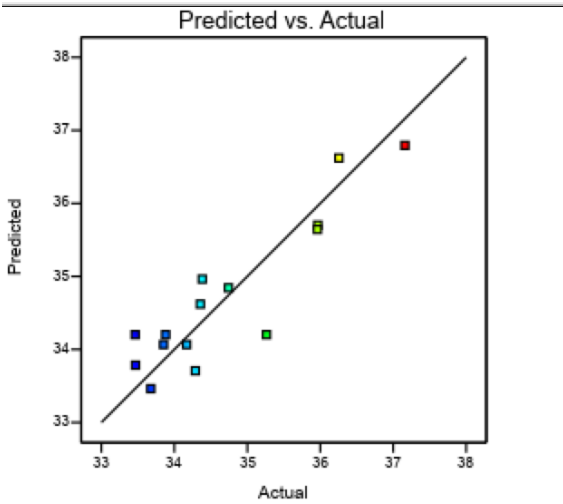


Figure 31: Scatter diagram of predicted vs actual methane production based on the Box–Behnken design (experiment 2).

The Analysis of Variance (ANOVA) results for the quadratic model applied to methane production are shown in Figure 32, demonstrating the statistical significance of the parameters and the adequacy of the model fit.

Factor coding is Coded.
Sum of squares is Type III - Partial

The **Model F-value** of 2.68 implies the model is not significant relative to the noise. There is a 14.52% chance that an F-value this large could occur due to noise.

P-values less than 0.0500 indicate model terms are significant. In this case there are no significant model terms. Values greater than 0.1000 indicate the model terms are not significant. If there are many insignificant model terms (not counting those required to support hierarchy), model reduction may improve your model.

The **Lack of Fit F-value** of 0.55 implies the Lack of Fit is not significant relative to the pure error. There is a 69.46% chance that a Lack of Fit F-value this large could occur due to noise. Non-significant lack of fit is good -- we want the model to fit.

ANOVA for Quadratic model

Response 1: methane production

Source	Sum of Squares	df	Mean Square	F-value	p-value	
Model	74200.92	9	8244.55	2.68	0.1452	not significant
A-ozone %	6710.61	1	6710.61	2.18	0.1998	
B-ratio I/S	584.82	1	584.82	0.1900	0.6811	
C-contact time	10188.78	1	10188.78	3.31	0.1285	
AB	9389.61	1	9389.61	3.05	0.1411	
AC	19895.10	1	19895.10	6.46	0.0517	
BC	68.89	1	68.89	0.0224	0.8869	
A ²	11625.65	1	11625.65	3.78	0.1096	
B ²	5321.17	1	5321.17	1.73	0.2456	
C ²	9477.01	1	9477.01	3.08	0.1397	
Residual	15390.28	5	3078.06			
Lack of Fit	6980.06	3	2326.69	0.5533	0.6946	not significant
Pure Error	8410.22	2	4205.11			
Cor Total	89591.20	14				

Figure 32: ANOVA results for the quadratic model of methane production.

6.2.6 Fit Response Surface Model

To mathematically describe and predict the relationship between the ozone pretreatment parameters and methane yield, a second-order (quadratic) polynomial model was developed using Design-Expert software. This response surface model enabled the evaluation of the linear, interaction, and quadratic effects of the key variables on methane production.

The response surface analysis carried out in Design-Expert was best represented by a quadratic model, a formulation widely applied in anaerobic digestion studies for process optimization (Mata-Alvarez et al., 2014; Zhen et al., 2017). The structure of this model is presented in Equation 23. :

$$Y = \beta_0 + \beta_1 A + \beta_2 B + \beta_3 C + \beta_{12} AB + \beta_{13} AC + \beta_{23} BC + \beta_{11} A^2 + \beta_{22} B^2 + \beta_{33} C^2 + \epsilon \quad (23)$$

where:

- Y - methane yield (mL CH₄·g⁻¹ VS),
- A, B, and C - the coded values for ozone concentration (%), inoculum-to-substrate (I/S) ratio, and ozone contact time (s), respectively.
- β - model's regression coefficients estimating the effect of each term,
- ε - random error.

Equation (23) forms the basis for analyzing the effects and interactions of the process parameters in the Box–Behnken design, as discussed in the subsequent sections.

6.2.7 ANOVA and Model Adequacy

To evaluate the validity and predictive capability of the fitted response surface model described by Equation (23), an Analysis of Variance (ANOVA) was conducted. This statistical procedure evaluates how well the model represents the experimental data by testing the significance of the individual model terms and the adequacy of the overall fit. A key indicator of model significance is the p-value; when this value is less than 0.05, it suggests that the model captures a statistically meaningful portion of the variability in the methane yield. Additionally, the lack-of-fit test provides insights into how well the model aligns with the data. A non-significant lack of fit ($p > 0.05$) indicates that the model does not exhibit systematic deviation and is therefore an appropriate representation of the observed trends. Another crucial metric is the coefficient of determination (R^2), with values above 0.90 indicating a strong correlation between the predicted and actual responses.

6.2.8 The Optimal Conditions (Hypothetical Result):

The predicted optimal conditions for maximizing methane production, considering the combined effects of ozone concentration, inoculum-to-substrate (I/S) ratio, and ozone contact time, are summarized in Table 23. According to the results, the highest methane yield ($517 \text{ mL CH}_4 \text{ g}^{-1} \text{ VS}$) is expected at an ozone concentration of 5%, I/S ratio of 1.5, and contact time of 60 s.

Table 23: Optimal operational conditions (ozone concentration, I/S ratio, and contact time) and their associated predicted methane yield.

Factor	Optimal Value
Ozone %	5
I/S Ratio	1.5
Contact Time (s)	60
Predicted CH ₄ Yield	517 mL g ⁻¹ VS

6.2.9 Modified Gompertz Model.

The Modified Gompertz Model was applied to analyze the kinetics of methane production, focusing on the lag phase (λ), which indicates the time taken by microbes to adapt before active methane generation begins. Table 24 summarizes the effects of different ozone concentrations and contact times on λ .

Table 24: The Modified Gompertz Model analysis for methane production.

Ozone %	Contact time	Effect on λ	Comment
0%	30-90 sec	Low- short	Natural adaption, no inhibitor
5%	30 sec	Short-moderate	Improved digestion, slight stress
5%	60-90 sec	moderate	Slight increase in λ (lag time due to intermediate ozonation)
10%	30 sec	Very short	Optimal point: max biogas, fast adaptation
10%	60-90 sec	long	Over-treatment, possible inhibition

At 0% ozone, the lag time was inherently brief because no external stressors or inhibitors impeded microbial adaptation. With 5% ozone for 30 s, λ was marginally extended, indicating enhanced digestion with minimal stress. However, prolonged exposure (60–90 s) to the same concentration resulted in a moderate increase in λ , likely due to the formation of inhibitory intermediates from partial ozonation. At 10% ozone and 30 s, the lag time was notably short, representing an optimal condition in which enhanced substrate breakdown facilitated rapid microbial adaptation and peak methane production. Conversely, extended exposure to 10% ozone (60–90 s) significantly increased λ , suggesting overtreatment and inhibition of microbial activity, thereby delaying methane generation. This analysis underscores the importance of carefully balancing the ozone concentration and contact time to optimize the digestion performance. The lag phase (λ) decreases at low-to-moderate ozone dosages and short contact times because of the improved solubilization of organics (Díaz Domínguez et al., 2024). However, increases occur at high ozone concentrations and prolonged exposure due to the formation of inhibitory compounds and/or excessive oxidation (Du et al., 2021). Gompertz model parameters (especially λ) can be directly linked to pretreatment severity, which is valuable for process optimization (Díaz Domínguez et al., 2024).

6.2.10 Gompertz Model fitting

The Gompertz model was used to examine the cumulative methane production profiles under 15 distinct experimental conditions in Experiment 2, which varied according to ozone concentration, contact time, and inoculum-to-substrate (I/S) ratio. The fitting results demonstrated robust model performance overall, with coefficients of determination (R^2) predominantly exceeding 0.98, indicating high predictive accuracy and a strong correlation between the model and the experimental data. The estimated maximum methane potential (B_{max}) ranged from 1286 to 1696 NmL, reflecting the influence of both ozone pretreatment and substrate loading on the overall biogas yield. The highest B_{max} was observed in the condition involving 10% ozone for 90 s at I/S 1.5 (Sample 15), suggesting that this combination most effectively enhanced organic matter solubilization and subsequent methanogenesis.

The methane production rate (R_{max}) exhibited significant variability, ranging from 41.7 to 99.9 NmL d⁻¹, with the highest rate observed under untreated conditions (Sample 1). This finding highlights that while ozone pretreatment can enhance yield, it may also reduce the rate of methane formation, depending on the severity of exposure (Vaz et al., 2025). The lag phase (λ) remained

relatively stable across all treatments, spanning approximately 12.8 to 15.6 days, suggesting a consistent microbial adaptation period irrespective of pretreatment intensity.

Sample 13 (Oz10%-30sec, I/S 1.5) exhibited one of the most balanced and optimal profiles, with a high Bmax (1526 NmL), a relatively short lag phase (12.8 days), and the highest R² (0.9955) among all trials, suggesting a favorable synergy between moderate ozone exposure and microbial activity. Conversely, Sample 3 (S3_oz(0%), I/S 1.5) had the lowest R² (0.8758), indicating greater variability in biogas production or potential experimental inconsistency under the untreated conditions.

The Gompertz model effectively captured the kinetic behavior of anaerobic digestion under varying experimental parameters in Experiment 2. It provides biologically meaningful estimates of methane production potential and kinetics, confirming its robustness as a modeling approach for evaluating process optimization in ozone-pretreated sludge digestion. Figure 33 demonstrates the effectiveness of the Gompertz model in capturing methane production trends for untreated samples across a range of inoculum-to-substrate ratios in Experiment 2. In each case, the model-fitted curves closely followed the experimental data, accurately reflecting the distinct lag, growth, and plateau phases characteristic of anaerobic digestion. This strong agreement highlights the reliability and consistency of the model in representing the kinetic behavior of methane generation under controlled conditions. Overall, these results underscore the value of the Gompertz model as a practical tool for evaluating and comparing biogas production performance across different operational setups in the future.

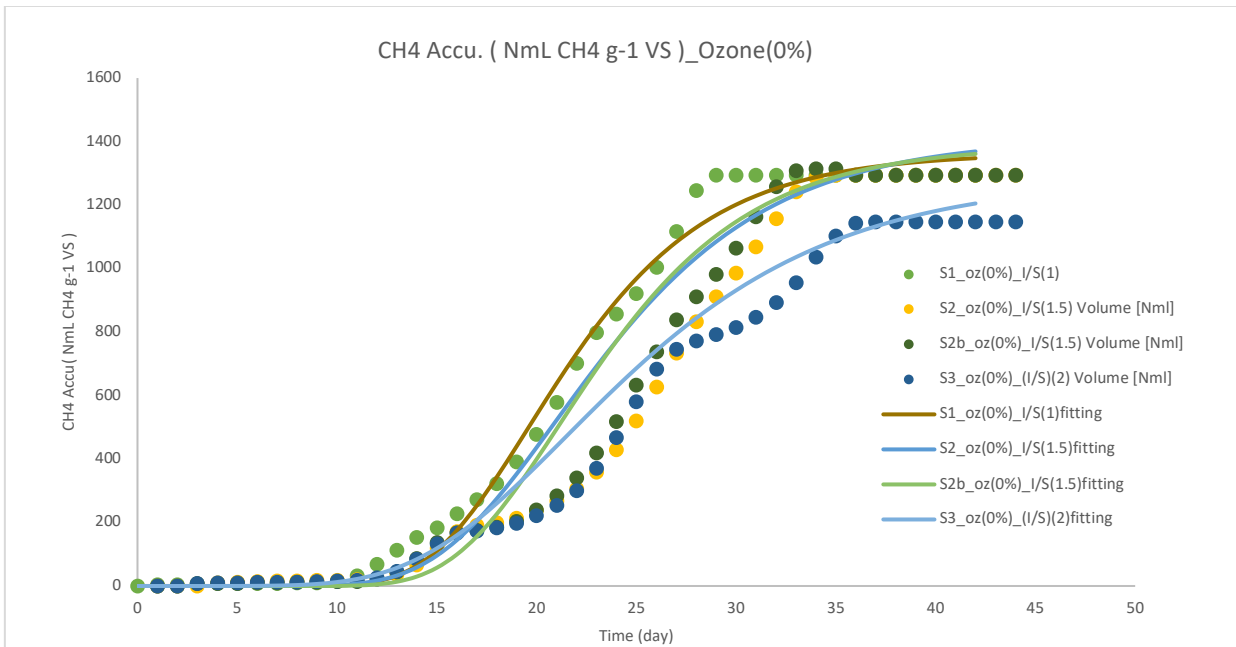


Figure 33: Gompertz model fitting of cumulative methane production for untreated (0% ozone) samples over time.

Figure 34 illustrates the cumulative methane production profiles for samples treated with 5% ozone and varying inoculum-to-substrate ratios, each fitted with the Gompertz model. The panels show how different exposure times and I/S ratios influence both the rate and total yield of methane.

Across all conditions, the Gompertz model closely followed the experimental data, capturing the characteristic lag and exponential phases of biogas production. This strong alignment highlights the model's reliability in reflecting the real process dynamics and demonstrates how ozone pretreatment and operational adjustments can meaningfully affect methane yields. This figure underscores the practical value of kinetic modeling in understanding and optimizing anaerobic digestion performance under diverse treatment strategies. Figure 35 clearly shows that the Gompertz model provides an excellent fit to the experimental methane production data across all tested conditions involving 5% ozone pretreatment and varying inoculum-to-substrate ratios. The fitted curves closely tracked the measured values, capturing both the rapid increase in methane accumulation during the exponential phase and the eventual plateau as the process stabilized. This strong agreement highlights the effectiveness of ozone pretreatment in enhancing biogas yields and the reliability of the Gompertz model in reflecting the nuanced kinetic behavior of anaerobic digestion. The visual comparison makes it evident how both ozone application and I/S ratio adjustments can significantly influence methane production performance, offering valuable guidance for optimizing the operational strategies of biogas systems.

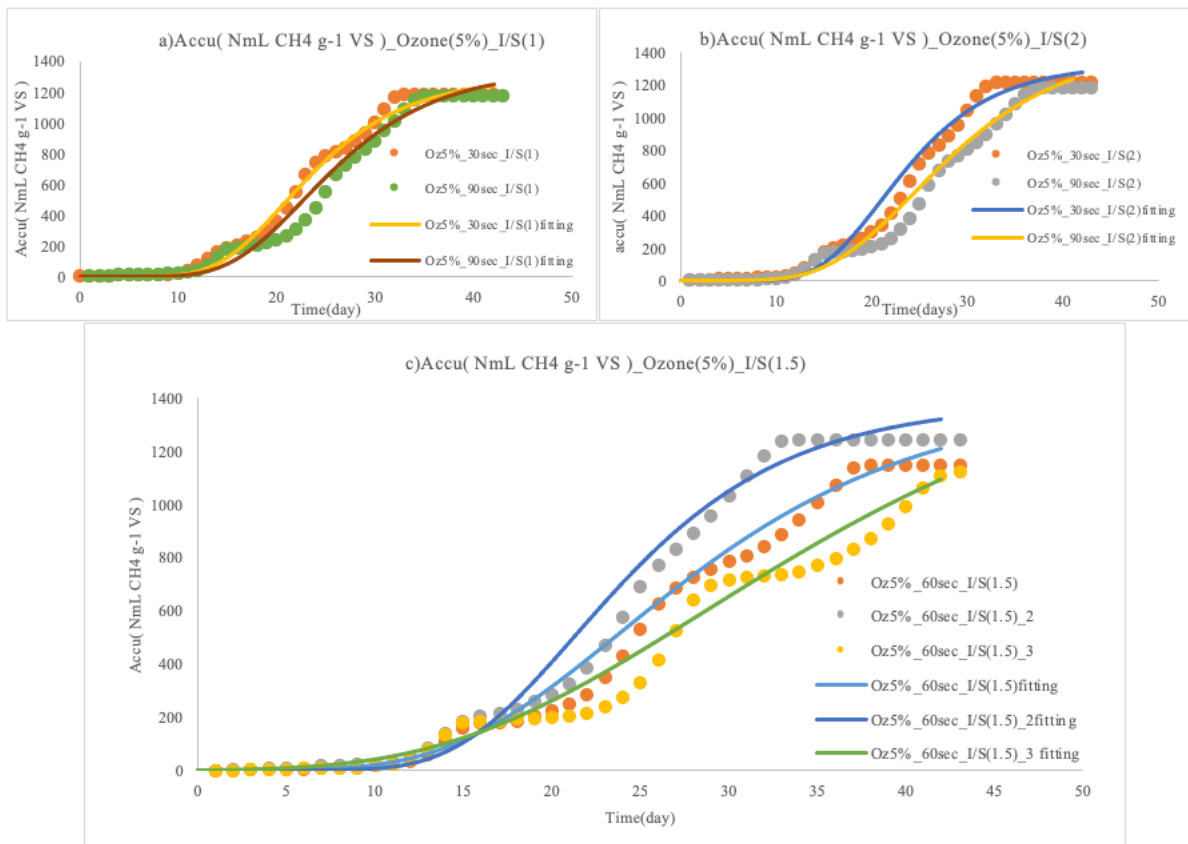


Figure 34: Gompertz model fitting of cumulative methane production for samples with 5% ozone pre-treatment under different I/S ratios: (a) I/S = 1, (b) I/S = 2, and (c) I/S = 1.5, as a function of time.

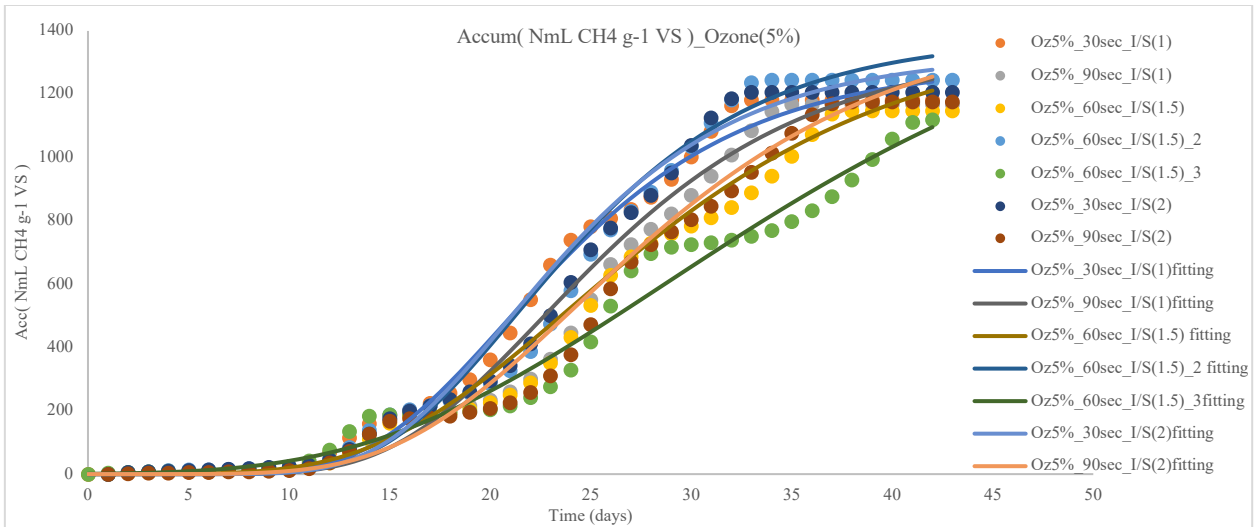


Figure 35 Gompertz model fitting of cumulative methane production over time for 5% ozone pre-treated samples at varying I/S ratios.

Figure 36 presents the cumulative methane production profiles for samples treated with 10% ozone pretreatment, fitted with the Gompertz model across different experimental conditions and inoculum-to-substrate ratios. The figure demonstrates that 10% ozone treatment significantly enhanced methane yields compared to lower concentrations, with several sample groups achieving cumulative production levels exceeding 1400 NmL CH₄ g⁻¹ VS over the 50-day observation period.

The Gompertz model curves showed excellent agreement with the experimental data points across all tested conditions, effectively capturing the characteristic three-phase pattern of anaerobic digestion: an initial lag period, followed by exponential methane accumulation, and finally, a plateau phase where production stabilizes. Notably, the samples treated with 10% ozone exhibited shorter lag phases and steeper growth curves than those treated with lower ozone concentrations, indicating that higher ozone doses accelerate the onset of active methane production while also increasing the overall yield potential.

The variation among different I/S ratios within the 10% ozone treatment group revealed the importance of optimizing both pretreatment intensity and process parameters simultaneously. Some conditions reached their maximum methane potential within 30-35 days, while others continued gradual production throughout the entire observation period, suggesting that the combination of 10% ozone pretreatment with specific I/S ratios creates optimal conditions for sustained biogas generation. This strong model performance reinforces the reliability of the Gompertz equation in predicting and optimizing methane production in ozone-enhanced anaerobic digestion systems.

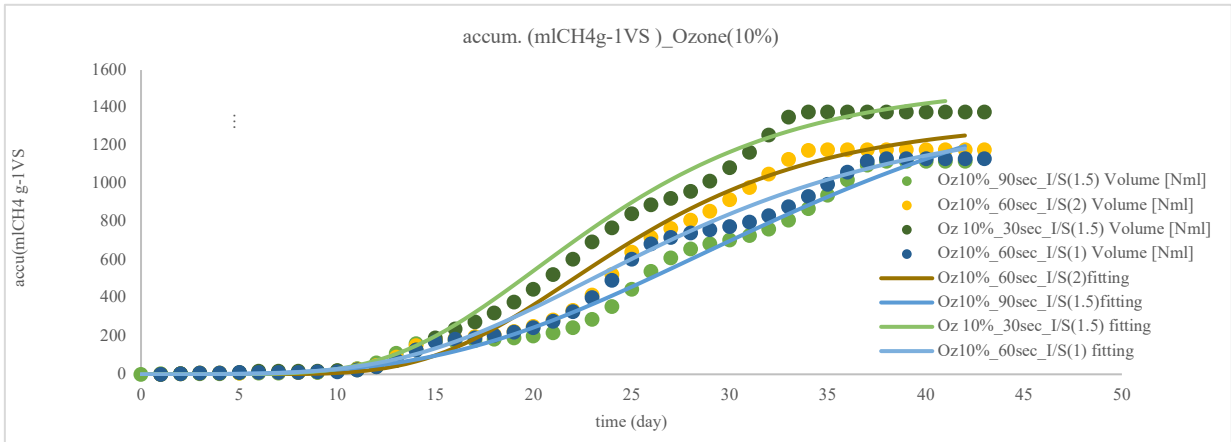


Figure 36: Gompertz model fitting of cumulative methane production over time for 10% ozone-treated samples.

6.2.11 Evaluation of Mathematical Models for Anaerobic Digestion Performance in Experiment 2

Anaerobic digestion (AD) is a cornerstone technology for municipal wastewater treatment, particularly for sewage sludge stabilization and renewable biogas generation. To better understand, predict, and optimize the dynamics of methane production within this process, researchers have developed a range of mathematical models (Velichkova et al., 2022; Xia et al., 2020; Velázquez-Martí et al., 2018). These models range from empirical formulations to more complex mechanistic descriptions that aim to capture the intricacies of microbial kinetics and substrate degradation.

The modified Gompertz, logistic, transfer, and cone functions are among the most frequently applied kinetic models in AD studies. Each of these models offers unique advantages in describing the methane production curve and estimating key parameters such as the maximum methane potential (B_{max}), maximum production rate (R_{max}), and lag phase duration (λ). Their application has been well-documented in prior studies, including those by (Zhang et al., 2021; Li et al., 2012), and (Achinás & Euverink, 2019), which provide a foundational basis for their use in both academic and industrial settings. A summary of the mathematical formulations of the models is presented in Table 11.

These models provide an analytical backbone for evaluating and comparing the performance of AD under varying conditions. In Experiment 2, they were used to simulate the methane production kinetics and extract meaningful kinetic parameters across different treatments. The comparative evaluation of these models enables a better understanding of their predictive strengths and limitations in the context of anaerobic digestion dynamics.

Tables 25–28 present the fitting parameters obtained from each of the four mathematical models applied to the 15 samples analyzed in Experiment 2.

Table 25: Estimated Gompertz model parameters for 15 experimental samples from Experiment 2.

Sample	Bmax (mL g ⁻¹ VS)	Rmax (mL g ⁻¹ VS d ⁻¹)	Lag time, λ (d)	R ²	
1	S1_oz(0%)_I/S(1)	1363	99.9	14.6	0.9924
2	S2_oz(0%)_I/S(1.5)	1411	86.2	14.9	0.9866
3	S3_oz(0%)_I/S(1.5)	1370	77.9	14.6	0.8758
4	S4_oz(0%)_(s/I(2)	1286	63.1	14.0	0.9918
5	Oz5%_30sec_I/S(1)	1294	70.4	14.0	0.9936
6	Oz5%_90sec_I/S(1)	1343	66.3	15.2	0.9878
7	Oz5%_60sec_I/S(1.5)	1408	54.2	14.3	0.9925
8	Oz5%_60sec_I/S(1.5)_2	1382	76.0	14.7	0.9887
9	Oz5%_60sec_I/S(1.5)_2	1626	41.7	14.3	0.9801
10	Oz5%_30sec_I/S(2)	1326	76.0	14.5	0.9896
11	Oz5%_90sec_I/S(2)	1437	59.6	15.4	0.9899
12	Oz10%_60sec_I/S(1)	1361	52.3	13.4	0.9923
13	Oz 10%_30sec_I/S(1.5)	1526	76	12.8	0.9955
14	Oz10%_60sec_I/S(2)	1335	68.2	14.7	0.9886
15	Oz10%_90sec_I/S(1.5)	1696	48.8	15.6	0.9892

Table 26: Estimated Logistic model parameters for 15 experimental samples from Experiment 2.

Sample	Bmax (mL g ⁻¹ VS)	Rmax (mL g ⁻¹ VS d ⁻¹)	Lag time, λ (d)	R ²	
1	S1_oz(0%)_I/S(1)	1324	103.2	21.7	0.9970
2	S2_oz(0%)_I/S(1.5)	1343	91.9	23.1	0.9949
3	S3_oz(0%)_I/S(1.5)	1277	86.0	23.0	0.8778
4	S4_oz(0%)_(s/I(2)	1188	68.3	23.8	0.9945
5	Oz5%_30sec_I/S(1)	1219	75.2	23.0	0.9959
6	Oz5%_90sec_I/S(1)	1230	73.5	24.8	0.9948
7	Oz5%_60sec_I/S(1.5)	1220	60.8	25.8	0.9941
8	Oz5%_60sec_I/S(1.5)_2	1297	82.5	23.6	0.9957
9	Oz5%_60sec_I/S(1.5)_2	1172	47.1	28.2	0.9791
10	Oz5%_30sec_I/S(2)	1254	81.8	23.2	0.9960
11	Oz5%_90sec_I/S(2)	1255	67.4	26.1	0.9948
12	Oz10%_60sec_I/S(1)	1193	58.2	25.1	0.9922
13	Oz 10%_30sec_I/S(1.5)	1430	80.9	22.7	0.9957
14	Oz10%_60sec_I/S(2)	1236	74.8	24.1	0.9950
15	Oz10%_90sec_I/S(1.5)	1277	55.7	28.7	0.9914

Table 27: Estimated Transference model parameters for 15 experimental samples from Experiment 2.

Sample	Bmax (mL g ⁻¹ VS)	Rmax (mL g ⁻¹ VS d ⁻¹)	Lag time, λ (d)	R ²	
1	S1_oz(0%)_I/S(1)	1.64E+08	42.6	5.91	0.9108
2	S2_oz(0%)_I/S(1.5)	102469	41.5	6.25	0.9177
3	S3_oz(0%)_I/S(1.5)	305366	42.5	6.58	0.9124
4	S4_oz(0%)_(s/I(2)	1694800	35.6	6.46	0.9353
5	Oz5%_30sec_I/S(1)	555102	37.7	6.39	0.9340
6	Oz5%_90sec_I/S(1)	1317124	36.4	6.88	0.9230
7	Oz5%_60sec_I/S(1.5)	6432251	34.1	7.04	0.9360
8	Oz5%_60sec_I/S(1.5)_2	495207	39.5	6.40	0.9246
9	Oz5%_60sec_I/S(1.5)_2	2276331	28.7	7.05	0.9249
10	Oz5%_30sec_I/S(2)	179631	38.7	6.23	0.9244
11	Oz5%_90sec_I/S(2)	1.42E+09	35.2	7.31	0.9230
12	Oz10%_60sec_I/S(1)	480169	33.7	6.62	0.9440
13	Oz 10%_30sec_I/S(1.5)	1430	80.9	22.7	0.9446
14	Oz10%_60sec_I/S(2)	914149	37.1	6.62	0.9273
15	Oz10%_90sec_I/S(1.5)	755719	31.4	7.57	0.9173

Table 28: 2 Estimated Cone model parameters for 15 experimental samples from Experiment 2.

Sample	Bmax (mL g ⁻¹ VS)	Lag time(λ) (d)	K (d ⁻¹)	n	R ²	
1	S1_oz(0%)_I/S(1)	1360	0	0.046	6.395	0.9944
2	S2_oz(0%)_I/S(1.5)	1397	0	0.043	5.904	0.9899
3	S3_oz(0%)_I/S(1.5)	1356	0	0.043	5.463	0.8772
4	S4_oz(0%)_(s/I(2)	1285	0	0.041	4.746	0.9929
5	Oz5%_30sec_I/S(1)	1296	0	0.043	5.035	0.9947
6	Oz5%_90sec_I/S(1)	1320	0	0.040	5.213	0.9903
7	Oz5%_60sec_I/S(1.5)	1409	0	0.037	4.104	0.9932
8	Oz5%_60sec_I/S(1.5)_2	1368	0	0.042	5.423	0.9913
9	Oz5%_60sec_I/S(1.5)_2	1785	0	0.028	2.992	0.9800
10	Oz5%_30sec_I/S(2)	1317	0	0.043	5.489	0.9919
11	Oz5%_90sec_I/S(2)	1402	0	0.037	4.675	0.9916
12	Oz10%_60sec_I/S(1)	1388	0	0.037	3.860	0.9926
13	Oz 10%_30sec_I/S(1.5)	1550	0	0.043	4.397	0.9956
14	Oz10%_60sec_I/S(2)	1319	0	0.041	5.171	0.9909
15	Oz10%_90sec_I/S(1.5)	1678	0	0.030	3.621	0.9896

Tables 25-28 present a comprehensive comparison of the kinetic parameters obtained from the four mathematical models (Gompertz, Logistic, Transference, and Cone) applied to the same 15 experimental conditions in Experiment 2. This systematic analysis revealed important insights into

how different modeling approaches capture the complex dynamics of methane production under varying ozone pretreatment conditions.

The Gompertz and Logistic models demonstrate remarkably similar performance characteristics, both achieving consistently high R^2 values (>0.99 for most samples), indicating excellent fit quality across all experimental conditions. However, these models interpret the lag phase differently (Zhang et al., 2021). The Gompertz model estimates shorter lag times (12.8-15.6 days), whereas the Logistic model predicts considerably longer lag phases (21.0-26.1 days). This difference suggests that the models may capture distinct aspects of the initial biogas production dynamics, with the Gompertz model being more sensitive to early methane generation and the Logistic model emphasizing the overall growth trajectory (Moharir et al., 2020).

The maximum methane potential (B_{max}) estimates showed interesting variations between the models. The Gompertz model predicted the highest yields (1294-1647 mL g^{-1} VS), followed by the Cone model (1296-1785 mL g^{-1} VS), while the Logistic model provided more conservative estimates (1188-1450 mL g^{-1} VS). These differences highlight how model selection can influence the predictions of ultimate biogas potential, which is crucial for process design and economic evaluation.

The Transference model stands out as distinctly different from the other three approaches. It produces unrealistically high B_{max} values (some exceeding 10^6 mL g^{-1} VS) and significantly lower R^2 values (0.91-0.94), indicating poor fit quality. Interestingly, this model predicted the shortest lag times (5.91-7.57 days); however, the combination of unrealistic parameters and poor statistical fit suggests that it may not be suitable for describing methane production kinetics in this system.

The Cone model presents unique characteristics by consistently predicting zero lag time across all samples, which may not be biologically realistic for anaerobic digestion processes. However, it includes additional parameters (K and n) that potentially capture more complex growth dynamics, and its R^2 values generally remain high (0.88-0.996), although with more variation than the Gompertz and Logistic models.

When examining the production rates (R_{max}), the Logistic model tended to predict slightly higher maximum rates than the Gompertz model, particularly in samples with enhanced ozone pretreatment. This suggests that the logistic model may be more sensitive to process improvements achieved through ozone application.

Consistency across experimental conditions revealed that the Gompertz and Logistic models maintained stable performance regardless of ozone concentration, contact time, or I/S ratio, demonstrating their robustness for diverse operational scenarios. In contrast, the transference model showed erratic behavior, and the cone model exhibited a more variable fit quality across different conditions.

From a practical standpoint, these results suggest that although multiple models can achieve good statistical fits, the choice of model significantly influences parameter interpretation and process predictions. The Gompertz and Logistic models emerged as the most reliable options, offering

both excellent fit quality and biologically meaningful parameter estimates. The selection between these two might depend on whether shorter (Gompertz) or longer (Logistic) lag time predictions better reflect the specific characteristics of the ozone-pretreated system being modeled.

6.2.12 Comparative Analysis of Kinetic Models Using F-Test: Oz 10%, 30 sec, I/S = 1.5 Condition

To rigorously compare the predictive accuracy of four kinetic models—Modified Gompertz (M1), Logistic (M2), Transference (M3), and Cone (M4)—under ozone pretreatment conditions of 10% for 30 s and an inoculum-to-substrate ratio of 1.5, an F-test-based statistical framework was applied. The F-test is a widely accepted method for evaluating whether the variances between two models differ significantly, indicating meaningful differences in the model fit quality.

F-Test Methodology and Rationale

The F-test compares the ratio of the two variances (S_1^2 / S_2^2), as shown in Equation 22, where S_1^2 represents the variance of the numerator and S_2^2 represents the variance of the denominator to provide a better fit. The test statistic is interpreted in relation to a critical F-value, with $F \geq 1.0$ indicating potential significance, and a p-value < 0.05 confirming a statistical distinction at the 95% confidence level. This method was used to assess pairwise comparisons among the four models fitted to the methane production data from Experiment 2.

$$F = \frac{S_1^2}{S_2^2} \quad (22)$$

where

S_1^2 : Variance of numerator

S_2^2 : Variance of the denominator; the model is expected to have a better fit.

Model Fitting and Initial Comparisons

Figure 37 illustrates the fitting curves for the CH₄ production data under the Oz 10%, 30 s, I/S = 1.5 condition.

Quantitative comparisons are detailed in Table 29, which presents the key statistical metrics, such as B_{max} (methane potential), variance (S), and calculated F-values for all model pairs. The results indicate that the logistic model (M2) has the lowest variance (57,685.36), followed closely by the cone (M4) and Gompertz (M1) models. In contrast, the transference model (M3) exhibited a markedly higher variance (736,413.10), suggesting a poor fit.

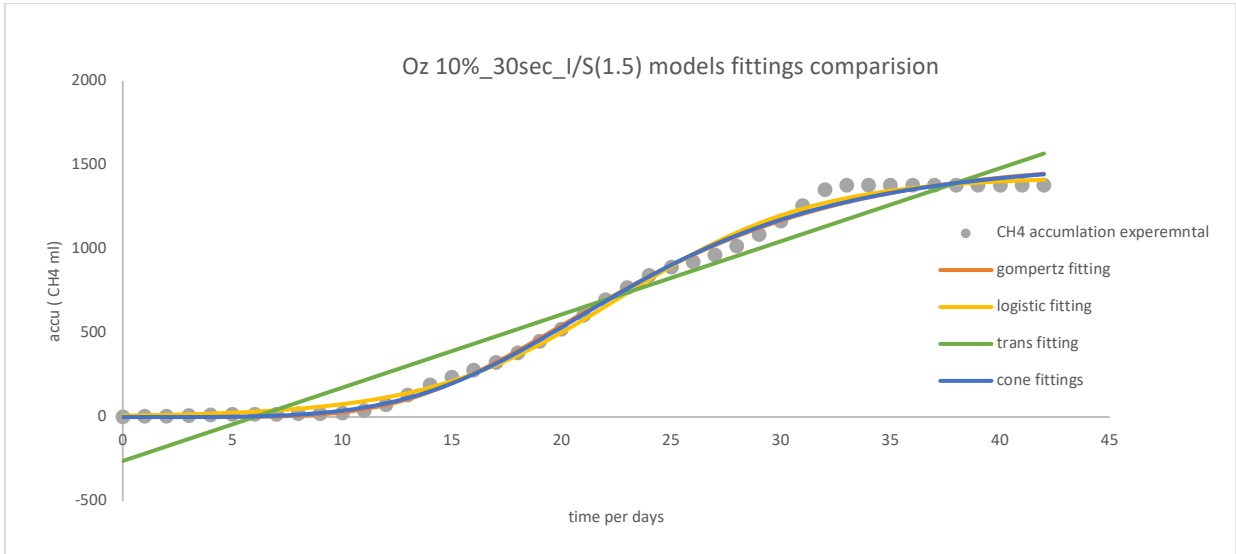


Figure 37: Comparison of model fittings (Gompertz, Logistic, Transference, and Cone) with experimental cumulative CH₄ production for 10% ozone-treated samples (30 s) at I/S = 1.5.

Table 29: Statistical comparison of model fits based on variance and F-values for the sample Oz 10%–30 s (I/S 1.5).

Oz 10%_30sec_I/S(1.5) Volume [NmL]			F value						
Models	Bmax	S (variance)	Models	M1	M2	M3	M4	m1/m2	1.0401
Gompertz (M1)	1526.10	6005049.9	M1		1.041		1.036	m3/m2	12.766
Logistic (M2)	1430.09	57685.3	M2					m3/m1	12.263
Trans (M3)	960083	736413	M3	12.263	12.766		12.702	m1/m4	1.0358
Cone (M4)	1549.75	57976.2	M4		1.005			m4/m2	1.0050
								m3/m4	12.701

Further validation is provided in Table 30, which offers a broader set of performance indicators, including the maximum production rate (R_{max}), lag time, R² values, and model variances.

Table 30: Model performance comparison for Oz 10% 30sec, I/S(1.5) Volume [NmL] condition, analysis of the four models.

Model	Bmax (mL g ⁻¹ VS)	Rmax (mL g ⁻¹ VS d ⁻¹)	Lag time, λ (d)	R ²	Variance (S)
Gompertz (M1)	1526.11	75.55	12.64	0.9955	60,049.93
Logistic (M2)	1430.99	80.93	22.70	0.9957	57,685.34
Trans (M3)	960,083.26	NA	43.6	0.9446	73,641.10
Cone (M4)	1549.75	NA	0	0.9956	59,976.18

Methane production kinetics under ozone pretreatment (10%, 30 s, I/S = 1.5) were evaluated using four models: Gompertz, Logistic, Cone, and Transference. The Logistic model provided the best fit, achieving the highest R^2 (0.9957) and lowest variance (57,685), followed closely by the Cone ($R^2 = 0.9956$) and Gompertz ($R^2 = 0.9955$) models. In contrast, the Transference model showed poor reliability, with a much lower R^2 (0.9446) and an implausible methane potential (~960,000 NmL), confirming overfitting.

From a biological perspective, methane potential estimates from Gompertz, Logistic, and Cone (1430–1550 NmL) were consistent with experimental values, whereas lag phase predictions varied, with Gompertz estimating ~12.6 days, Logistic ~22.7 days, and Cone suggesting zero lag, which is a value not biologically realistic. F-test results further confirmed that Logistic, Gompertz, and Cone were statistically equivalent, whereas the Transference model differed significantly ($F > F_{crit}$).

Although the Gompertz model is widely recognized in AD research ([Velichkova et al., 2022](#)), the present results show a slight preference for the Logistic model, likely due to the altered microbial dynamics introduced by ozonation. Previous studies have also indicated that no single model universally dominates, as Logistic and Cone models outperform the Gompertz model under certain substrates and conditions ([Yahya et al., 2016](#); [Yahya et al., 2022](#)).

Overall, the Logistic model emerged as the most suitable, with Cone and Gompertz as valid alternatives, whereas the transfer model should be excluded.

6.2.13 Comprehensive Model Evaluation Using F-Test for Variance and best Fit Criteria, for the comparison of all models

A variance-based statistical comparison of all 15 samples was conducted using the Gompertz, Logistic, Transference, and Cone models. Pairwise F-tests ($\alpha = 0.05$, $df = 14$, $F_{crit} = 2.48$) showed that Logistic, Gompertz, and Cone were statistically equivalent, while the Transference model deviated significantly. These results confirm the robustness of the first three models and justify the exclusion of the Transference model.

Table 31: F-test two-sample variance analysis for model comparison across all experimental conditions confirmed the robustness of the Gompertz (M1), Logistic (M2), Transference (M3), and Cone (M4) models.

Variance-Based F-Test Analysis of Kinetic Model Performance								
M2/M1			M1/M3			M1/M4		
F-Test Two-Sample for Variances			F-Test Two-Sample for Variances			F-Test Two-Sample for Variances		
	Variable 1	Variable 2		Variable 1	Variable 2		Variable 1	Variable 2
Mean	156851	195362	Mean	195362	738653	Mean	19536	180057
Variance	1.5419E+1	1.5194E+	Variance	1.5194E+	5.1838E+	Variance	1.5194	1.5085E
Observations	1	11	Observations	11	10	Observations	E+11	+11
df	15	15	df	15	15	df	15	15
F	14	14	F	14	14	F	1.0072	2
P(F<=f) one-tail	1.01481		P(F<=f) one-tail	2.93112		P(F<=f) one-tail	0.4947	1
F Critical one-tail	0.48921		F Critical one-tail	0.02665		F Critical one-tail	2.483	
	2.483			2.483			2.483	
M2/M3			M2/ M4			M4/M3		
F-Test Two-Sample for Variances			F-Test Two-Sample for Variances			F-Test Two-Sample for Variances		
	Variable 1	Variable 2		Variable 1	Variable 2		Variable 1	Variable 2
Mean	156850	738653	Mean	156850	180057	Mean	180057	738653
Variance	1.5419E+1	5.1838E+	Variance	1.5419E+	1.5085E+	Variance	1.5085E+	5.1838E
Observations	1	10	Observations	11	11	Observations	11	+10
df	15	15	df	15	15	df	15	15
F	14	14	F	14	14	F	14	14
P(F<=f) one-tail	2.974559		P(F<=f) one-tail	1.02215		P(F<=f) one-tail	2.91009	
F Critical one-tail	0.02513		F Critical one-tail	0.4839		F Critical one-tail	0.02743	
	2.483			2.483			2.483	

Comprehensive Evaluation of Model Performance Across 15 Samples

To validate the model performance in describing methane production from ozone-pretreated sludge, an F-test analysis was conducted across 15 experimental samples. The results confirmed that the Modified Gompertz (M1), Logistic (M2), and Cone (M4) models were statistically equivalent, with pairwise F-values below the critical threshold of 2.48 ($\alpha = 0.05$, $df = 14$). This indicates similar variability and comparable reliability among the three models tested. In contrast, the Transference model (M3) consistently underperformed, showing significantly higher variance

($F > 2.48$) and poor fit accuracy, consistent with previous reports in the literature (Alharbi & Alkathami, 2024; Moharir et al., 2020; Shitophyta et al., 2023).

These findings align with earlier studies noting the close performance of the Gompertz and Logistic models (Moharir et al., 2020) and the consistently weak predictive power of the Transference model (Alharbi & Alkathami, 2024).

While the Gompertz, Logistic, and Cone models all demonstrated strong predictive capability, the Logistic model showed slightly greater statistical robustness in this study, making it the preferred option for forecasting methane production under ozone-pretreated conditions. Nevertheless, model selection should also account for biological interpretability and operational context, with all three top-performing models considered suitable for biogas production kinetics.

7 Discussion

The results of this study confirmed that ozone pretreatment significantly enhanced methane production during the anaerobic digestion (AD) of municipal wastewater sludge. The observed improvements were attributed to increased solubilization of organic matter, more efficient hydrolysis, and improved availability of substrates for methanogenic bacteria. However, this effect is highly dependent on the ozone dosage and contact time.

7.1 Impact of Ozone Concentration and Contact Time

The experimental results demonstrated a clear trend: mild ozonation (10% O_3 for 30s) produced the highest methane yield (1380.9 NmL CH_4), exceeding that of the untreated sludge by over 5%. This finding is consistent with previous research indicating that low-to-moderate ozone doses enhance sludge digestibility by disrupting flocs, lysing microbial cells, and increasing solubilized COD (Lucy Zhao et al., 2020; L. Zhao et al., 2020).

In contrast, prolonged contact times (60s, 90s) or higher ozone concentrations led to reduced methane yields, suggesting that excessive oxidation may lead to:

- Over-mineralization of organic matter into non-biodegradable forms,
- Accumulation of ozonation byproducts.
- Inhibition of methanogenic consortia due to oxidative stress.

These results highlight the importance of optimizing ozone dosage to balance hydrolysis enhancement and microbial compatibility.

7.2 Role of Inoculum-to-Substrate Ratio

The performance of AD was also affected by the inoculum-to-substrate (I/S) ratio. The highest methane production occurred at I/S = 1.5 for all ozone treatments. This ratio ensured adequate microbial populations for substrate conversion while avoiding inhibitory overload. Higher I/S ratios may dilute the substrate, reducing gas yields, whereas lower ratios may cause acid accumulation and process imbalance (L. Zhao et al., 2020).

This aligns with the literature, which suggests that I/S ratios between 1.0 and 2.0 are generally effective for co-digestion systems, particularly when pretreatments are applied.

7.3 Methane Kinetics and Gompertz Model

Modeling using the modified Gompertz equation provides valuable insights into the dynamics of methane production. Optimal ozonation (10%, 30s) reduced the lag phase (λ) and increased the methane production rate (R_{\max}), indicating enhanced microbial activity and quicker system start-up.

Conversely, the extended lag and reduced R_{\max} observed at 90s ozone contact under 10% suggests microbial inhibition, reinforcing that excessive ozonation may harm microbial ecology, particularly methanogens.

The strong model fit ($R^2 > 0.95$ across conditions) confirmed the reliability of the Gompertz equation for predicting biogas kinetics under ozone-pretreated conditions.

7.4 Integration with Literature and Novelty

These results are in agreement with multiple studies demonstrating ozone's dual role as a solubilization enhancer and potential inhibitor. Tyagi & Lo (2011) reported that low ozone doses can improve methane yields by 40–70%, whereas Zhen et al. (2017) observed no significant reductions at high doses due to over-oxidation and cellular toxicity.

This study is distinguished by its systematic evaluation of contact time, which is often overlooked in ozonation studies. The results underscore that not only ozone dose but also exposure duration is a critical operational parameter.

Furthermore, the integration of co-digestion principles (I/S ratio variation) with ozone pretreatment contributes to the understanding of synergistic strategies for maximizing biogas yield from WWTP sludge.

7.5 Practical Implications and Environmental Significance

The results of this study provide practical and strategic insights for wastewater treatment plants (WWTPs) seeking to enhance energy recovery and improve process efficiency. Specifically, the application of low-dose, short-duration ozone pretreatment has demonstrated clear benefits in improving methane yield, reducing the need for chemical conditioners, and enhancing sludge

dewaterability. These improvements collectively contribute to more efficient sludge management and potential cost savings for wastewater treatment plants.

Notably, the study identified that an ozone concentration of 10% with a 30-second contact time represents an optimal balance, significantly enhancing hydrolysis and boosting methane production. However, higher ozone doses or extended exposure may negatively affect microbial activity, thereby diminishing biogas output. Additionally, an inoculum-to-substrate (I/S) ratio of 1.5 provided the most effective microbial-to-substrate balance for digestion efficiency.

Kinetic analysis using the Gompertz model further confirmed the accelerated biogas formation under ozone treatment, validating its predictive value for process optimization. These findings align with the existing literature and offer a scalable and environmentally responsible approach to sludge valorization (Chen et al., 2008; Neumann et al., 2016). Nevertheless, before adopting this strategy on a full scale, WWTPs must conduct thorough cost-benefit assessments and energy audits. Due to the high energy demand associated with ozone generation, integrating renewable energy sources or selectively applying pretreatment to specific sludge fractions could enhance overall sustainability.

7.6 Comparison between kinetic model's fittings

A comparative analysis of four microbial growth models (Gompertz M1, Logistic M2, Transference M3, and Cone M4) for biogas production under ozone pretreatment revealed critical insights. Statistical equivalence ($F < 2.48$, $p > 0.05$) was observed among M1, M2, and M4, with all three demonstrating strong fits ($R^2 > 0.95$) and comparable variance in standard error estimates (SEE: 38,81–60,05) 1. However, the Logistic model (M2) exhibited marginally superior performance, achieving the highest R^2 (0.997) and lowest SEE (38,81) in key experimental conditions (e.g., Oz 10% 30s, I/S=1.5), while maintaining biologically plausible parameters for maximum biogas potential (B_{max} : 1323–1430 NmL) and growth rates (R_{max} : 80–103 NmL/day) 1. In contrast, the transference model (M3) showed significantly higher variance ($F > 2.93$, $p < 0.03$ vs. other models) and unrealistic parameter estimates (e.g., $B_{max} = 960$ NmL), indicating poor suitability for these kinetics 1. These results align with the literature showing Gompertz/logistic models as robust choices for anaerobic digestion modeling, although substrate-specific variations in lag phase interpretation (Gompertz $\lambda = 12$ –16 days vs. Logistic $\lambda = 22$ –29 days) warrant consideration for process optimization.

8 Conclusions

This study demonstrated that ozone gas pretreatment significantly enhanced methane production from municipal wastewater sludge during anaerobic digestion. By systematically investigating the effects of ozone concentration, exposure time, and inoculum-to-substrate (I/S) ratio, this study identified the critical operational parameters that influence biogas yield. Ozone gas pretreatment significantly enhances methane production from municipal wastewater sludge during anaerobic digestion. Through a systematic assessment of ozone concentration, exposure time, and the (I/S) ratio, this study determined the critical operational parameters affecting biogas production.

The optimal pretreatment condition (10% ozone concentration with a 30-second contact time), achieved a methane yield of approximately 1381 NmL CH₄, representing an improvement of over 5% compared to untreated sludge. When normalized per gram of volatile solids (VS), the yield reached 736 NmL CH₄ g⁻¹ VS, closely approaching the theoretical potential predicted by the Buswell and Mueller equation (≈ 517 mL CH₄ g⁻¹ VS), thus validating the experimental results.

Kinetic analysis using the modified Gompertz model revealed that optimal ozone pretreatment shortened the lag phase and accelerated the methane production. Conversely, excessive ozone doses or prolonged exposure reduced yields, likely due to the accumulation of inhibitory oxidation byproducts or over-mineralization, highlighting the importance of balancing oxidative strength and microbial tolerance.

The inoculum-to-substrate ratio was another critical factor, with a ratio of 1.5 maintaining process stability, buffering capacity, nutrient availability, and pH balance during digestion. This underscores the intricate interplay between the biological and chemical variables in optimizing anaerobic performance.

A comparative assessment of four kinetic models—Gompertz, Logistic, Transference, and Cone—demonstrated that while all models provided reasonable fits, the Gompertz and Logistic models exhibited superior agreement with the experimental data. Statistical evaluation using the F-test confirmed the Gompertz model as the most suitable ($p < 0.05$), offering reliable interpretability and predictive performance under tested conditions.

In summary, ozone pretreatment represents a promising strategy for enhancing methane recovery from wastewater sludge when applied under optimized conditions. The integration of kinetic modeling supports robust process monitoring and provides guidance for scale-up application. Future research should focus on pilot-scale validation, energy efficiency optimization, and the development of hybrid pretreatment approaches, such as combining ozone with thermal or chemical methods, to further improve the sustainability, efficiency, and cost-effectiveness of anaerobic digestion technologies.

9 References

1. Achinas, S., & Euverink, G. J. W. (2016). Theoretical analysis of biogas potential prediction from agricultural waste. *Resource-Efficient Technologies*, 2(3), 143-14
2. Achinas, S., & Euverink, G. J. W. (2019). Effect of combined inoculation on biogas production from hardly degradable material. *Energies*, 12(2), 217.
3. Afroze, N., George, N., Mingu, K., & Yazdanpanah, A. (2023, 2023/12/06). Effects of trace elements on digester performance and microbial community response in anaerobic digestion systems. *Environmental Technology*, 44(27), 4157-4172.
4. Al Seadi, T., Drog, B., Fuchs, W., Rutz, D., & Janssen, R. (2013). Biogas digestate quality and utilization. In *The biogas handbook* (pp. 267-301). Elsevier.
5. Alharbi, M., & Alkathami, B. S. (2024). Modeling of Biogas Production of Camel and Sheep Manure Using Tomato and Rumen as Co-Substrate via Kinetic Models. *Journal of Ecological Engineering*, 25(8).
6. Amani, T., Nosrati, M., & Srekrishnan, T. (2010). Anaerobic digestion from the viewpoint of microbiological, chemical, and operational aspects—a review. *Environmental Reviews*, 18(NA), 255-278.
7. Angelidaki, I., & Ahring, B. (1994). Anaerobic thermophilic digestion of manure at different ammonia loads: effect of temperature. *Water Research*, 28(3), 727-731.
8. Angelidaki, I., Ellegaard, L., & Ahring, B. K. (2003). Applications of the anaerobic digestion process. *Biomethanation ii*, 1-33.
9. Apha Awwa, W. (2005). Standard methods for the examination of water and wastewater. *APHA WEF AWWA*.
10. Apha Awwa, W. (2017). Standard methods for the examination of water and wastewater ,23th eddition. *APHA WEF AWWA*.
11. Appels, L., Baeyens, J., Degrève, J., & Dewil, R. (2008). Principles and potential of the anaerobic digestion of waste-activated sludge. *Progress in energy and combustion science*, 34(6), 755-781.
12. Ataa Fosua, B., Ren, L., Qiao, W., Zhang, J., Gao, Y., Fu, X., Yu, D., & Dong, R. (2023, 12/16). Restoring the Stability of Long-Term Operated Thermophilic Anaerobic Digestion of Maize Straw by Supplying Trace Elements. *Processes*, 11, 3440.
13. Bakhshi, Z., Jauffur, S., & Frigon, D. (2018). Assessing energy benefits of operating anaerobic digesters at low temperature with solids pre-ozonation. *Renewable Energy*, 115, 1303-1311.
14. Batstone, D. J., Keller, J., Angelidaki, I., Kalyuzhnyi, S. V., Pavlostathis, S. G., Rozzi, A., Sanders, W., Siegrist, H., & Vavilin, V. A. (2002). The IWA anaerobic digestion model no 1 (ADM1). *Water science and technology*, 45(10), 65-73.
15. Bolzonella, D., Fatone, F., Pavan, P., & Cecchi, F. (2005). Anaerobic fermentation of organic municipal solid wastes for the production of soluble organic compounds. *Industrial & Engineering Chemistry Research*, 44(10), 3412-3418.
16. Bougrier, C., Delgenès, J. P., & Carrère, H. (2008). Effects of thermal treatments on five different waste activated sludge samples solubilisation, physical properties and anaerobic digestion. *Chemical Engineering Journal*, 139(2), 236-244.
17. Braguglia, C., Gianico, A., & Mininni, G. (2011). Laboratory-scale ultrasound pre-treated digestion of sludge: heat and energy balance. *Bioresource technology*, 102(16), 7567-7573.

18. Buswell, A., & Mueller, H. (1952). Mechanism of methane fermentation. *Industrial & Engineering Chemistry*, 44(3), 550-552.
19. Carlsson, M., Lagerkvist, A., & Morgan-Sagastume, F. (2012). The effects of substrate pre-treatment on anaerobic digestion systems: a review. *Waste management*, 32(9), 1634-1650.
20. Carvalho, A. C. P. T. (2010). *Estudo Integrado Para Transporte, Tratamento, Valorização e Destino Final das Lamas Produzidas na ETAR de Sobreiras, na ETAR do Feixo Universidade do Porto (Portugal)*].
21. Chen, Y., Cheng, J. J., & Creamer, K. S. (2008). Inhibition of anaerobic digestion process: a review. *Bioresource technology*, 99(10), 4044-4064.
22. Chu, L., Yan, S., Xing, X.-H., Sun, X., & Jurcik, B. (2009). Progress and perspectives of sludge ozonation as a powerful pretreatment method for minimization of excess sludge production. *Water Research*, 43(7), 1811-1822.
23. Demirel, B., & Scherer, P. (2008). The roles of acetotrophic and hydrogenotrophic methanogens during anaerobic conversion of biomass to methane: a review. *Reviews in Environmental Science and Bio/Technology*, 7, 173-190.
24. Díaz Domínguez, E., Ibañez López, M. E., Mañinia, J., Fernández-Morales, F. J., & García Morales, J. L. (2024). Impact of Nanoparticle Addition and Ozone Pre-Treatment on Mesophilic Methanogenesis in Temperature-Phased Anaerobic Digestion. *Applied Sciences*, 14(20), 9504.
25. Du, H., Wu, Y., Wu, H., & Li, F. (2021). Effect of ozone pretreatment on characteristics of dissolved organic matter formed in aerobic and anaerobic digestion of waste-activated sludge. *Environmental Science and Pollution Research*, 28(3), 2779-2790.
26. Efebor, U., Onokwai, A., Onokpita, E., & Okonkwo, U. (2024). Response surface methodology application for the optimization of biogas yield from an anaerobic Co-digestion process. *environment*, 10, 12.
27. Esplugas, S., Bila, D. M., Krause, L. G. T., & Dezotti, M. (2007). Ozonation and advanced oxidation technologies to remove endocrine disrupting chemicals (EDCs) and pharmaceuticals and personal care products (PPCPs) in water effluents. *Journal of hazardous materials*, 149(3), 631-642.
28. Gonde, L. (2023). *The Effect of pH Control on Ammonium Release in Anaerobic Digestion University of Pretoria (South Africa)*].
29. Hammadi, N., Zegrar, M., Nemnich, S., Dey, Z., Remaoun, S.-M., Naouel, B., & Tilmatine, A. (2016). Development of high-voltage high-frequency power supply for ozone generation. *J. Eng. Sci. Technol*, 11(5), 755-767.
30. Harirchi, S., Wainaina, S., Sar, T., Nojourni, S. A., Parchami, M., Parchami, M., Varjani, S., Khanal, S. K., Wong, J., & Awasthi, M. K. (2022). Microbiological insights into anaerobic digestion for biogas, hydrogen or volatile fatty acids (VFAs): a review. *Bioengineered*, 13(3), 6521-6557.
31. Hu, J. (2013). Anaerobic digestion of sludge from brackish RAS: CSTR performance, analysis of methane potential and phosphatase, struvite cry-stallization. *C:/Users/77780971/Desktop/MSc. _thesis-Jianmei_Hu. pdf*.
32. Junior, I. V., de Almeida, R., & Cammarota, M. C. (2021). A review of sludge pretreatment methods and co-digestion to boost biogas production and energy self-sufficiency in wastewater treatment plants. *Journal of Water Process Engineering*, 40, 101857.

33. Kalogo, Y., Monteith, H., & Eng, P. (2012). STATE OF SCIENCE REPORT: ENERGY AND RESOURCE RECOVERY FROM SLUDGE.
34. Karim, K., Hoffmann, R., Klasson, T., & Al-Dahhan, M. (2005). Anaerobic digestion of animal waste: Waste strength versus impact of mixing. *Bioresource technology*, *96*(16), 1771-1781.
35. Kumari, U., & Gupta, P. (2024). Evaluation and optimization of the different process parameters of mild acid pretreatment of waste lignocellulosic biomass for enhanced energy procreation. *Applied biochemistry and biotechnology*, *196*(7), 3765-3785.
36. Li, L., Kong, X., Yang, F., Li, D., Yuan, Z., & Sun, Y. (2012, 2012/03/01). Biogas Production Potential and Kinetics of Microwave and Conventional Thermal Pretreatment of Grass. *Applied biochemistry and biotechnology*, *166*(5), 1183-1191.
37. Li, P., Zhao, H., Cheng, C., Hou, T., Shen, D., & Jiao, Y. (2024). A review on anaerobic co-digestion of sewage sludge with other organic wastes for methane production: Mechanism, process, improvement and industrial application. *Biomass and Bioenergy*, *185*, 107241.
38. Li, Y., Park, S. Y., & Zhu, J. (2011). Solid-state anaerobic digestion for methane production from organic waste. *Renewable and sustainable energy reviews*, *15*(1), 821-826.
39. Liu, F., Rotaru, A.-E., Shrestha, P. M., Malvankar, N. S., Nevin, K. P., & Lovley, D. R. (2012). Promoting direct interspecies electron transfer with activated carbon. *Energy & Environmental Science*, *5*(10), 8982-8989.
40. Mary, C. T., Swarnalatha, K., & Harishma, S. J. (2024, 2024/01/11). Experimental analysis on the effects of trace metals as micronutrients in enhancing biomethane production. *Sustainable Energy Research*, *11*(1), 3.
41. Mata-Alvarez, J., Dosta, J., Romero-Güiza, M., Fonoll, X., Peces, M., & Astals, S. (2014). A critical review on anaerobic co-digestion achievements between 2010 and 2013. *Renewable and sustainable energy reviews*, *36*, 412-427.
42. Meegoda, J. N., Li, B., Patel, K., & Wang, L. B. (2018). A review of the processes, parameters, and optimization of anaerobic digestion. *International journal of environmental research and public health*, *15*(10), 2224.
43. Moharir, S., Bondre, A., Vaidya, S., Patankar, P., Kanaskar, Y., & Karne, H. (2020). Comparative analysis of the amount of biogas produced by different cultures using the modified Gompertz model and Logistic model. *European Journal of Sustainable Development Research*, *4*(4), em0141.
44. Nakakubo, R., Møller, H., Nielsen, A., & Matsuda, J. (2008, 12/01). Ammonia Inhibition of Methanogenesis and Identification of Process Indicators during Anaerobic Digestion. *Environmental Engineering Science - ENVIRON ENG SCI*, *25*, 1487-1496.
45. Neumann, P., Pesante, S., Venegas, M., & Vidal, G. (2016). Developments in pre-treatment methods to improve anaerobic digestion of sewage sludge. *Reviews in Environmental Science and Bio/Technology*, *15*, 173-211.
46. Neves, L., Goncalo, E., Oliveira, R., & Alves, M. (2008). Influence of composition on the biomethanation potential of restaurant waste at mesophilic temperatures. *Waste management*, *28*(6), 965-972.
47. Nguyen, V. K., Chaudhary, D. K., Dahal, R. H., Trinh, N. H., Kim, J., Chang, S. W., Hong, Y., La, D. D., Nguyen, X. C., & Ngo, H. H. (2021). Review on pretreatment techniques to improve anaerobic digestion of sewage sludge. *Fuel*, *285*, 119105.

48. Nickel, K. (2000). Ultrasonic disintegration of biosolids—benefits, consequences and new strategies. *proteins*, 700, 71.
49. Oliveira, B. D. L. (2017). Controlo e avaliação do sistema de tratamento de águas residuais da ETAR de Gaia Litoral e ETAR de Febros.
50. Pilli, S., Bhunia, P., Yan, S., LeBlanc, R., Tyagi, R., & Surampalli, R. (2011). Ultrasonic pretreatment of sludge: a review. *Ultrasonics sonochemistry*, 18(1), 1-18.
51. [Record #21 is using a reference type undefined in this output style.]
52. Qaseem, A., Kansagara, D., Forcica, M. A., Cooke, M., & Denberg, T. D. (2016, Jul 19). Management of Chronic Insomnia Disorder in Adults: A Clinical Practice Guideline From the American College of Physicians. *Ann Intern Med*, 165(2), 125-133.
53. Qiuyuan, W., Tiejian, Z., Liyong, Z., Meichun, L., Biao, Z., Junliang, L., & Yongkai, W. (2023). Effects of Carbon to Nitrogen Ratio on Anaerobic Co-digestion by Mixing Human Manure with Straw in Rural Areas. *Environmental Science & Technology (10036504)*, 46(12).
54. Rajagopal, R., Massé, D. I., & Singh, G. (2013). A critical review on inhibition of anaerobic digestion process by excess ammonia. *Bioresource technology*, 143, 632-641.
55. Riffat, R., Dararat, S., & Krongthamchat, K. (1999). Anaerobic processes. *Water environment research*, 71(5), 656-676.
56. Ripley, L. E., Boyle, W. C., & Converse, J. C. (1986). Improved alkalimetric monitoring for anaerobic digestion of high-strength wastes. *Journal (Water Pollution Control Federation)*, 406-411.
57. Ruiz-Hernando, M., Martinez-Elorza, G., Labanda, J., & Llorens, J. (2013). Dewaterability of sewage sludge by ultrasonic, thermal and chemical treatments. *Chemical Engineering Journal*, 230, 102-110.
58. Sánchez, E., Borja, R., Weiland, P., Travieso, L., & Martín, A. (2000, 2000/03/01). Effect of temperature and pH on the kinetics of methane production, organic nitrogen and phosphorus removal in the batch anaerobic digestion process of cattle manure. *Bioprocess Engineering*, 22(3), 247-252.
59. Shitophyta, L., Arnita, A., & Wulansari, H. (2023). Evaluation and modelling of biogas production from batch anaerobic digestion of corn stover with oxalic acid. *Res. Agric. Eng*, 69, 151-157.
60. Sichler, T. C., Montag, D., Barjenbruch, M., Mauch, T., Sommerfeld, T., Ehm, J.-H., & Adam, C. (2022, 2022/09/05). Variation of the element composition of municipal sewage sludges in the context of new regulations on phosphorus recovery in Germany. *Environmental Sciences Europe*, 34(1), 84.
61. Syaichurrozi, I., Rusdi, R., Hidayat, T., & Bustomi, A. (2016). Kinetics studies impact of initial pH and addition of yeast *Saccharomyces cerevisiae* on biogas production from tofu wastewater in Indonesia. *International Journal of Engineering Transactions B Applications*, 29(8), 1037-1046.
62. Tundisi, J. G., & Matsumura-Tundisi, T. (2011). *Recursos hídricos no século XXI*. Oficina de textos.
63. Tyagi, V. K., & Lo, S.-L. (2011, 2011/09/01). Application of physico-chemical pretreatment methods to enhance the sludge disintegration and subsequent anaerobic digestion: an up to date review. *Reviews in Environmental Science and Bio/Technology*, 10(3), 215-242.

64. Vaz, T., Domingues, S., Martins, R. C., Gomes, J., & Quina, M. J. (2025). Ozonation to enhance methane production in anaerobic digestion of olive oil industry wastewater. *Journal of Environmental Chemical Engineering*, 117888.
65. Velázquez-Martí, B., Meneses-Quelal, O. W., Gaibor-Chavez, J., & Niño-Ruiz, Z. (2018). Review of mathematical models for the anaerobic digestion process. In *Anaerobic Digestion*. IntechOpen.
66. Velichkova, P., Ivanov, T., & Lalov, I. (2022). Development of simplified models for optimization of biochemical methane potential procedure. *J. Chem. Technol. Metall*, 57(4).
67. Von Gunten, U. (2003). Ozonation of drinking water: Part I. Oxidation kinetics and product formation. *Water Research*, 37(7), 1443-1467.
68. Wainaina, S., Lukitawesa, Kumar Awasthi, M., & Taherzadeh, M. J. (2019). Bioengineering of anaerobic digestion for volatile fatty acids, hydrogen or methane production: a critical review. *Bioengineered*, 10(1), 437-458.
69. Wang, J. L., & Xu, L. J. (2012). Advanced oxidation processes for wastewater treatment: formation of hydroxyl radical and application. *Critical reviews in environmental science and technology*, 42(3), 251-325.
70. Weemaes, M., Grootaerd, H., Simoens, F., & Verstraete, W. (2000). Anaerobic digestion of ozonized biosolids. *Water Research*, 34(8), 2330-2336.
71. Xia, J., Sun, H., Ma, X., Huang, K., & Ye, L. (2020). Ozone pretreatment of wastewater containing aromatics reduces antibiotic resistance genes in bioreactors: the example of p-aminophenol. *Environment International*, 142, 105864.
72. Yahya, M., Herrmann, C., Ismaili, S., Jost, C., Truppel, I., & Ghorbal, A. (2022). Kinetic studies for hydrogen and methane co-production from food wastes using multiple models. *Biomass and Bioenergy*, 161, 106449.
73. Yasar, A., Ahmad, N., Chaudhry, M., Rehman, M., & Khan, A. (2007). Ozone for Color and COD Removal of Raw and Anaerobically Biotreated Combined Industrial Wastewater. *Polish Journal of Environmental Studies*, 16(2).
74. Zhang, H., An, D., Cao, Y., Tian, Y., & He, J. (2021). Modeling the methane production kinetics of anaerobic co-digestion of agricultural wastes using sigmoidal functions. *Energies*, 14(2), 258.
75. Zhao, L., Caro, E., Holman, D. B., Gzyl, K. E., Moate, P. J., & Chaves, A. V. (2020, 2020-November-02). Ozone Decreased Enteric Methane Production by 20% in an in vitro Rumen Fermentation System [Original Research]. *Frontiers in microbiology*, Volume 11 - 2020.
76. Zhao, L., Caro, E., Holman, D. B., Gzyl, K. E., Moate, P. J., & Chaves, A. V. (2020). Ozone Decreased Enteric Methane Production by 20% in an in vitro Rumen Fermentation System. *Front Microbiol*, 11, 571537.
77. Zhao, S., & Baik, O. D. (2012). Application of ultrasound as pretreatment for extraction of podophyllotoxin from rhizomes of *Podophyllum peltatum*. *Ultrasonics sonochemistry*, 19(1), 22-31.
78. Zhen, G., Lu, X., Kato, H., Zhao, Y., & Li, Y.-Y. (2017). Overview of pretreatment strategies for enhancing sewage sludge disintegration and subsequent anaerobic digestion: Current advances, full-scale application and future perspectives. *Renewable and sustainable energy reviews*, 69, 559-577.

79. Zhou, J., Xu, W., Wong, J. W., Yong, X., Yan, B., Zhang, X., & Jia, H. (2015). Ultrasonic and Thermal Pretreatments on Anaerobic Digestion of Petrochemical Sludge: Dewaterability and Degradation of PAHs. *PLoS One*, *10*(9), e0136162.